# STRENGTH DEGRADATION OF LAMINATED COMPOSITES UNDER HYGROTHERMAL LOADING CONDITIONS

**A**
**Thesis Report**

**Submitted in partial fulfilment of the requirement for the award of degree**

**MASTER OF ENGINEERING**
**in**
**CAD/CAM & ROBOTICS**


**Submitted By**
**Sushma Singh**
**(Roll No. 800881020)**


**Under Guidance of**


**Dr. Abhijit Mukherjee**
**Director**
**Thapar University, Patiala**

**Dr. Rahul Chhibber**
**Assistant professor**
**Deptt. Of Mechanical Engg.**
**Thapar University, Patiala**



**DEPARTMENT OF MECHANICAL ENGINEERING**
**THAPAR UNIVERSITY**
**PATIALA-147004, INDIA**

# CERTIFICATE

This is to certify that the work done in this thesis report titled "**Strength Degradation of Laminated Composites under Hygrothermal Loading Conditions**" submitted in partial fulfilment of requirement for the award of **Master of Engineering Degree in CAD/CAM/Robotics** in the Mechanical Engineering Department of Thapar University, Patiala, is an authentic record of work carried out by me under the guidance of **Dr. Abhijit Mukherjee, Director, Thapar University, Patiala and Dr. Rahul Chhibber, Assistant Professor, Mechanical Engineering Department, Thapar University, Patiala.**

The matter embodied in this report has not been submitted in part or full to any other university or institute for the award of any degree.

**Dated:** 15/7/10

Deepa
**(A.Deepa)**

This is to certify that above declaration made by the student concerned is correct to the best of my knowledge & belief.

Dr. Abhijit Mukherjee
Director
Thapar University, Patiala

Rahul Chhibber
Dr. Rahul Chhibber
Assistant Professor
Deptt. of Mechanical Engg.
Thapar University, Patiala

Dr. S.K. Mohopatra
Professor & HOD
Deptt. of Mechanical Engg.
Thapar University, Patiala

Dr. R.K. Sharma
Dean
Deptt. of Academic Affairs
Thapar University, Patiala

# ACKNOWLEDGEMENT

I express my deep sense of gratitude and respects to my guide **Dr. Abhijit Mukherjee**, Director, Thapar University, Patiala and **Dr. Rahul Chhibber**, Department of Mechanical Engineering, Thapar University, Patiala for their keen interest and valuable guidance, strong motivation and constant encouragement during the course of the work. I thank them for their great patience, constructive criticism and myriad useful suggestions apart from invaluable guidance to me. I am sure that the knowledge gained through my association with my supervisors shall go a long way in helping me to realize my goals in life.

I owe my thanks to Dr. S. K. Mohapatra, Head of Department of Mechanical Engineering for his kind support.

I am thankful to Dr. H. Bhunia, Assistant professor, Department Of Chemical Engineering for his kind support.

I am thankful to Ms.Neeraj, Mr.Gurusewak singh, Mr.Purshottam for kind help and suggestions at very stages of my work.

I am highly thankful to other faculty members and workshop staff of Mechanical Department, TU, Patiala for their intellectual support.

I am also thankful to BASF construction chemicals(India) private limited for supplying us generously with MBrace E-Glass fibre sheet, carbon fibre sheet,Epoxy,Saturant etc.for this Experimentation.

Finally, I would like to express my deepest gratitude to my parents and family, without whom I am nothing, to provide me great opportunities, everlasting support, big encouragement and lots of love.

**Date:** **(A.Deepa)**

**Roll No: 800881001**

# ABSTRACT

Fiber-reinforced polymer (FRP) composites are becoming increasingly popular materials for reinforcing and/or strengthening concrete members. FRPs have high strength, light weight, excellent resistance to aggressive environments, and represent a very effective solution to the deterioration problem caused by the corrosion of steel reinforcement in structural concrete.

FRPs materials, as is known, are influenced by environmental conditions such as freezing and thawing, moisture, temperature, solar radiation, and aggressive chemical agents that occur during their service life. The degrading effect of environmental actions on the mechanical properties of FRPs reduces the durability of concrete structures. As a consequence, for an efficient use of FRPs as substitutes for traditional steel reinforcements in reinforced concrete structures, an analysis of the durability of FRP materials considering all possible deteriorating conditions is necessary.

One of the most important environmental factors affecting the durability of FRPs is the temperature variation. In hot-climate regions, the concrete structures reinforced with FRP rebars, in fact, are continuously subjected to thermal actions corresponding to daily temperature variations. So, the natural environmental conditions represent a source of degrading effect that needs accurate investigations in evaluating the durability of FRPs.

This thesis presents some results of an ongoing experimental program undertaken to investigate the suitability of FRP laminated composites working in natural environment conditions. The experimental investigations performed include thermal, with temperature value of $45^0$C, water wetting and drying cycles, tensile and bending tests of GFRP (Glass FRP) and CFRP (Carbon FRP) after their conditioning.

The mechanical and physical properties tensile strength, Flexural strength, capacitance, micro hardness, diffusivity and area of fraction of FRP laminates, determined from hygrothermal exposure, are compared with those of the unexposed laminated composites. The mechanical degradation (strength reduction and decrease in the elastic modulus) is then analyzed and discussed. The degradation is also analysed at macroscopic and microscopic levels by using SEM analyses of the exposed and unexposed specimen. An attempt has been made to relate macroscopic and microscopic behaviors.

# CONTENTS

# LIST OF FIGURES

# LIST OF TABLES

# CHAPTER-1
# INTRODUCTION

## 1.1.Basic definitions[2]

### 1.1.1. Composite

Composite is a structure or an entity made up of distinct components.

### 1.1.2. Composite material

Composite materials (or composites for short) are engineered materials made from two or more constituent materials with significantly different mechanical properties and which remain separate and distinct within the finished structure.

Composites are combinations of two materials in which one of the materials, called the **reinforcing phase**, is in the form of fibres, sheets, or particles, and are embedded in the other materials called the **matrix phase** as shown in Fig. 1.1.

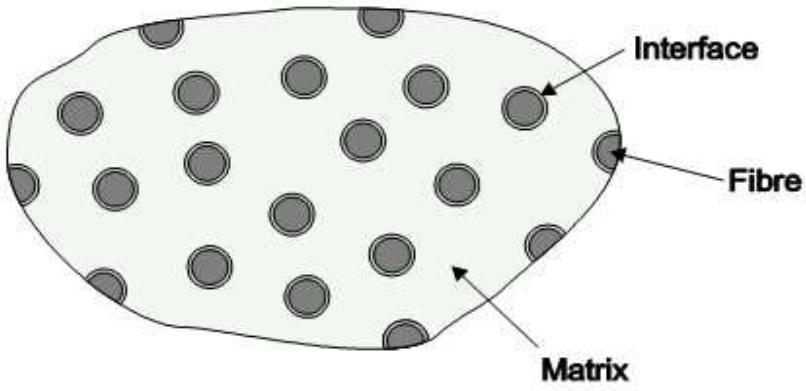


**Fig. 1.1**: phases of a composite system [3]

The primary phase, having a continuous character, is called **matrix**. Matrix is usually more ductile and less hard phase. It holds the dispersed phase and shares a load with it**.**

The second phase (or phases) is embedded in the matrix in a discontinuous form. This secondary phase is called dispersed phase. Dispersed phase is usually stronger than the matrix, therefore it is sometimes called **reinforcing phase.**

Composite materials are anisotropic in nature .so, the material properties at a certain point, vary with direction or depend on the orientation of axis as shown in Fig. 1.2.

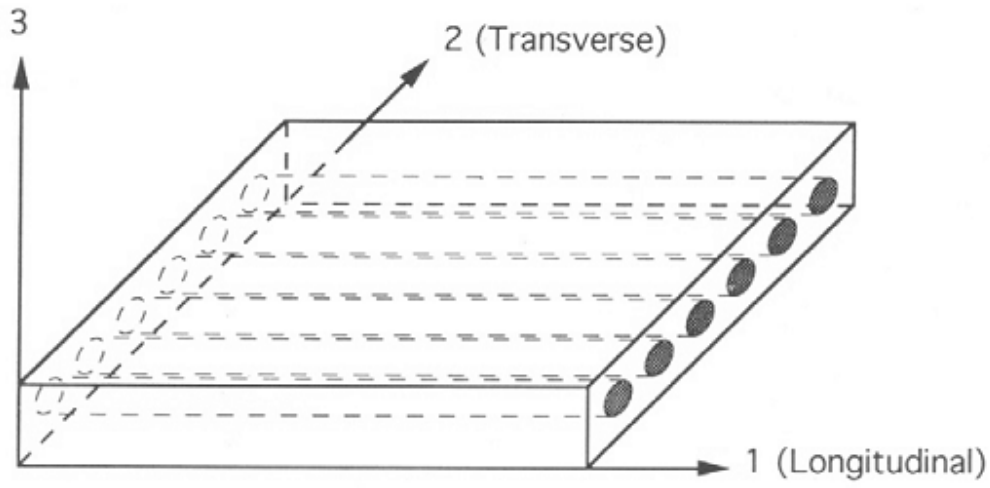


**Fig. 1.2**: Unidirectional ply and Principal coordinate axis [33]

## 1.2. Classification of composites [1]

### 1.2.1. Fibre reinforced plastics

Fibre-reinforced composite materials can be divided into two main categories normally referred to as short fibre-reinforced materials and continuous fibre-reinforced materials.

Fibre-reinforced polymers or FRPs include wood (comprising cellulose fibres in a lignin and hemicellulose matrix), carbon-fibre reinforced plastic or CFRP, and glass-reinforced plastic or GRP. If classified by matrix then there are thermoplastic composites, short fibre thermoplastics, long fibre thermoplastics or long fibre-reinforced thermoplastics. There are numerous thermoset composites, but advanced systems usually incorporate aramid fibre and carbon fibre in an epoxy resin matrix.

## 1.2.2. Sandwich structures [34]

Sandwich structures consist of high strength composite facing sheets bonded to a light weight foam or honey comb core as shown in Fig. 1.3. Sandwich structures have extremely high flexural stiffness to weight ratios and are widely used in aerospace structures. The design flexibility offered by these and other configurations is obviously quiet attractive to designers, and the potential now exists to design not only the structure, but also the structural material itself.

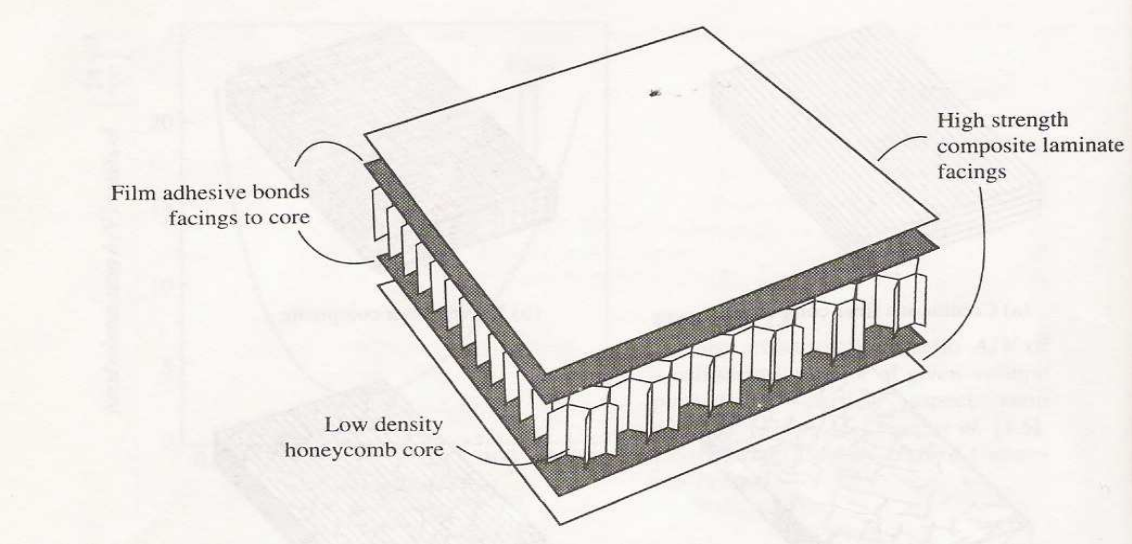


**Fig. 1.3:** Composite sandwich structure [34]

### 1.2.3. Polymer- matrix composites

Polymer matrix composites are constructed of components such as carbon, boron, and graphite and aramind fibres bound together by an organic polymer matrix such as epoxy, polyester, and urethane. Drawbacks of polymer matrix composites includes low operating temperatures, high coefficients of thermal and moisture expansion, and low elastic properties in certain directions.

### 1.2.4. Metal -Matrix Composites

Metal matrix composites consist of metal alloys reinforced with continuous fibres, short fibres or particulates. Because of their use of metals as matrix materials they have a higher temperature resistance than polymer matrix composites but in general are heavier.

### 1.2.5. Ceramic -Matrix Composites

Ceramic matrix composites are classes of structural materials reinforcement such as SiC fibres embedded in a ceramic matrix such as $Al_2O_3$, $Si_3N4$ or SiC. The reinforcements can be continuous fibres, chopped fibres, small discontinuous whisker platelets or particulates. This combination of a fibre and ceramic matrix makes ceramic matrix composites more attractive for applications where both high mechanical properties and extreme service temperatures are desired.

### 1.2.6. Carbon -Carbon Composites

Carbon-carbon composites consist of carbon fibre reinforcements embedded in a carbonaceous matrix. Carbon-carbon is a superior structural material for applications where resistance to high temperatures and thermal shocks is required. Reinforcement of a carbon matrix gives advantages such as ability to withstand high temperatures, low density and good tensile strengths, high fatigue resistance etc. Draw backs include high cost, low shear strength and susceptibility to oxidations at high temperatures.

### 1.2.7. Hybrid composites

Hybrid composites defined as a composite material system derived from the integration of dissimilar materials at least one of which is a basic composite material. A hybrid composite material blends the desirable properties of two or more types of materials into a single material system.

### 1.2.8. Engineered wood [1]

Engineered wood includes a wide variety of different products such as plywood as shown in Fig. 1.4, oriented strand board, wood plastic composite , Pykrete , Plastic-impregnated or laminated paper or textiles, Arborite, Formica and Micarta. Other engineered laminate composites, such as Mallite, use a central core of end grain balsa wood, bonded to surface skins of light alloy or GRP. These generate low-weight, high rigidity materials.

**Fig.1.4**: Plywood [1]

## 1.3. Benefits of Composites [1]

1. Weight
   a. Light weight
   b. Weight distribution
2. Strength and Stiffness
   a. High strength-to-weight ratio
   b. Directional strength and/or stiffness
3. Surface Properties
   a. Corrosion resistance
   b. Weather resistance
   c. Tailored surface finish
4. Thermal Properties
   a. Low thermal conductivity
   b. Low coefficient of thermal expansion
5. Electric Property
   a. High dielectric strength
   b. Non-magnetic
   c. Radar transparency

## 1.4. Differences with other materials

1. End material is formed during production process, in most cases in the end form of the end product.
2. Materials habits are also determined by production/curing process
3. Fibrous composites are more versatile than metals and can be tailored to meet performance needs and complex design requirements.
4. Higher specific strength (material strength/density material). Aramide and Carbon Fibre reinforced epoxies have approx. 4 to 6 times higher spec. tensile strength than steel or aluminum
5. Great fatigue endurance especially for aramide and carbon reinforced epoxies, compared with metals.

## 1.5. Properties of composites

1. Posses excellent strength and stiffness
2. They are very light materials
3. They possess high resistance to corrosion, chemicals and other weathering agents.
4. They can be moulded to any shape and size with required mechanical properties in different directions.
5. High strength to weight ratio
6. High creep resistance
7. High tensile strength at elevated temperature

## 1.6. Applications of composite materials [34]

1. Aerospace components (tails, wings, fuselages, propellers) as shown in Fig. 1.5, boat and scull hulls, bicycle frames and racing car bodies.

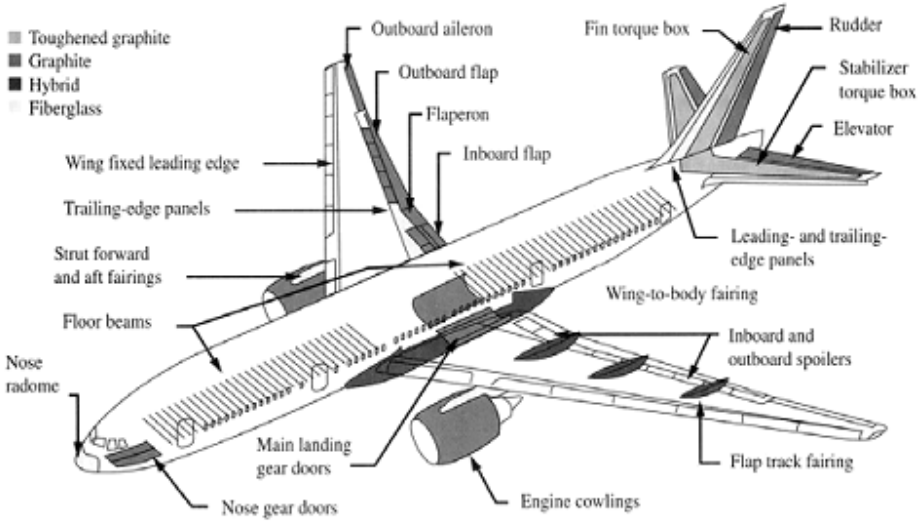


**Fig. 1.5**: Boeing 777 commercial airliner

2. Carbon composite is a key material in today's launch vehicles and spacecraft. It is widely used in solar panel substrates, antenna reflectors and yokes of spacecraft. It is also used in payload adapters, inter-stage structures and heat shields of launch vehicles.
3. The shell composed of CosmoLite, a thermoplastic fibre-reinforced composite and the exterior surface SpectraLite which incorporates DuPont Surlyn, an impact-resistant coating found on golf balls.

## 1.7. Classification of FRP

A fibre-reinforced plastic is a composite material comprising a polymer matrix reinforced with fibres. The fibres are usually fibreglass, carbon, or aramid, while the polymer is usually an epoxy, vinyl ester or polyester thermosetting plastic. FRP's are commonly used in the aerospace, automotive, marine, and construction industries.

### 1.7.1. Based on type of fibre [1]

#### 1.7.1.1. Glass-fibre reinforced plastic

Glass-reinforced plastic (GRP) is a composite material or fibre-reinforced plastic made of a plastic reinforced by fine glass fibres. Thermosetting plastics like vinyl ester or epoxy are normally used for GRP production. More recently alternatives have been developed. The glass can be in the form of a chopped strand mat or a woven fabric.

Composite materials (such as reinforced concrete), the two materials act together, each overcoming the deficits of the other. Whereas the plastic resins are strong in compressive loading and relatively weak in tensile strength, the glass fibres are very strong in tension but have no strength against compression. By combining the two materials, GRP becomes a material that resists both compressive and tensile forces well. The two materials may be used uniformly or the glass may be specifically placed in those portions of the structure that will experience tensile loads.

**Types of glass fibres used for structural reinforcements:**

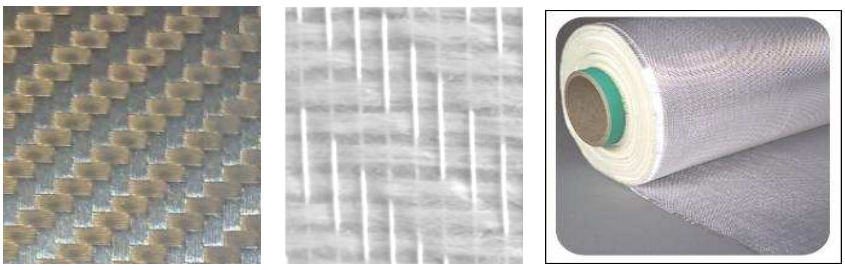

**Fig. 1.6**: Glass fibres [5]

There are two types of glass fibres used in GFRP, E-glass and S-glass as shown in Fig. 1.6. S-glass is chemically different, is stronger, more expensive and is only used in special applications in the aerospace industry. E-glass is most commonly used as a chopped strand mat, but fibreglass is also woven into a wide variety of cloths. Some of these are woven

roving, double-bias, tri-axial, Quad-axial. Depending on the application, there are 4 types of resin used with fibreglass- polyester, vinyl ester, epoxy and phenol.

**Properties of GFRP**

1. High strength-to-weight ratio
2. High modulus of elasticity-to-weight ratio
3. Good corrosion resistance
4. Good insulating properties
5. Low thermal resistance

**Applications of GFRP**

1. Pods, domes and architectural features where a light weight is necessary.
2. Bodies for automobiles, such as the Chevrolet Corvette and Studebaker Avanti.
3. Aircraft wings and fuselage sections.
4. FRP tanks and vessels: FRP is used extensively to manufacture chemical equipments and tanks and vessels.
5. F-broadcasting antennas are often mounted inside a glass-reinforced plastic cylinder on the pinnacle of a broadcasting tower
6. Housings for radar systems

### 1.7.1.2. Carbon-fibre reinforced plastic [3]

**Fig. 1.7**: carbon fibres [6]

Carbon fibre reinforced plastic or (CFRP or CRP), is a strong, light and very expensive composite material or fibre reinforced plastic as shown in Fig.1.7. Similar to glass-reinforced plastic, which is sometimes simply called fibreglass, the composite material is commonly referred to by the name of its reinforcing fibres. The plastic is most often epoxy, but other plastics, such as polyester, vinyl ester or nylon, are also sometimes used. Some composites contain both carbon fibre and fibreglass reinforcement. Less commonly, the term graphite-

reinforced plastic is also used. The characteristics and applications of carbon fibre are shown in Table 1.1, properties of CFRP laminates are shown in Table 1.3.

**Types of carbon fibres used for structural reinforcement**

1. Ultra – high modulus (modulus>450Gpa)
2. High modulus (modulus between 350-450Gpa)
3. Intermediate modulus (modulus between 200-350Gpa)
4. Low modulus and high strength (modulus<100Gpa & tensile strength>3.0Gpa)
5. Super high-tensile (tensile strength>4.5Gpa)
6. PAN-based carbon fibre
7. Pitch based carbon fibre
8. Mesosphere pitch-based carbon fibre
9. Isotropic pitch-based carbon fibre
10. Rayon –based carbon fibre
11. Gas phase-grown carbon fibre
12. Type-I, high-heat-treatment carbon fibres (HTT), where final heat treatment temperature should be above 2000$^{o}$C and can be associated with high-modulus type fibre.
13. Type-II, intermediate-heat-treatment carbon fibres (IHT), where final heat treatment temperature should be around or above 1500$^{o}$C and can be associated with high-strength type fibre.
14. Type-III, low-heat-treatment carbon fibres, where final heat treatment temperatures not greater than 1000$^{o}$C. These are low modulus and low strength materials.

**Table 1.1: Characteristics and Applications of Carbon Fibres**

| Characteristics | Applications |
|---|---|
| 1. Physical strength, specific toughness, light weight | Aerospace, road and marine transport, sporting goods |
| 2. High dimensional stability, low coefficient of thermal expansion, and low abrasion | Missiles, aircraft brakes, aerospace antenna and support structure, large telescopes, optical benches, waveguides for stable high-frequency (GHz) precision measurement frames |
| 3. Good vibration damping, strength, and toughness | Audio equipment, loudspeakers for Hi-fi equipment, pickup arms, robot arms |
| 4. Electrical conductivity | Automobile hoods, novel tooling, casings and bases for electronic equipments, EMI and RF shielding, brushes |
| 6. Fatigue resistance, self-lubrication, high damping | Textile machinery, genera engineering |
| 7. Chemical inertness, high corrosion resistance | Chemical industry; nuclear field; valves, seals, and pump components in process plants |
| 8. Electromagnetic properties | Large generator retaining rings, radiological equipment |

**Table 1.2. Basic properties of fibres and other materials**

| Material Type | Tensile Strength(MPa) | Tensile Modulus(MPa) | Typical Density(g/cc) | Specific Modulus |
|---|---|---|---|---|
| Carbon HS | 3500 | 160 - 270 | 1.8 | 90 – 150 |
| Carbon IM | 5300 | 270 - 325 | 1.8 | 150 – 180 |
| Carbon HM | 3500 | 325 - 440 | 1.8 | 180 – 240 |
| Carbon UHM | 2000 | 440+ | 2.0 | 200+ |
| Aramid LM | 3600 | 60 | 1.45 | 40 |
| Aramid HM | 3100 | 120 | 1.45 | 80 |
| Aramid UHM | 3400 | 180 | 1.47 | 120 |
| Glass - E glass | 2400 | 69 | 2.5 | 27 |
| Glass - S2 glass | 3450 | 86 | 2.5 | 34 |
| Glass – quartz | 3700 | 69 | 2.2 | 31 |
| Aluminum Alloy (7020) | 400 | 1069 | 2.7 | 26 |
| Titanium | 950 | 110 | 4.5 | 24 |

### 1.7.2. Based on Type of Matrix

#### 1.7.2.1. Thermoset composites [1]

**Polyester resin**, tends to have yellowish tint, and is suitable for most backyard projects. Its weaknesses are that it is UV sensitive and can tend to degrade over time, and thus generally is also coated to help preserve it. It is often used in the making of surfboards and for marine applications. Its hardener is a MEKP, and is mixed at 14 drops per oz. MEKP is composed of methyl ethyl ketone peroxide, a catalyst. When MEKP is mixed with the resin, the resulting chemical reaction causes heat to build up and cure or harden the resin.

**Vinyl ester resin** tends to have a purplish to bluish to greenish tint. This resin has lower viscosity than polyester resin, and is more transparent. This resin is often billed as being fuel resistant, but will melt in contact with gasoline. This resin tends to be more resistant over time to degradation than polyester resin, and is more flexible. It uses the same hardener as polyester resin (at the same mix ratio) and the cost is approximately the same.

**Epoxy resin** is almost totally transparent when cured. In the aerospace industry, epoxy is used as a structural matrix material or as structural glue.

**Shape memory polymer** (SMP) resins have varying visual characteristics depending on their formulation. These resins may be epoxy-based, which can be used for auto body and outdoor equipment repairs; cyanate-ester-based, which are used in space applications; and acrylate-based, which can be used in very cold temperature applications, such as for sensors that indicate whether perishable goods have warmed above a certain maximum temperature. These resins are unique in that their shape can be repeatedly changed by heating above their glass transition temperature ($T_g$). When heated, they become flexible and elastic, allowing for easy configuration. Once they are cooled, they will maintain their new shape. The resins will return to their original shapes when they are reheated above their $T_g$.The advantage of shape memory polymer resins is that they can be shaped and reshaped repeatedly without losing their material properties, and these resins can be used in fabricating shape memory composites.

### 1.7.2.2. Thermoplastic Composites [34]

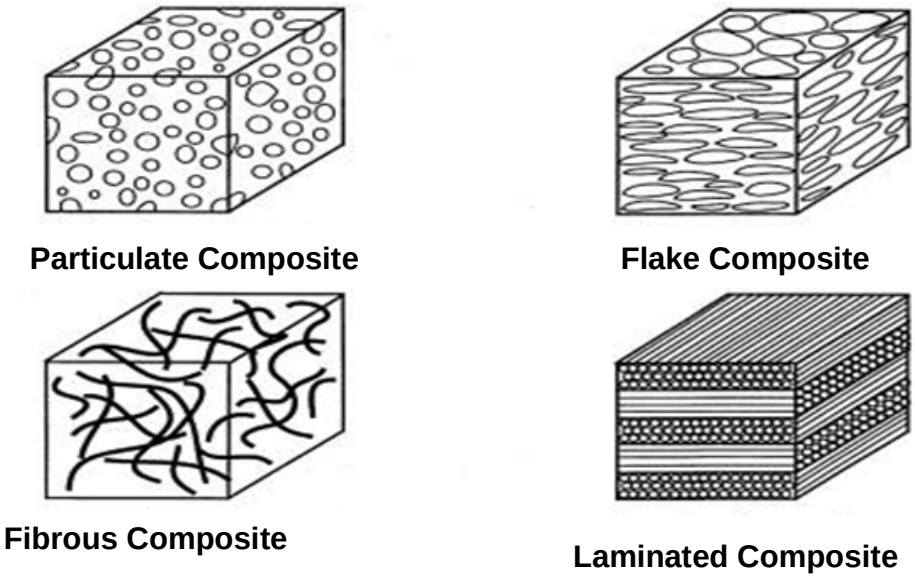


**Fig. 1.8**: Thermo plastic composites

#### 1.7.2.2.1. Fibrous composites

Dispersed phase in form of fibres improves strength, stiffness and Fracture Toughness of the material, impeding crack growth in the directions normal to the fibre. The strengthening effect is higher in long-fibre (continuous-fibre) reinforced composites than in short-fibre (discontinuous-fibre) reinforced composites.

**Short-fibre reinforced composites**, consisting of a matrix reinforced with a dispersed phase as shown in Fig.1.8 in form discontinuous fibres have a limited ability to share load.

**Long-fibre reinforced composites**; load applied is carried mostly by the dispersed phase - fibres. Matrix in such materials serves only as a binder of the fibres keeping them in a desired shape and protecting them from mechanical or chemical damages.

#### 1.7.2.2.2. Particulate composites

Particulate Composites consists of a matrix reinforced with a dispersed phase in form of particles as shown in Fig.1.8. Effect of the dispersed particles on the composite properties depends on the particles dimensions. Large dispersed phase particles have low strengthening effect but they are capable to share load applied to the material, resulting in increase of

stiffness and decrease of ductility. Hard particles dispersed in a softer matrix increase wear and abrasion resistance. Soft dispersed particles in a harder matrix improve mach inability and reduce coefficient of friction. Composites with high electrical conductivity matrices and with refractory dispersed phase (tungsten, molybdenum) work in high temperature electrical applications.

#### 1.7.2.2.3. Laminated composites [34]

Laminate composites consist of layers with different anisotropic orientations as shown in Fig.1.9 or of a matrix reinforced with a dispersed phase in form of sheets. When a fibre reinforced composite consists of several layers with different fibre orientations, it is called multilayer (angle-ply) composite.

Laminate composites provide increased mechanical strength in two directions and only in one direction, perpendicular to the preferred orientations of the fibres or sheet, mechanical properties of the material are low.

Laminated fibre reinforced composite materials are a hybrid class of composite materials involving both fibrous composite materials and lamination techniques. Purpose of lamination is to tailor the directional dependence of strength and stiffness of a composite material to match the loading environment of the structural element.

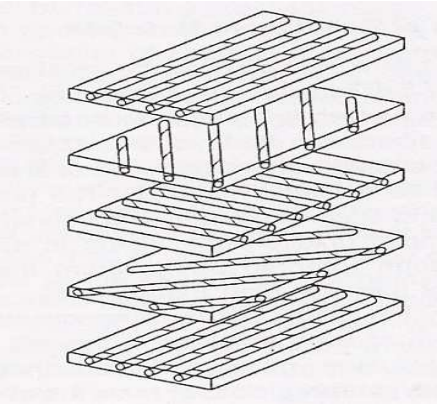

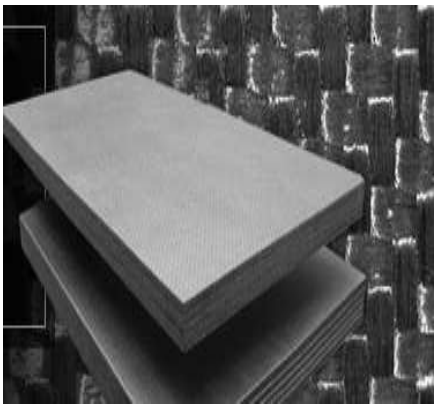

**Fig 1.9:** Laminated composite [37]

**Properties that can be emphasized by lamination are**

1. Strength
2. Stiffness
3. Low weight
4. Corrosion resistance
5. Wear resistance
6. Thermal insulation
7. Acoustical insulation

**Table 1.3. Properties of CFRP laminates**

| Property | laminates |
|---|---|
| Tensile strength,[MPa] | >2500 |
| Modulus of elasticity,[GPa] | 130-300 |
| Thickness [mm] | 1.0-2.0 |
| Ultimate strain [%] | 0.2-1.8 |

**Applications**[34]

1. Rocket motor cases, boat hulls, aircraft wing panels, tennis rackets, golf club shafts, etc.

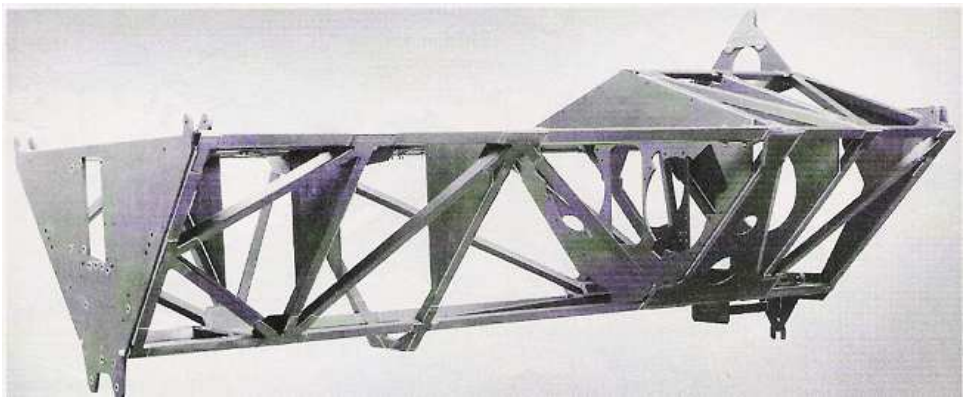

**Fig 1.10**: Optical bench for space application

2. Helicopter rotor blades as shown in Fig.1.11 are made of laminated composites and sandwich structures.

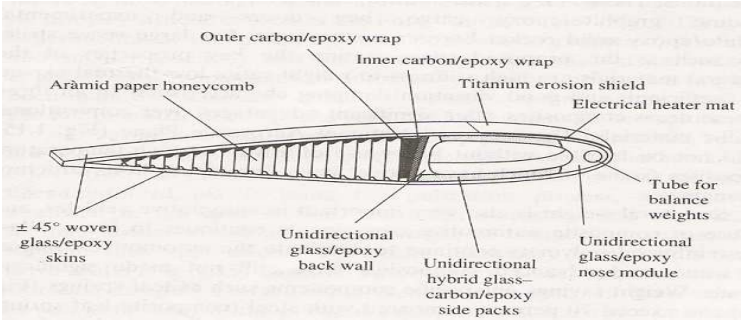


**Fig. 1.11**: Helicopter Rotor blade

3. Aircraft blades are made up of carbon-carbon laminates as shown in Fig.1.12, automobiles use composites for drive shafts manufacturing.

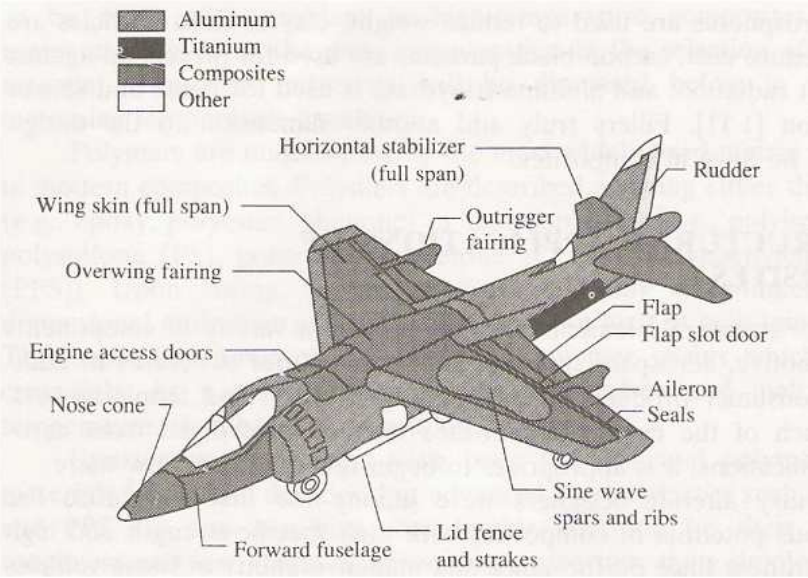


**Fig. 1.12:** Composite structures on the AV-8B fighter Air craft

## 1.7.3. Delamination Effects of laminated composites [4]

**Delamination** is a mode of failure for composite materials. Mode of failure is also known as 'failure mechanism'. In laminated materials repeated cyclic stresses, impact, and so on can cause layers to separate as shown in Fig.1.13, forming a mica-like structure of separate layers, with significant loss of mechanical toughness.

Delamination also occurs in reinforced concrete structures subject to reinforcement corrosion, in which case the oxidized metal of the reinforcement is greater in volume than the original metal. The oxidized metal therefore requires greater space than the original reinforcing bars, which causes a wedge-like stress on the concrete. This force eventually overcomes the relatively weak tensile strength of concrete, resulting in a separation (or delamination) of the concrete above and below the reinforcing bars.

The cause of fibre pull-out (another form of failure mechanism) and delamination is weak bonding. Thus, delamination is an insidious kind of failure as it develops inside of the material, without being obvious on the surface, much like metal fatigue.

**Fig. 1.13**: Delaminating CFRP under compressive load [7]

Delamination failure may be detected in the material by its sound; solid composite has bright sound, while delaminated part sounds dull, reinforced concrete sounds solid, whereas delaminated concrete will have a light drum-like sound when exposed to a dragged chain

pulled across its surface. Bridge decks in cold climate countries which use de-icing salts and chemicals are commonly subject to delamination and as such are typically scheduled for annual inspection by chain-dragging as well as subsequent patch repairs of the surface. Other nondestructive testing methods are used, including embedding optical fibres coupled with optical time domain reflectometer testing of their state, testing with ultrasound, radiographic imagining, and infrared imaging.

## 1.7.4. Construction methods of laminated composites [2]

### Hand lay-up operation

Resin is mixed with a catalyst (e.g. butanox LA) or hardener if working with epoxy, otherwise it will not cure (harden) for days/ weeks. Next, the mold is wetted out with the mixture. The sheets of fibreglass are placed over the mold and rolled down into the mold using steel rollers. The material must be securely attached to the mold, air must not be trapped in between the fibreglass and the mold. Additional resin is applied and possibly additional sheets of fibreglass. Rollers are used to make sure the resin is between all the layers, the glass is wetted throughout the entire thickness of the laminate, and any air pockets are removed. The work must be done quickly enough to complete the job before the resin starts to cure. Various curing times can be achieved by altering the amount of catalyst employed.

### Spray lay-up operation

The fibreglass spray lay-up process is similar to the hand lay-up process but the difference comes from the application of the fibre and resin material to the mold. Spray-up is an open-molding composites fabrication process where resin and reinforcements are sprayed onto a mold. The resin and glass may be applied separately or simultaneously "chopped" in a combined stream from a chopper gun. Workers roll out the spray-up to compact the laminate. Wood, foam or other core material may then be added, and a secondary spray-up layer imbeds the core between the laminates. The part is then cured, cooled and removed from the reusable mold.

### Pultrusion operation

Pultrusion is a manufacturing method used to make strong light weight composite materials, in this case fibreglass. Fibres (the glass material) are pulled from spools through a device that coats them with a resin. They are then typically heat treated and cut to length. Pultrusions can be made in a variety of shapes or cross-sections such as a W or S cross-section. The word pultrusion describes the method of moving the fibres through the machinery. It is

pulled through using either a hand over hand method or a continuous roller method. This is opposed to an extrusion which would push the material through dies.

## 1.7.5. Environmental Effects on laminated Composite Materials [1]

During normal operation time, composite structures are subjected to environmental attacks, which include changes in temperature and moisture. These effects are called hygrothermal effects.

Fibre reinforced polymers (FRP) are being increasingly used in many structural applications due to their excellent mechanical and corrosion resistance characteristics. FRP sheets and strips are being used to strengthen waterfront concrete structures, such as piers and wharves. The FRP reinforcements are bonded to beams, piles, and decks using structural adhesives. Adhesive strength can be affected by both short-term and long-term environmental exposure. In the current study, short-term effects of temperature, moisture, and chloride content on the FRP adhesion are evaluated using pull-off tests. Three structural adhesives were chosen to assess the effects of three different temperatures and four different relative humidities on the FRP adhesion to concrete cubes. In the case of concrete piles exposed to marine conditions, the effect of superficial chloride content on the short-term bond strength was also investigated. It was shown that high relative humidity may reduce bond strength below acceptable levels

### 1.7.5.1. Categorization of Effects

**Physical and chemical effects**

Moisture absorption and desorption processes in polymer matrix composites depend on the current hygrothermal state and on the environment. Basically the moisture content in the material affects the glass transition temperature of the matrix. Polymerization process is a function of the hygrothermal properties of the constituents and the composites current hygrothermal state. Material degradation and corrosion can also be related to hygrothermal factors.

**Effects on mechanical properties**

Time dependent properties such as the tensile modulus and shear modulus may vary with temperature and moisture concentration, failure and strength characteristics, specially interfacial and matrix dominated ones, may depend on temperature and humidity

**Hygrothermal elastic effects**

The composite material undergoes reversible deformations related to thermal expansion and moisture expansion coefficients. Intra laminar and inter laminar stresses are developed as a result of the thermo elastic and hydro elastic inhomogenity and anisotropy of the material.

# CHAPTER-2
# LITERATURE REVIEW

**Hiroshi Saito and Isao Kimpara [2009]** evaluated the damage evolution behavior by considering the effect of the textile structure and water absorption. Damage observation was conducted by the integration of non-destructive and direct observation methods. Candidate textile reinforcements were T300-3k plain woven fabric (PW) and T700S-12k multi-axial knitted fabric (MA). The effect of water absorption on the performances of compression after impact (CAI) and PIF were small in PW CFRP laminates. Conversely, PIF properties of water-absorbed MA CFRP laminates drastically decreased than that of dry ones. CAI strength was not affected by water absorption. PIF performance of dry MA CFRP was fairly higher than that of the others. From the precise observation, some evidences of interfacial deterioration caused by water absorption were confirmed in both PW and MA CFRP laminates

**Toshio Ogasawara, Yuichi ishida, and Tetsuokasai [2009],** examined the effect of fullerene dispersion on the mechanical properties of carbon-fibre reinforced epoxy matrix composites (CFRPs). Mechanical properties such as tension, compression, open-hole compression, compression after impact (CAI), binding, short beam shear, and interlaminar fracture toughness were evaluated for $[0]_8$, $[90]_{16}$, $[45/0/-45/90]_{2S}$ laminates. Tension and compression strengths increased 2–12% by dispersing 0.5% of fullerene into the matrix resin. Furthermore, interlaminar fracture toughness of the composite was improved by about 60%. It was revealed that a small amount of fullerene (0.1–1 wt. %) increased the failure strain of epoxy resin itself, thereby improving the CFRP strength.

**F.Elgabbas, A.A.Ei-Ghandour, A.A.Abdeelrahman and A.S.Ei-Dieb [2009],** conducted experimental–analytical investigation on the structural behavior of precast prestressed hollow core RC slabs strengthened in flexure by CFRP laminates. Externally bonded and near surface mounted (NSM) laminates were used. The CFRP area and using transverse anchorage were also investigated. Results demonstrated that NSM technique resulted in optimum strengthening efficiency. The increased bond strength also resulted in full activation of the NSM laminates at failure. However, the NSM flexural strengthening level should be carefully designed to avoid unfavorable shear-tension failure mode. Moderate efficiency was associated with the externally bonded technique due to the premature de-bonding. However, this efficiency was optimized by using transverse CFRP laminates as anchorage, which re-directed de-bonding further away from the laminates' ends and delayed failure, but at much lower deformations than those of the control slab. A rational analytical study was conducted.

**Reaza.chaudhuri and Paulseide [2009]** employed the equilibrium/compatibility method, which is a semi-analytical post-processing method for computation of hitherto unavailable through-thickness variation of interlaminar (transverse) shear stresses in the vicinity of the bi-layer interface circumferential re-entrant corner line of an internal part-through circular cylindrical hole weakening an edge-loaded laminated composite plate. A Co-type triangular composite plate element, based on the assumptions of transverse inextensibility and layer-wise constant shear-angle theory (LCST), is utilized to first compute the in-plane stresses and layer-wise through-thickness average interlaminar shear stresses, which serve as the starting point for computation of through-thickness distribution of interlaminar shear stresses in the vicinity of the bi-layer interface circumferential re-entrant corner line of the part-through hole. The same stresses computed by the conventional equilibrium method (EM) are, in contrast, in serious error in the presence of the bi-layer interface circumferential re-entrant corner line singularity arising out of the internal part-through hole, and are found to violate the interfacial compatibility condition. The computed interlaminar shear stress can vary from negative to positive through the thickness of a cross-ply plate in the neighborhood of this kind of stress singularity

**B. Kolesnikov, I. Herbeck and A. Fink [2008],** explained about the structural joining essential for the development of composite aerospace structures: every structural interconnection means a disturbance of an optimized structure resulting in an increase in overall structural weight. The lightweight potential of advanced, high-performance fibre composite materials is affected more strongly by mechanical fastening techniques than by conventional metallic materials due to the low shear and bearing capabilities of CFRP materials. Local embedding of thin titanium layers into the composite laminate in the coupling region results in a considerable improvement in structural efficiency of bolted and riveted joints in CFRP structures. This improvement is not only obvious in the increase in shear and bearing capabilities, but also in the resulting possibilities for a design no longer burdened by local material thickening, eccentricities and additionally excited local bending stresses. This report displays experimental results demonstrating the advantageous influence of titanium hybridization on specific characteristics of CFRP-materials, thus proving the mechanical potential of CFRP/titanium hybrid materials when used as an advanced reinforcement technique for highly loaded composite joints.

**Alaattin Aktas and Ibrahim Uzun[[2008],** investigated about the effect of sea water on the bearing strength behavior of the woven glass fibre composite in this paper. the ratio of the edge distance to the pin diameter, and the ratio of the specimen width to the pin diameter(w/d) were symmetrically varied during experiments. In order to provide the real environmental conditions, specimen were tied to a ship, making voyage in the Sea of Marmara having 2.2% of salt and 22-26$^{oC}$ of surface temperature, with a stainless wire to

keep the specimen in to sea. The specimen was kept into sea 1, 2 and 4 months. The experiments were carried out according to the ASTM D953. The results show that while the bearing values obtained from the specimen kept into sea for four months decrease considerably with respect to 1 and 2 months. But the failure modes for all configurations are the same mode. Failure distance of the pin displacement increases with the increasing of immersing period owing to softening of the specimen.

**Z.sereir and E.A. Adda-Bedia [2007],** worked for the reduction of the hygroscopic stresses at the edges of the hybrid composite for the symmetrical and constant environmental conditions in this paper. We noted during our search that the hygroscopic stresses calculated by the analytical method are maximum at both the edges of the laminated composite, in particular at the first times of the moisture diffusion. Therefore, a probable degradation of the laminated plates can be produced at the two edges. In this context and in order to limit these maximum stresses, we made some applications on hybrid composites in graphite/epoxy with polymer matrix. Firstly, we carried out a calculation of the moisture concentration from the initial until the saturation time, for two applications suggested A and B, of a hybrid composite. Secondly, we calculated the hygroscopic stresses for each application (cases A and B). An appropriate choice of the stacking hybrid sequences $[\theta/-\theta]$ will be useful considerably in the reduction of these hygroscopic stresses.

**B.Pradhan and S.K.Panda [2006],** has given about their investigation on the influence of ply lay up and the interaction of residual thermal stresses and mechanical loading on the interlaminar asymmetric embedded delamination crack growth behavior in this paper. Two sets of full three-dimensional thermo-elastic finite element analyses have been performed for the interlaminar elliptical delaminations, which may be due to manufacturing defects or other reasons and are located symmetrically with respect to the midplane in a quasi-isotropic FRP composite laminate layup. Depending upon the through-the-thickness location of the embedded elliptical delaminations, four different laminate configurations have been considered. Strain energy release rate (SERR) procedures have been employed to assess the delamination crack growth characteristics at the interfaces. It is found that the individual fracture modes exhibit asymmetric and non self-similar crack growth behavior along the delamination front depending upon the location of the interfacial delaminations; ply sequence and orientation and thermo-elastic anisotropy of the laminate.

**B.Pradhan and Saroja Kanta Panda [2006],** studied about the thermo elastic effect of material anisotropy and curing stresses on interlaminar embedded elliptical delamination fracture characteristics in multiply laminated fibre-reinforced polymeric (FRP) composites in this paper. Two sets of full three-dimensional finite element analyses have been performed to calculate the displacements and interlaminar stresses along the delaminated interface responsible for the delamination onset and propagation. Modified crack closure integral

methods based on the concepts of linear elastic fracture mechanics have been followed to evaluate the individual modes of strain energy release rates along the delamination front. It is shown that the individual modes of energy release rates vary along the delamination front depending on the ply sequence, orientation, and thermo elastic material anisotropy of the constituting laminate. This causes the anisotropic and non-self similar delamination propagation along the interface. The asymmetric and nonuniform variations in the nature of energy release rate plots obtained in a thermo mechanical loading environment are significant when curing stress effects are included in the numerical analysis and hence should be taken into account in the designs of laminated FRP composite structures

**E.C Botelho, I.C.Pardini and M.C. Rezende [[2006],** studied about the environmental factors, such as humidity and temperature, can limit the applications of composites by deteriorating the mechanical properties over a period of time. Environmental factors play an important role during the manufacture step and during composite's life cycle. The degradation of composites due to environmental effects is mainly caused by chemical and/or physical damages in the polymer matrix, loss of adhesion at the fibre/matrix interface, and/or reduction of fibre strength and stiffness. Composite's degradation can be measure by shear tests because shear failure is a matrix dominated property. In this work, the influence of moisture in shear properties of carbon fibre/epoxy composites (laminates $[0/0]_s$ and $[0/90]_s$) have been investigated. The interlaminar shear strength (ILSS) was measured by using the short beam shear test, and Iosipescu shear strength and modulus ($G_{12}$) have been determinated by using the Iosipescu test. Results for laminates $[0/0]_s$ and $[0/90]_s$, after hygrothermal conditioning, exhibited a reduction of 21% and 18% on the interlaminar shear strength, respectively, when compared to the unconditioned specimen. Shear modulus follows the same trend. A reduction of 14.1 and 17.6% was found for $[0/0]_s$ and $[0/90]_s$, respectively, when compared to the unconditioned specimen. Micro structural observations of the fracture surfaces by optical and scanning electron microscopes showed typical damage mechanisms for laminates $[0/0]_s$ and $[0/90]_s$.

**X.W.Wag, I.Pont Lezica, J.M.Harris, F.J.Guild and M.J.Pavier [2005],** explained about causes of delaminations reduction in the compressive strength of a composite material and multiple delaminations cause greater strength reduction than single ones. Since realistic damage such as that resulting from an impact consists of multiple delaminations, it is of interest to understand the mechanism of strength reduction for laminates containing multiple delaminations. In this work, compression testing of glass fibre reinforced plastic specimen containing single and multiple embedded delaminations was carried out. Finite element modeling was used to gain further understanding of the mechanisms of compressive failure. Reasonable agreement between finite element predictions and experimental measurements were found for the whole range of delamination geometries that were tested. It is

demonstrated that the maximum reduction in strength for a multiple occurs when the delaminations split the laminate into sub-laminates of similar thickness.

**W. J. Hwang, Y.T. Park and W. Hwag [2005],** studied about the effect of notching on fibre-reinforced metal laminates (FML). 3-2 layup carbon fibre aluminium laminates specimen containing a circular hole were employed in notch tests. The notch effect for a composite laminate was investigated and compared with carbon/ epoxy composites and aluminium sheets. The degradation of notch strength for carbon fibre aluminium laminates was smaller than for carbon/ epoxy composites. The point and average stress criteria were used in the notch strength analysis. A finite width correction factor was also used. The strength degradation models involve a single parameter that is a function of the hole size and the characteristic length. These models were compared with experimental data and good agreement was found.

**J.Lee and C.Soutis [2005],** studied the effect of laminate thickness on the compressive behaviour of composite laminates was investigated through systematic experimental work using the stacking sequences, $[0_4]_{ns}$, $[45/0/-45/90]_{ns}$ and $[45_n/0_n/-45_n/90_n]_s$ ($n$=2–8) with a 3 mm diameter open hole at the centre. Parameters such as fibre volume fraction, void content, fibre waviness and interlaminar stresses, influencing compressive strength with increasing laminate thickness were also studied experimentally and theoretically. Furthermore the stacking sequence effects on failure strength of multidirectional laminates were examined. For this, two different scaling techniques were used: (1) ply-level technique $[45_n/0_n/-45_n/90_n]_s$ and (2) sub laminate level technique $[45/0/-45/90]_{ns}$. An apparent thickness effect existed in the lay-up with blocked plies, i.e. unidirectional specimen ($[0_4]_{ns}$) and ply-level scaled multidirectional specimen ($[45_n/0_n/-45_n/90_n]_s$). Fibre waviness and void content were found to be main parameters contributing to the thickness effect on the compressive failure strength. However, the compressive strength of the sub laminate level scaled specimen ($[45/0/-45/90]_{ns}$) was almost unaffected regardless of the specimen thickness (since ply thickness remains constant). From the investigation of the stacking sequence effect, the strength values obtained from the sub laminate level scaled specimen were slightly higher than those obtained from the ply level scaled specimen. This applied to all specimen thicknesses regardless of the presence of an open hole. The reason for this effect was explained by the fibre waviness, void content, free edge effect and stress redistribution in blocked 0° plies and unblocked 0° plies. Finally the average strengths of open hole specimen obtained from both stacking sequences increased with increasing specimen thickness. The measured failure strengths were compared with the predicted values.

**S.kellas, J.Morton and P.T Curtis [2003],** studied the effect of several hygrothermal environments upon the uniaxial strength of centre-notched laminates, fabricated from a

standard carbon fibre-reinforced epoxy system was investigated. Conditioned dry or wet specimen were tested in either tension or compression in a range of test temperatures: room temperature, 90°C, or 130°C. Two stacking sequences were studied: $(\pm 45°/0°_3/\pm 45°/0°)_s$ denoted A, and $(0°/\pm 45°/0°_2/\pm 45°/0°)_s$ denoted B. In the case of sequence A, two notch geometries were considered: a sharp 10 mm notch, and a circular 5 mm diameter hole; sequence B was investigated with a sharp notch only. Results indicated that, in general, the hygrothermal environments considered had a beneficial effect upon tensile strength and a detrimental effect upon compressive strength. The interactions of damage modes responsible for the observed behavior have been isolated and schematically represented. It has been shown that such interactions depend upon the notch geometry as well as upon the stacking sequence.

**P.K.Ray, A.Bhushan, T.Bera, R.Ranjan, U.Mohanty, S.Vadhera, B.C.Ray [2003],** investigated the effect of absorbed moisture on the mechanical properties of E-Glass/Epoxy composite. It is now well known that the exposure of polymeric composites in moist environments, under both normal and sub-zero conditions, leads to certain degradation of its mechanical properties which necessitates proper understanding of the correlation between the moist environment and the structural integrity. Environments similar to several that in real life, like marine environments, the high temperature excursions (thermal spikes) experienced by the undercarriage of VTOL aircraft, or even natural weathering conditions were tried to be regenerated and an attempt was made to understand their impact on the fibre-matrix adhesion property. The tensile and bending properties were determined under hydrothermal conditions and the effect of thermal spike on the interlaminar shear strength (ILSS) values of the composite under different conditions were also discussed. The changes in glass transition temperature (Tg) and investigations through scanning electron microscopy (SEM) showed that E-Glass/epoxy composites quite sensitive to environmental conditioning.

**M.Raghavendra1, C.M.Manjunatha, M.Jeeva Peter, C.V.Venugopal and H.K.Rangavittal[2004],** Glass fibre reinforced polymer matrix (GFRP) woven fabric composite material was tested to determine tensile, compressive and in-plane shear (IPSS) strength under both room temperature(RT) and hot-wet conditions. Prior to testing, hot-wet specimen were hygrothermally aged in an environmental chamber, maintained at 71 $^oC$ and 85 % relative humidity (RH) until moisture absorption of about 1 wt. % was attained. Tests were performed in a computer controlled 100kN servo-hydraulic test machine. For hot-wet tests, a split type environmental chamber was fixed to the machine which was also maintained at 71$^oC$ and 85 % RH. The test data obtained was statistically analyzed to determine mean strength and B-basis design allowables. In general, hot-wet strength was lower by about 11% to 18%, compared to strength at RT. Presence of moisture in the epoxy

matrix, in the fibre-matrix interface and the chemical attack of moisture on the glass fibres are thought be the main reasons for reduced strength of GFRP material in hot-wet condition.

**Buket Okutan [2002]** conducted a numerical and experimental study to determine the failure of mechanically fastened fibre-reinforced laminated composite joints. E/glass–epoxy composites were manufactured to fabricate the specimen. Mechanical properties and strengths of the composite were obtained experimentally. Tests have been carried out on single pinned joints in $[0/90/0]_s$ and $[90/0/90]_s$ laminated composites. A parametric study considering geometries was performed to identify the failure characteristics of the pin-loaded laminated composite. Data obtained from pin-loaded laminate tests were compared with the ones calculated from a finite element model (PDNLPIN computer code). Damage accumulations in the laminates were evaluated by using Hashin's failure criteria combined with the proposed property degradation model. Based on the results, ply orientation and geometries of composites could be crucial for pinned laminated composite joints.

**M. A. Aiello and L. Ombres [2000]**, presented the effect of temperature and moisture on the mechanical properties of FRP (Fibre-Reinforced Polymer) reinforcements. FRP rebars made from glass and aramid fibres were subjected to cyclic thermal actions at temperatures ranging between 20 and $70^{O}C$, typical of natural hot-climate environments. Tensile tests were also carried out on FRP rebars. The effect of moisture was investigated by cyclic wetting and drying the FRP rebars under laboratory conditions before their testing in tension. Finally, the elastic modulus and tensile strength of the FRP rebars exposed to these cyclic actions were compared with those obtained for unexposed ones, in order to evaluate the mechanical damage caused by environmental conditions.

**C.Soutis, N.A. Fleck and P.T. Curtis [1991],** described the static compressive response of T800/924C carbon fibre/epoxy $[(\pm 45/0_2)_3]_s$ laminates containing a single or two circular holes. Penetrant-enhanced X-ray radiography, laminate deply and scanning electron microscopy are employed to observe damage initiation and propagation. Failure is due to 0° fibre micro buckling surrounded by delamination. For all geometries investigated, the micro buckled region initiates at the hole boundary at approximately 80% of the failure strength. The micro buckle band extends stably under increasing load before becoming unstable at a critical micro buckle length of 2–3 mm. The final fracture surface is almost perpendicular to the loading direction. A two-dimensional finite element analysis is used to study the interaction effect between a pair of 5 mm diameter holes as a function of hole spacing; for no interaction the hole centers should be placed at least four hole diameters apart.

**C.Soutis and N.A.Fleck [1990],** conducted experimental and theoretical studies on the compressive failure of carbon/epoxy, T800/924C, composite laminates. Static tests were carried out to investigate the mechanics of uniaxial compressive failure in multidirectional

unnotched $[(\pm 45/0_2)_3]_s$ plates. Fibre micro buckling in the 0° plies is the critical damage mode which causes fracture of the composite plate. A series of experiments was also carried out to determine the failure in compressively loaded $[(\pm 45/0_2)_3]_s$ laminates with circular holes. X-ray radiography and scanning electron microscopy were used to observe damage initiation and propagation. Failure is initiated as matrix cracking. With increasing load fibre micro buckling, surrounded by delamination, occurs at the edges of the hole at locations of high in-plane compressive stress. When damage reached a critical state the laminate failed catastrophically. Finally, a theoretical model is presented for predicting the static strength of notched laminates. Theoretical predictions are compared with experimental data for specimen containing circular holes of different sizes. Agreement of theory with test data is acceptable.

Following are the Gaps found in literature review

1. The flexural strength and flexural modulus data of laminates were not found in hygrothermal conditions only analytical calculations have been done.
2. Tensile properties of laminates have been assessed but laminates were not exposed to hygrothermal loading conditions
3. The micro hardness data, moisture absorption comparison with capacitance was not discussed in case of laminates
4. Effect of delamination at the interface of laminated composites under bending loads has not been studied so far.
5. The laminated composites subjected to bending and tensile pre-loads mechanical properties and exposed to hygrothermal loading for long period have not been reported in the literature.

# CHAPTER-3
# PROBLEM FORMULATION

FRP composites are extensively used in airframe structural applications. Carbon (CFRP), Glass (GFRP) are the most commonly used composite materials used composite materials in composite industry.

Wide-spread use of fibre reinforced polymers (FRP) in construction is hampered in this part of world due to lack of long-term durability and performance data, especially in a tropical environment. Hence effort is required to fully comprehend the GFRP and CFRP response under natural and accelerated moisture and temperature conditions.

From the gaps in literature an attempt was made to fulfil the gaps like capacitance comparison with moisture absorption, studying bending and tensile load effects on laminated composites and finding out micro hardness results due to hydrothermal loading of laminated composites and studying the mechanical and physical property degradation in GFRP and CFRP laminates.

The presented work was an attempt to study the effect of moisture & heat on **GFRP and CFRP laminated composites**. The changes occurring in the physical composition & mechanical properties of the composite material under natural and accelerated conditions had been studied.

For the achieving the objective an experimental setup was prepared. The aim of the experiment was to study the combined effect of parameters moisture and temperature & study *the* rate & magnitude of damage of the chosen laminated composite material which further helped in studying the response of the composite to the given hygrothermal load.

The natural degradation of material takes long time to show appreciable results so we had chosen accelerated degradation condition to have results in short duration of time. The material was pre-stretched and pre-bended in order to form some cracks so as to allow water to seep at a faster rate, the specimen were held in experimentation for pre-decided time periods & then tested for their tensile and bending strength by loading in tension and bending. The presented work was mainly carried out on the first two sets of specimen i.e. holding time of 1 & 2 months.

The work provided some insight in the performance and durability of laminated composite materials under tropical environment and this laboratory data might be useful to model the performance and durability of real time components under similar environmental conditions.

# CHAPTER-4
# EXPERIMENTATION

## 4.1. Fabrication of specimen

### 4.1.1. Specimen Specifications

Commercially available GFRP and CFRP sheets had been used for making specimen. The sheets were placed along $0^0$ orientation side for cutting the specimen
ASTM standard D3037/3039 and D790 were used to decide the specifications of tensile and bending specimen and dimensions of specimens are shown in Fig.4.1-Fig.4.6.

#### 4.1.1.1. Specifications

**For tensile testing**

| | | |
|---|---|---|
| Length of the specimen | : | 500mm |
| Width of the specimen | : | 15mm |
| Thickness of the specimen | : | 3mm (for GFRP) & 4.32mm (for CFRP) |
| Tab length | : | 100mm |
| Tab thickness | : | 0.8mm (approx.) |

**For bending test**

| | | |
|---|---|---|
| Length of the specimen | : | 250mm |
| Width of the specimen | : | 15mm |
| Thickness of the specimen | : | 3mm (for GFRP) & 4.32mm (for CFRP) |

#### 4.1.1.2. Specimen dimensions

**For bending test**

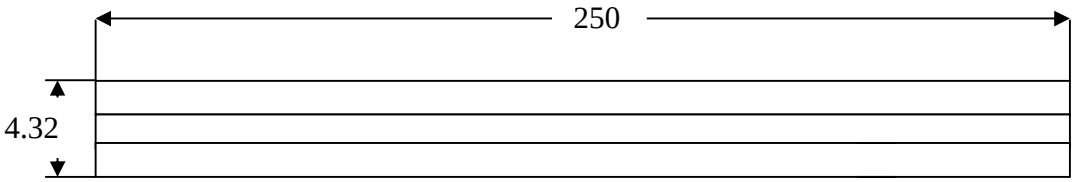


**Fig. 4.1:** For laminated CFRP composite
All dimensions are in mm

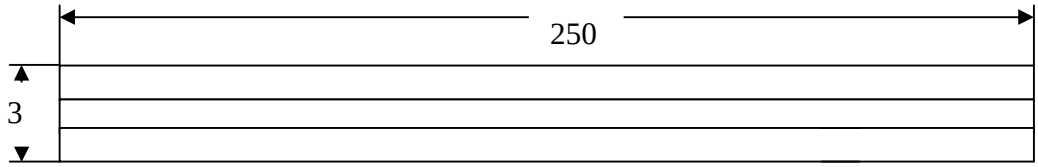


**Fig 4.2:** For laminated GFRP composite
All dimensions are in mm

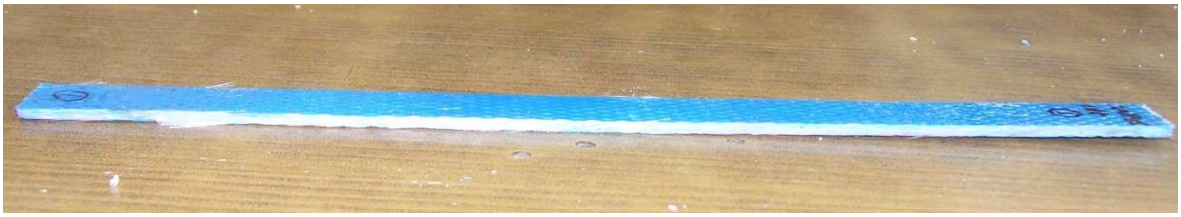

**Fig. 4.3:** Bending laminated composite

**For tensile test**

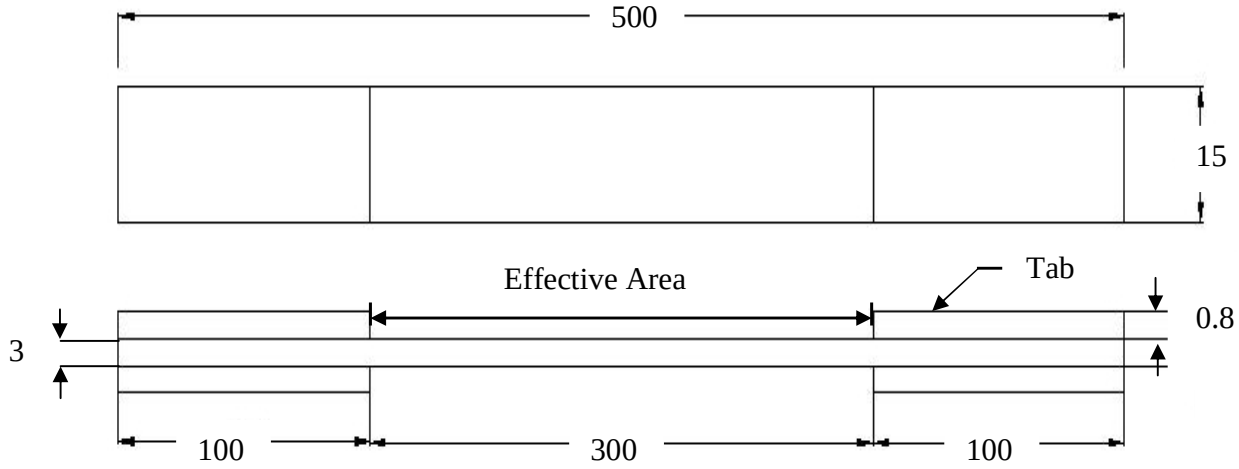


**Fig. 4.4:** For laminated GFRP composite
All dimensions are in mm

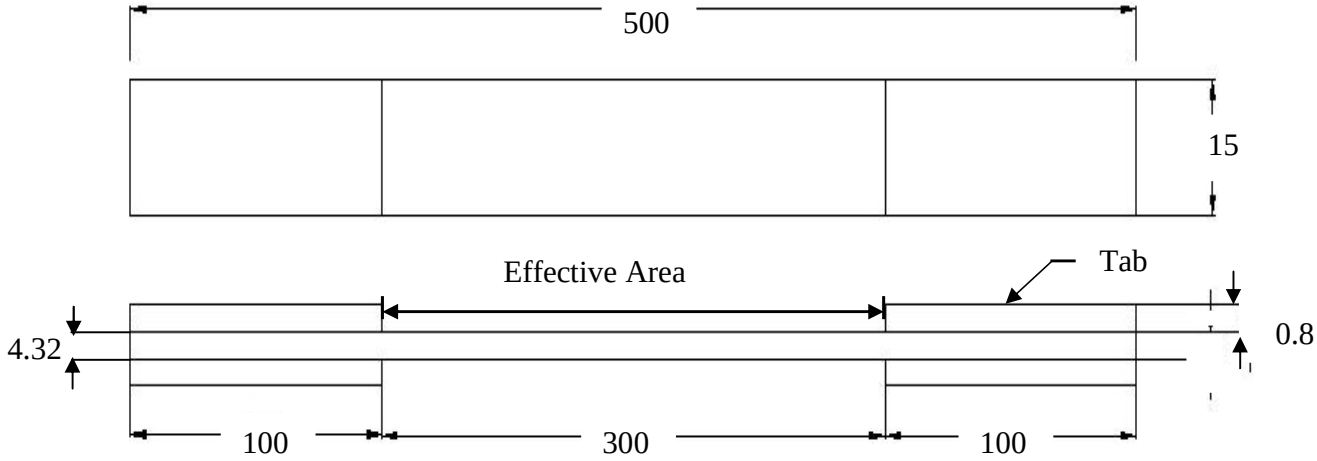


**Fig. 4.5:** For laminated CFRP composite
All dimensions are in mm

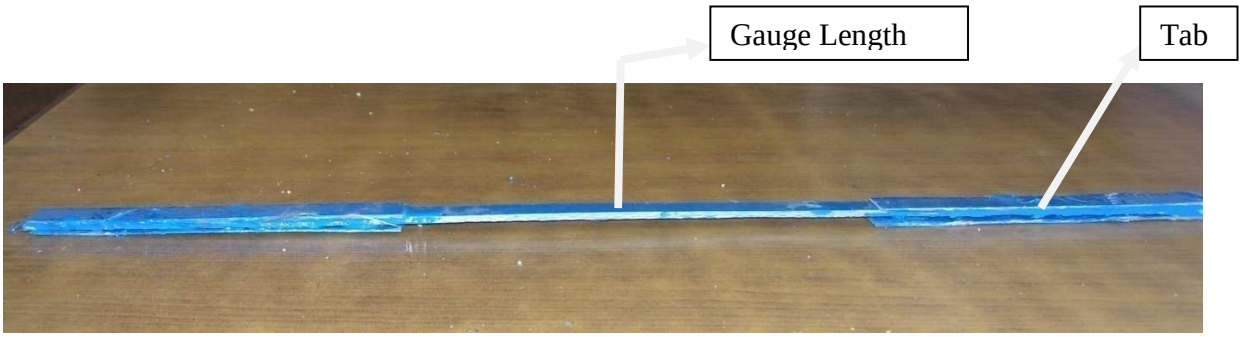


**Fig. 4.6:** Tensile laminated composite

The specimen is fully immersed in to the water bath with the help of thread, specimen details are represented on page marker for easy identification of specimen while removing the specimen at required time period for further calculation of required parameters in order to estimate degradation of the fibre.

### 4.1.2. Cutting of sheets

**Fig. 4.7**: Glass fibre sheet

**Fig. 4.8:** Carbon fibre sheet

For our experiments we purchased unidirectional woven fabric roll of GFRP and CFRP with width of 5oCm and 3oCm respectively having $0^0$ fibre orientation. The sheets were initially cutted from the roll more than the required specimen size as shown in Fig.4.7 and Fig. 4.8 in order to remove flaws at ends after curing.

### 4.1.3. Mixing of epoxy

Epoxy resin was used to coat the sheets in order to make a composite material. This resin consists of two parts:

a) Base
b) Hardener

Base is thick blue liquid which was considered as main ingredient and orangish coloured hardener was added to it to help it in settling down by starting the exothermic reactions. Both base and hardener were mixed (by weight) in a container in ratio of 100: 40 respectively.

**Fig. 4.9:** Hardener and Epoxy

**Fig. 4.10**: Mixing Of Epoxy and Hardener

After putting the base and hardener in required quantity, the mixture was stirred continuously by manual process as shown in Fig.4.10 so that the mixing takes place in proper manner. If mixing was not done properly the material would not settle well. Also if the ratio of the hardener was more than the pot life of the material would have been lesser. We prepared the amount which was consumed in 20-30 min. otherwise epoxy would have settled in container itself. Approx. 300gms of epoxy was needed to apply to both side of sheet in our case.

### 4.1.4. Applying resin on sheet

The epoxy was applied on sheet using a steel scrapper as shown in Fig.4.11 by carefully spreading it evenly on all sides of sheet. It was made sure that there are no air bubbles present entrapped inside the epoxy applied on sheet otherwise it would create a flaw there. After applying epoxy another sheet is placed in same direction and once again epoxy coating is given to create a laminated sheet. The coat could be applied on other side if required after drying of the specimen. The full curing of sheet was done as shown in Fig.4.12 by leaving it under ambient temperature for at least seven days before processing further.

**Fig 4.11:** Applying resin on sheet

**Fig 4.12:** After resin application

### 4.1.5. Sizing of sheet for specimen and tabs

Once the epoxy was fully cured, we cut the sheet to actual specimen size using the circular saw machine shown in Fig.4.13 which would cut it into required size of 15mm x 500mm as shown in Fig.4.15 for tensile and15mm x 250mm for bending shown in Fig.4.17. After obtaining the long cured strips of the resin coated FRP sheets, the tensile specimen were further tabbed on each side of either ends. The tabs were cut in size of 100mm x 15mm as shown in Fig.4.16 with Treadle shearing machine shown in Fig.4.14.

**Fig. 4.13:** Circular saw

**Fig. 4.14:** Treadle shearing machine

**Fig. 4.15:** Specimen before tab

**Fig 4.16:** Tab specimen

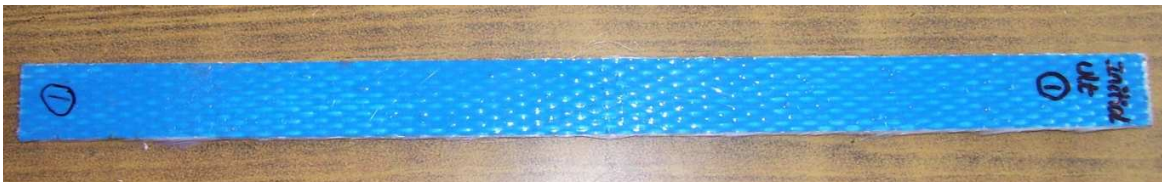

**Fig.4.17: B**ending specimen

### 4.1.6. Placing of tabs on specimen

The specimen had to be tabbed on either side on two ends. We had to again prepare the mixture of epoxy as discussed before and carefully apply it on the either side of specimen. The tabs were now placed on either side of epoxy pasted specimen (with epoxy coated side of tab on upper side). The epoxy would act as binder between tab and actual specimen. Two paper clamps were placed on either tabbed side to hold tabs in place and also to apply pressure while epoxy between them was getting dried as shown in Fig.4.18.

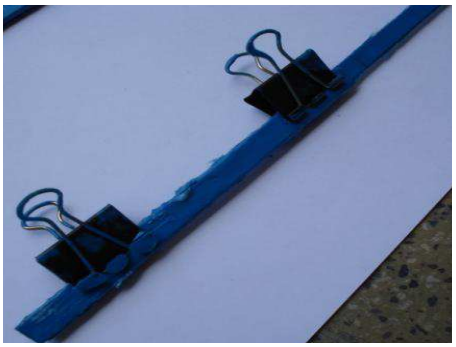

**Fig. 4.18:** Placing of tab

**Fig.4.19:** Tabbed specimen

Once the specimen was dried, paper clamps used to hold tabs in place were removed. Specimen was again cured for 5 days before they were put to any testing. A single specimen finally would have four tabs (in total) on either side of both ends as shown in Fig.4.19. This specimen was ready now for any kind of further testing.

## 4.2. Experimental setup

An experimental setup shown in Fig.4.20 is prepared to carryout accelerated aging tests in order to evaluate the performance of pre-stretched and pre-bended GFRP and CFRP laminated specimen. The field environment similar to tropical climate had been simulated.


**Fig. 4.20**: Experimental setup

The pre-stretched and pre-bended GFRP and CFRP specimen were immersed in a water bath which was maintained at 45$^{o}$C for different time periods under accelerated environmental exposure. The specimen were removed from bath at regular time period for evaluating tensile strength, flexural strength, moisture absorption and SEM images.

### 4.2.1. Setup fabrication

Setup shown in Fig. 4.20 basically consists of

1. Two water baths
2. Heating element
3. RTD sensor
4. Temperature controller
5. Solid state relay

#### 4.2.1.1. Water bath

The experimental setup consists of two water baths shown in Fig.4.21 and Fig.4.22 made up of plastic filled with normal water. One of the baths is maintained at 45$^{o}$C for thermal aging of specimen and the other at normal environment condition to check the natural degradation.


**Fig. 4.21:** Water bath ($T_1$)

**Fig. 4.22:** Natural degradation bath ($T_5$)

#### 4.2.1.3. Heating element

The setup temperature was maintained with the help of heating rod of wattage 1000 kW as shown in Fig.4.23 connected via temperature controller with single phase connection. As temperature reaches to required value the power supply of rod was cut off by temperature controller.


**Fig. 4.23:** Heating element and RTD sensor

**4.2.1.4.** RTD (Resistance Temperature Detector) sensor

One of the water baths was provided with RTD sensor as shown in Fig.4.23. It senses temperature of water bath at given time and input was sent to the controller which controls the system as per set value.

**4.2.1.5.** Temperature controller

For thermal aging of specimen the water bath was maintained at specified temperature, temperature controller was connected with the bath along with relay cutoff as shown in Fig.4.24.

Proportional-integral-derivative (PID) control was used to maintain the temperature. On the controller display we had to feed the “Set Value” of temperature indicated in green and the “Process Value” of temperature would be indicated in the red, which was the output from the RTD sensor. First time we had to set the controller to auto-tune mode so that it could adjust itself according to the input variables. Once the bath had attained the set value the controller cuts off its supply and after sometime it senses the temperature had gone below set value it again starts heating to obtain set value.

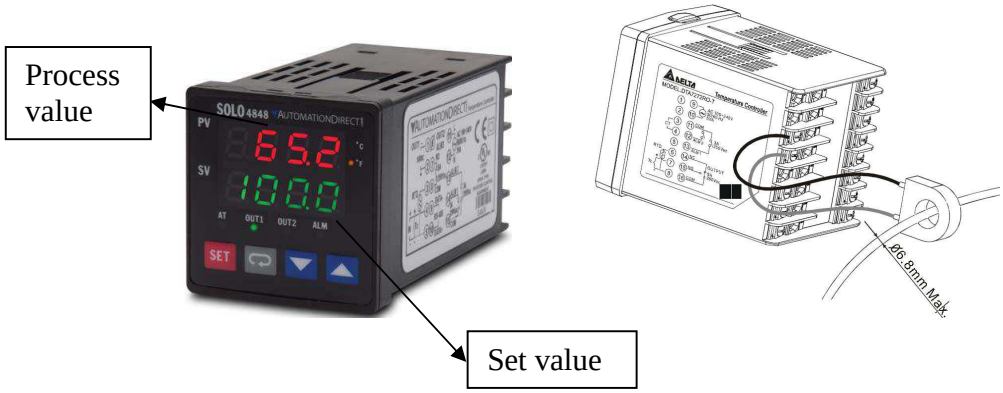


**Fig. 4.24:** Temperature controller

The connections of controller are shown below in the Fig.4.25 as given by its manufacturer. It consists of terminals named with different numbers. Each terminal is having specific input or output requirements. Terminal 1 and 2 here were connected to the power supply of 220Volts with live at 1 and neutral at 2. The relay was connected to the terminals at 3 & 4 with respective positive and negative connections. The live terminal of the heating element was connected to the T1 terminal of the relay and neutral was connected to the power input. The RTD Sensor was connected to the terminals 7, 8 & 9 as shown in circuit diagram.

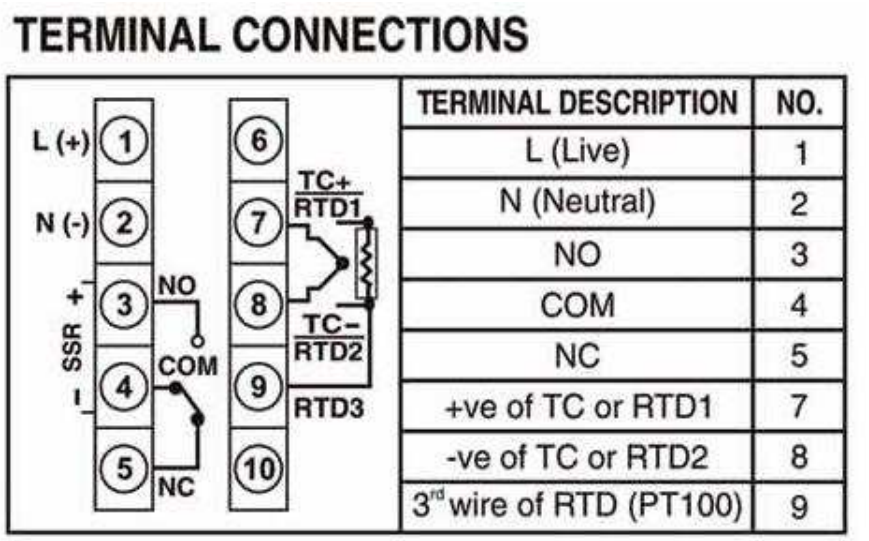


**Fig. 4.25:** Circuit diagram of connections

The temperature controller was needed to be secured at some place so we fabricated a display panel out of wood. The front face was provided with four holes of the size of the controller outer cover specifications i.e. 48 X 48mm. The difference of about 200mm was kept within back of controller and the wall it was attached. The distance was kept more so as to provide accessibility as well as good air circulation to dispose of heat generated as shown in Fig.4.26.

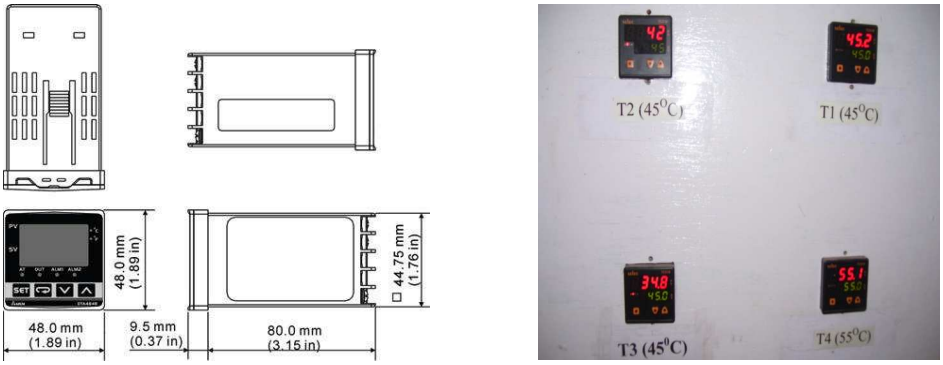


**Fig. 4.26:** Temperature display panel

**4.2.1.6.** Solid State Relays (SSR)

The solid state relay shown in Fig.4.27 was required to break the circuit in case of overloading. It controlled the switching of the heating element and acted as a switch. It helped in protecting controller for any kind of overload or short circuiting.


**Fig. 4.27:** Solid state relay

## 4.3. Testing Methods used in Experimentation

### 4.3.1. Tensile testing

**Fig. 4.28:** UTM testing machine

**Fig. 4.29:** Specimen in jaws

A Universal Tensile testing machine shown in Fig.4.28 and Fig.4.29 was used for the testing of the FRP specimen for its tensile strength. The test specimen had been prepared according to ASTM-D-3790 standard. The initial pre-stretching of specimen was done and all the pre-stretched specimen were tested until they break indicating the peak load and ultimate stress value they can bear at required time period to estimate the degradation in the same machine.

### 4.3.2. Three point bending test

Three point bending tests of hygrothermally treated specimen were carried out in using instron as shown in Fig.4.30 and Fig.4.31. The test specimen had been prepared according to ASTM-D-790 standard. The three point bend test results can be taken as indications of strength degradation of composites after they had been hygrothermally treated.


**Fig. 4.30:** Three point bend test machine

**Fig. 4.31:** Specimen positioning

### 7.3.3. Capacitance Test


**Fig. 4.32:** LCR meter

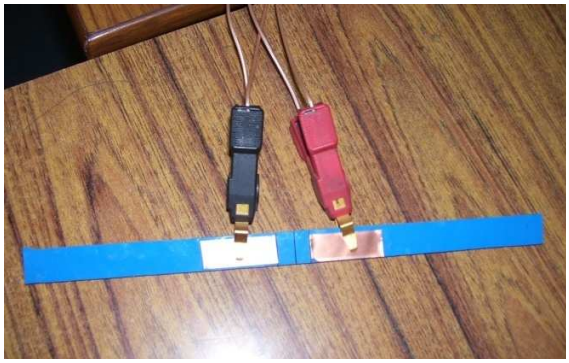

**Fig. 4.33:** Specimen with terminals attached

The capacitance and impedance readings of the specimen by using RCL meter as shown in Fig.4.32. The frequency had been varied from 50Hz to 1MHz and voltage is 1V. This capacitance and impedance readings were used to relate the moisture absorption rate with capacitance. For this copper strips were used to create magnetic field in the specimen as shown in Fig.4.33 and capacity reading through the thickness were obtained.

### 4.3.4. Micro hardness test

**Fig. 4.34:** Display of indent

**Fig. 4.35:** Micro hardness equipment

Micro hardness test (shown in Fig.4.35)' of specimen were taken in order to estimate the hardness of specimen before and after thermal treatment of the specimen. The load applied was 200gm and VHN values were determined by applying this load by using a calibration distance of 50 units in quantinet software as shown in Fig.4.34 used for image analysing. The dwell time used during load application was 20 seconds. An indent is formed in diamond shape as shown in Fig.4.36, used for calculating VHN as shown in figure below.

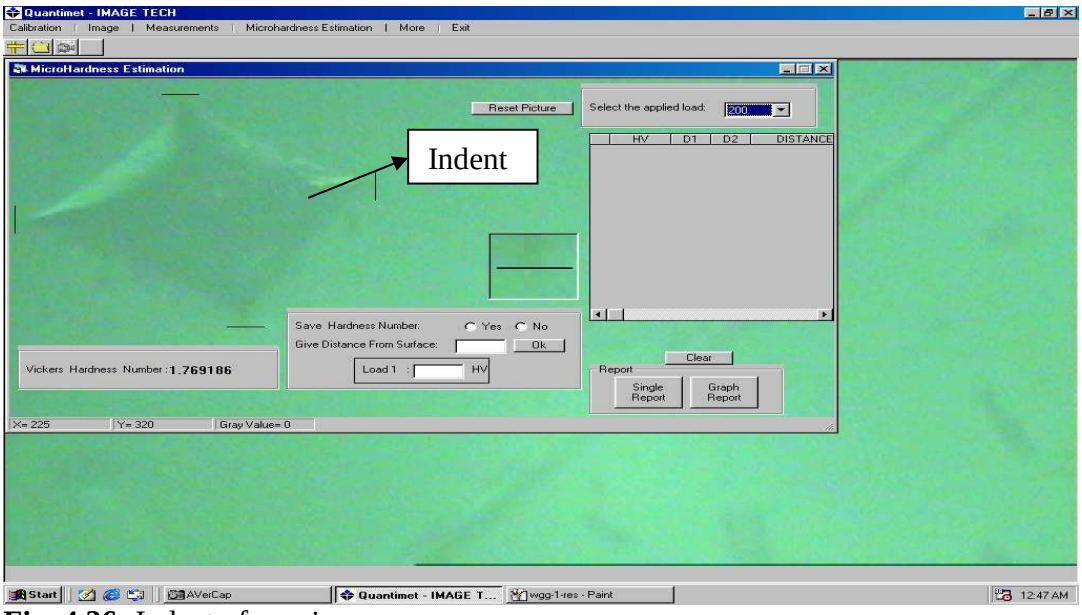


**Fig. 4.36:** Indent of specimen

### 4.3.5. SEM (Scanning Electron Microscope)


**Fig. 4.37:** Gold coating equipment

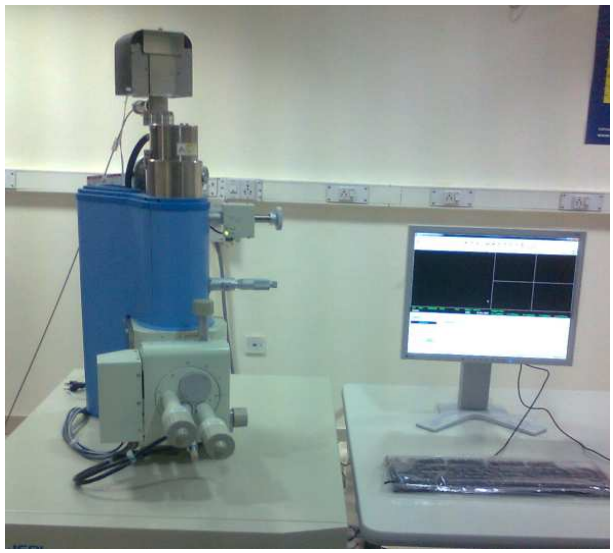

**Fig. 4.38:** SEM machine

Scanning electronic microscope shown in Fig.4.38 was used to test FRP specimen microstructure. The dimensioning of specimen was done according to block size of machine. The polishing of specimen was done by using Gold coating equipment as shown in the Fig.4.37. The polished specimen was used to estimate the microstructure of specimen at magnification factor of 2000X and 1500X.

After microstructure estimatmation image analyser test was carried out in order to find circularity of fibre, area fraction, and change in microstructure of specimen before and after hygrothermal treatment.

## 4.4. Percentage Weight Gain and Apparent Moisture diffusivity Calculation

Weight gain of the preconditioned specimen was carefully monitored by weighing multiple specimen periodically, with precautions taken to remove the surface moisture by wiping them before weighing. Percentage weight gain was determined as

$$M = \frac{(weight\ of\ the\ specimen) - (weight\ of\ the\ dry\ specimen)}{weight\ of\ the\ dry\ specimen} \times 100$$

Assuming that the moisture absorption process follows Fick's law, the apparent moisture diffusivity, D, can be determined as,

$$D = \pi\left(\frac{h}{4Mm}\right)^2 \left(\frac{M2 - M1}{\sqrt{t2} - \sqrt{t1}}\right)^2 \left(1 + \frac{h}{Le} + \frac{h}{w}\right)^{-2}$$

Where,

Le = length of the specimen
W = width of the specimen
M1 = moisture content at time t1
M2 = moisture content at time t2
Mm = % weight gain

Here,

Le = 250mm (Bending)
Le = 500mm (Tensile)
W = 15mm
Mm = percentage weight gain of specimen calculated by using the equation M.

## 4.5. Test matrices

**Table 4.1:** initial testing specimen

| **Specimen name** | **No. of specimen** | | **Total specimen** |
|---|---|---|---|
| | **tensile** | **bending** | |
| CFRP | 4 | 4 | 8 |
| GFRP | 4 | 4 | 8 |
| Total specimen | | | 16 |

**Table 4.2:** Test matrix (natural degradation)

| **Test type** | **Specimen type** | **Bath name** | **Holding time** | **No. of specimen for pre-stretching and pre-bending** | | | | **no.of specimen for final testing** | **Total specimen** |
|---|---|---|---|---|---|---|---|---|---|
| | | | | **30%** | **50%** | **70%** | **Without load** | | |
| bending | CFRP | T6 | 1month | 1 | 1 | 1 | 1 | 4 | 4 |
| | | | 2months | 1 | 1 | 1 | 1 | 4 | 4 |
| | GFRP | | 1month | 1 | 1 | 1 | 1 | 4 | 4 |
| | | | 2months | 1 | 1 | 1 | 1 | 4 | 4 |
| tensile | CFRP | | 1month | 1 | 1 | 1 | 1 | 4 | 4 |
| | | | 2months | 1 | 1 | 1 | 1 | 4 | 4 |
| | GFRP | | 1month | 1 | 1 | 1 | 1 | 4 | 4 |
| | | | 2months | 1 | 1 | 1 | 1 | 4 | 4 |
| **Total specimen** | | | | | | | | | 32 |

**Table 4.3:** Test matrix (for accelerated aging)

| **Test type** | **Specimen type** | **Bath name** | **Holding time** | **No. of specimen for pre-stretching and pre-bending** | | | | **no. of specimen for final testing** | **Total specimen** |
|---|---|---|---|---|---|---|---|---|---|
| | | | | **30%** | **50%** | **70%** | **Without load** | | |
| bending | CFRP | T2 | 1month | 3 | 3 | 3 | - | 9 | 9 |
| | | | 2months | 3 | 3 | 3 | - | 9 | 9 |
| | GFRP | | 1month | 3 | 3 | 3 | - | 9 | 9 |
| | | | 2months | 3 | 3 | 3 | - | 9 | 9 |
| tensile | CFRP | | 1month | 3 | 3 | 3 | - | 9 | 9 |
| | | | 2months | 3 | 3 | 3 | - | 9 | 9 |
| | GFRP | | 1month | 3 | 3 | 3 | - | 9 | 9 |
| | | | 2months | 3 | 3 | 3 | - | 9 | 9 |
| Weight gain (bending) | CFRP | | 10days | 1 | 1 | 1 | 1 | 4 | 4 |
| | | | 20days | 1 | 1 | 1 | 1 | 4 | 4 |
| | | | 30days | 1 | 1 | 1 | 1 | 4 | 4 |
| | | | 40days | 1 | 1 | 1 | 1 | 4 | 4 |
| | GFRP | | 10days | 1 | 1 | 1 | 1 | 4 | 4 |
| | | | 20days | 1 | 1 | 1 | 1 | 4 | 4 |
| | | | 30days | 1 | 1 | 1 | 1 | 4 | 4 |
| | | | 40days | 1 | 1 | 1 | 1 | 4 | 4 |
| Weight gain (tensile) | CFRP | | 10days | 1 | 1 | 1 | 1 | 4 | 4 |
| | | | 20days | 1 | 1 | 1 | 1 | 4 | 4 |
| | | | 30days | 1 | 1 | 1 | 1 | 4 | 4 |
| | | | 40days | 1 | 1 | 1 | 1 | 4 | 4 |
| | GFRP | | 10days | 1 | 1 | 1 | 1 | 4 | 4 |
| | | | 20days | 1 | 1 | 1 | 1 | 4 | 4 |
| | | | 30days | 1 | 1 | 1 | 1 | 4 | 4 |
| | | | 40days | 1 | 1 | 1 | 1 | 4 | 4 |
| **Total specimen** | | | | | | | | | 136 |

**Table 4.4:** Test matrix (for weight gain specimen)

| Test type | Specimen type | Bath name | Holding time | No. of specimen for pre-stretching and pre-bending | | | | no. of specimen for final testing | Total specimen |
|---|---|---|---|---|---|---|---|---|---|
| | | | | 30% | 50% | 70% | Without load | | |
| Weight gain (bending) | CFRP | T2 | 3days, 6days, 9days& 12days | 1 | 1 | 1 | 1 | 4 | 4 |
| | GFRP | | 3days, 6days, 9days& 12days | 1 | 1 | 1 | 1 | 4 | 4 |
| Weight gain (tensile) | CFRP | | 3days, 6days, 9days& 12days | 1 | 1 | 1 | 1 | 4 | 4 |
| | GFRP | | 3days, 6days, 9days& 12days | 1 | 1 | 1 | 1 | 4 | 4 |

In above experiment according to the planned test matrix numbers of specimen were estimated initially as 200. The tensile test of actual specimen was first conducted on a Universal Testing Machine to determine the actual failure load (peak load) the specimen can bear. On basis of that failure load the loading weight for specimen was calculated. The first set of specimen which would be stretched and bended to 30%, 50%& 70% of failure load and at temperature variation of 45$^{o}$C would be taken out of bath after a time of 1 & 2 months and would be checked for its tensile strength and flexural strength. One failed specimen under each load would also be tested for micrograph shown in Table 4.1 and Table 4.3.

The natural degradation specimen was kept at ambient conditions for a period of 1& 2 months shown in Table 4.2. After that they would also be tested in similar manner. The weight specimen tested shown in Table 4.4 for capacitance and moisture rate at regular time periods. The micro hardness readings of all specimen were taken at required time periods.

# CHAPTER-5
# RESULTS AND DISCUSSIONS

## 5.1. Macroscopic Behavior

The parameters discussed are flexural strength, flexural modulus, tensile strength, tensile modulus, percentage weight gain, capacitance, moisture diffusivity.

**Holding parameters:**

- Normal Water bath ($T_2$)
- $T_2$ bath Temperature: 45$^o$C
- Water bath ($T_5$) at natural condition
- $T_5$ bath temperature: Room temperature

### 5.1.1. Mode of Failure (Macroscopic Visual Observations)

As per the visual observation the initial specimen (Fig.5.1) had fine shiny epoxy coating and the failure of specimen under uniaxial tensile load showed a broom type failure due to typical sudden and violent release of stored elastic energy as shown in Fig.5.2. The specimen under bending load showed a crack at the middle of GFRP specimen where as CFRP specimen has no crack during initial bending.

After 1 month of exposure of specimen in water baths there was heavy visible scale formation (Fig 5.3) on the entire specimen of water bath ($T_2$) when compared to water bath ($T_5$). Surface observation showed that a thin layer of salt is deposited on surface. But still specimen showed considerable strength and flexibility on bending. Broom type failure was visible in GFRP specimen and abrupt failure in case of CFRP specimen during tensile test as shown in Fig.5.4. While in case of bending, hair line cracks were generated at the middle of the specimen of both GFRP and CFRP.

After 2 months of natural exposure in water bath ($T_5$) degradation observation and scaling (Fig.5.5) was comparatively low as compared to water tank $T_2$ maintained at 45$^o$C. The second month degradation of specimen in tank $T_5$ was more visible as compared to first month observations.

For 2 months of hygrothermal exposure in water bath $T_2$ observations of heavy degradation of fibre and scaling were noted as compared to first month specimen. Clean Abrupt failure like cleavage edge was visibly observed as shown in Fig.5.6. The specimen had lost their flexibility completely and was easily broken by slight bending with hands as compared to one month exposed specimen. Abrupt failure had occurred in both CFRP and GFRP specimen during tensile. In case of bending, the hair line cracks were clearly visible at the point where load is applied.

### 5.1.1.1. Initial specimen images before start of experimentation

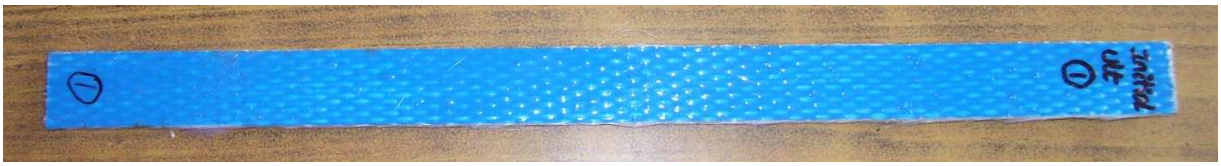

**a)**

**b)**

**Fig. 5.1:** a) Bending specimen b) Tensile specimen

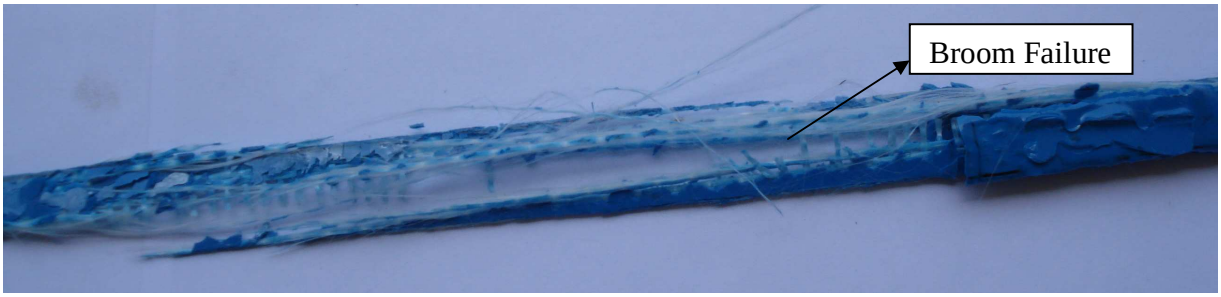


**a)**

**b)**

**Fig. 5.2:** Failure of a) GFRP b) CFRP laminates of initial specimen

### 5.1.1.2. Specimen after one month of degradation

**a)**

**b)**

**Fig. 5.3**: Scaling of a) CFRP b) GFRP laminates after one month

**a)**

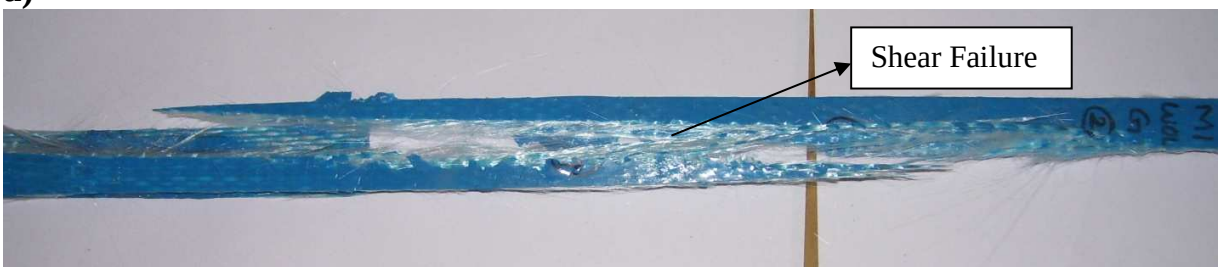


**b)**

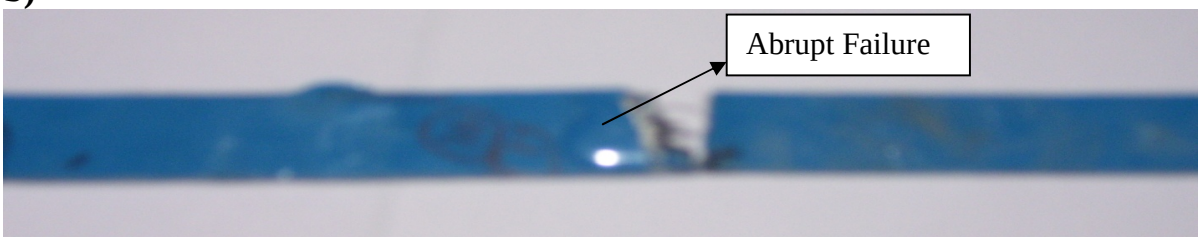


**c)**

**Fig. 5.4:** Failure of a) CFRP b) GFRP laminates after one month

### 5.1.1.3. Specimen after two months of degradation

**a)**

**b)**

**Fig. 5.5:** Scaling of a) CFRP b) GFRP laminates after two months

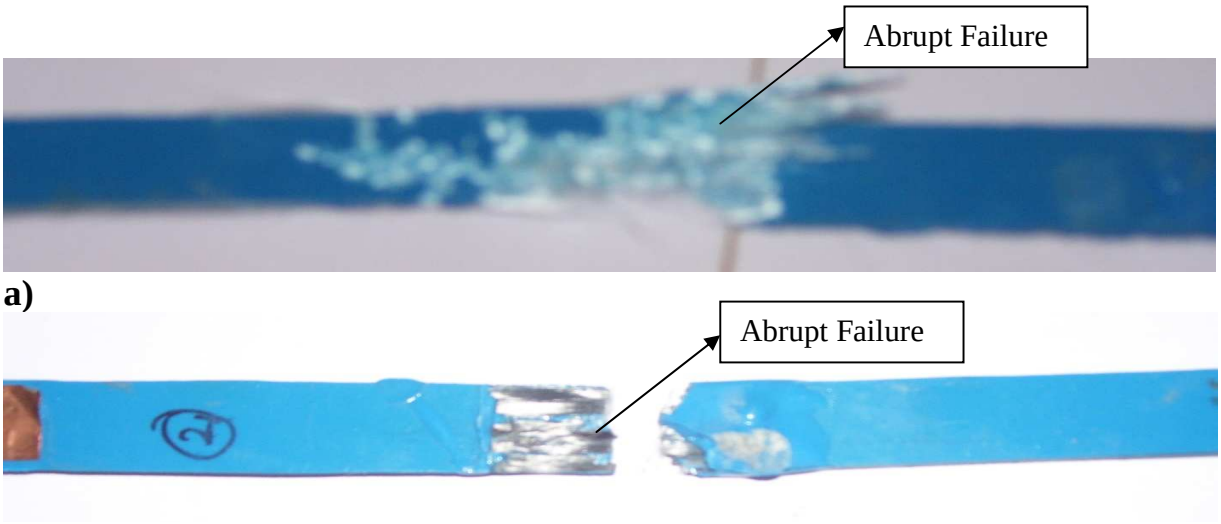


**Fig. 5.6:** Failure of a) CFRP b) GFRP laminates after two months

### 5.1.2. Bending test results of laminated specimen

**5.1.2.1.** Initial graphs of bending specimen before experiment

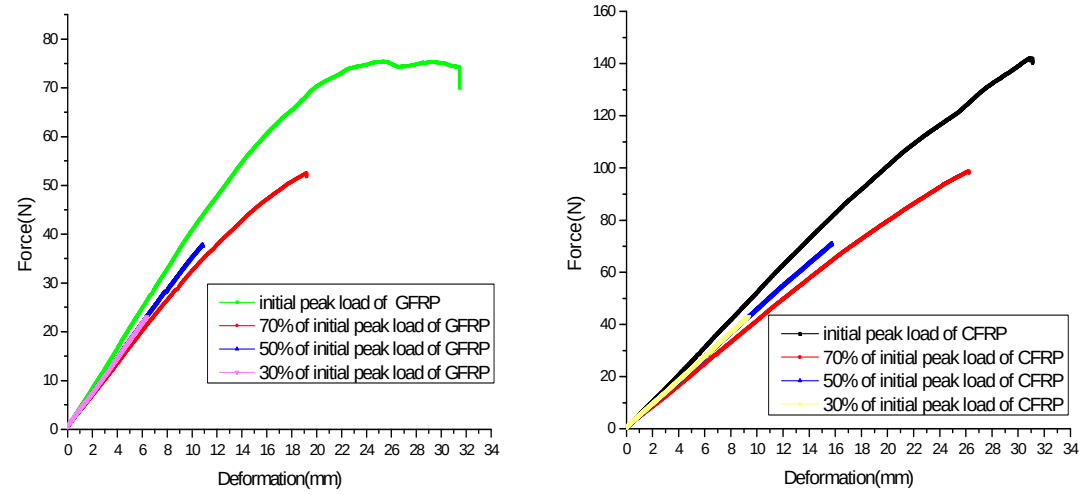


a) b)

**Fig. 5.7:** Initial graphs of **a)** GFRP at various loads b**)** CFRP at various loads

The initial peak loads of both GFRP and CFRP from graphs were calculated to estimate strength degradation of specimen after hygrothermal treatment. The peak loads shown in 70%UFL, 50%UFL, 30%UFL graphs were pre-bended specimen loads as shown in Fig.5.7.

### 5.1.2.2. Bending test results of water tank ($T_2$) for two months

The following results of bending specimen kept at 45°C were depicted as follows

**5.1.2.2.1**. Bending graphs of specimen loaded at 30%UFL

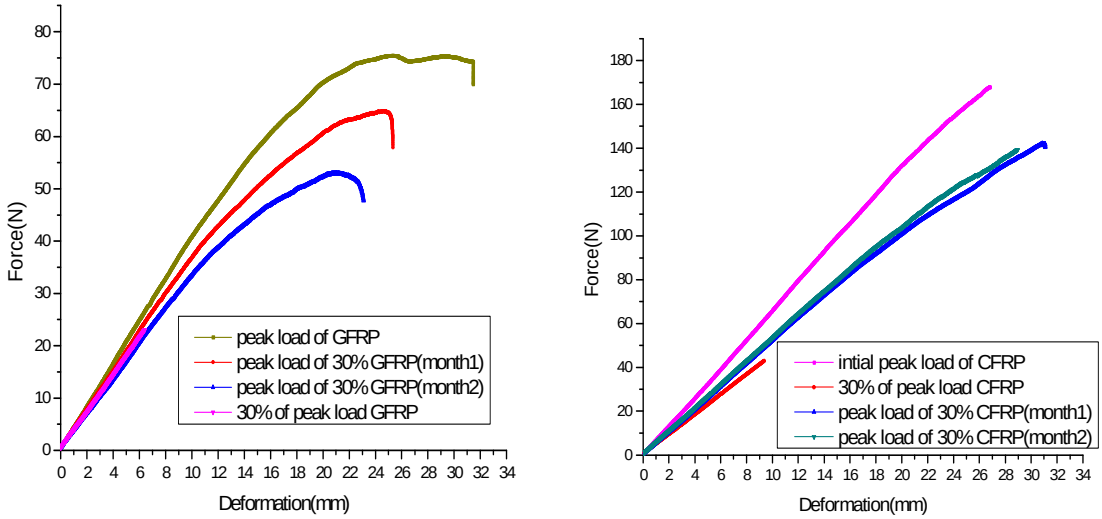


a) b)

**Fig. 5.8:** Peak load graph of a) GFRP 30% UFL b) CFRP 30% UFL

**5.1.2.2.2.** Bending graphs of specimen loaded at 50%UFL

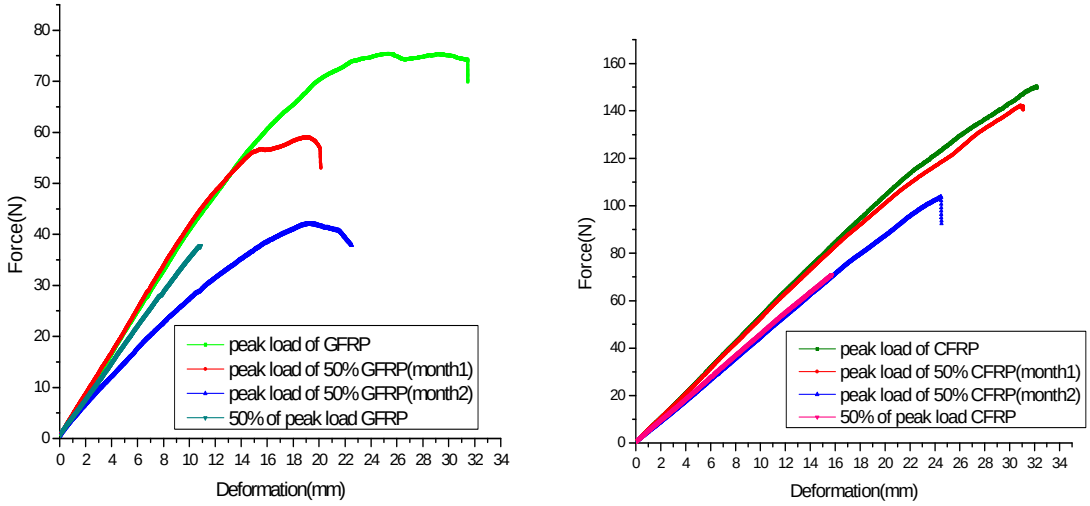


a) b)

**Fig. 5.9:** Peak load graph of a) GFRP 50% UFL b) CFRP 50% UFL

**5.1.2.2.3.** Bending graphs of specimen loaded at 70%UFL

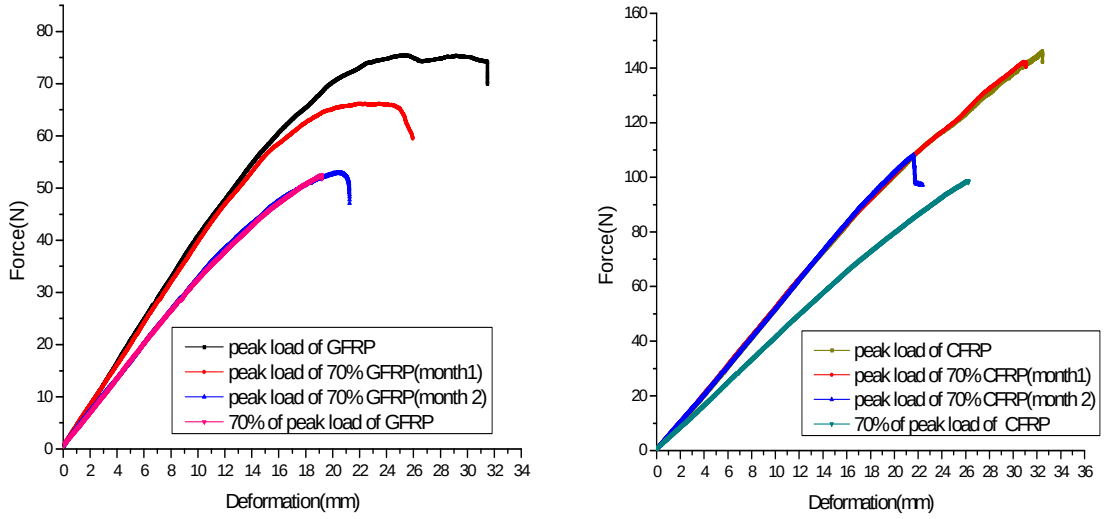


a) b)

**Fig. 5.10:** peak load graph of a) GFRP 70% UFL b) CFRP 70% UFL

From the above Fig.5.8 to Fig.5.10 we came to know that the peak loads of GFRP and CFRP laminates were decreasing from first month to second month. When compared with initial, second month specimen have considerable decrease in peak load. The Flexural strength and Flexural modulus of laminated composites after and before hygrothermal treatment had decreased as shown in the Table 5.1 and Table 5.2.

**Table 5.1:** Percentage decrease in flexural strength of GFRP laminates at various loads

| Specimen name | Flexural load(N) | Flexural strength(MPa) | Flexural modulus(MPa) | %Decrease in strength |
|---|---|---|---|---|
| initial GFRP | 75.4 | 168 | 20300 | 0 |
| GFRP 30% loading(month 1) | 64.4 | 144 | 18200 | 14.3 |
| GFRP 30% loading(month 2) | 53.0 | 118 | 16400 | 29.8 |
| GFRP 50% loading(month 1) | 59.0 | 131 | 20300 | 22.02 |
| GFRP 50% loading(month 2) | 42.1 | 93.5 | 13600 | 44.3 |
| GFRP 70% loading(month 1) | 66.1 | 147 | 19200 | 12.5 |
| GFRP 70% loading(month 2) | 52.9 | 118 | 15800 | 29.8 |

**Table 5.2:** Percentage decrease in Flexural strength of CFRP laminates at various loads

| Specimen name | Flexural load(N) | Flexural strength(MPa) | Flexural Modulus(MPa) | %Decrease in strength |
|---|---|---|---|---|
| initial CFRP | 151.0 | 162 | 10900 | 0 |
| CFRP 30% loading(month 1) | 142.2 | 152 | 8540 | 6.17 |
| CFRP 30% loading(month 2) | 141.1 | 151 | 8390 | 6.79 |
| CFRP 50% loading(month 1) | 150.5 | 161 | 8510 | 0.62 |
| CFRP 50% loading(month 2) | 103.8 | 111 | 7050 | 31.5 |
| CFRP 70% loading(month 1) | 146.3 | 157 | 8230 | 3.09 |
| CFRP 70% loading(month 2) | 108.0 | 116 | 8110 | 28.4 |

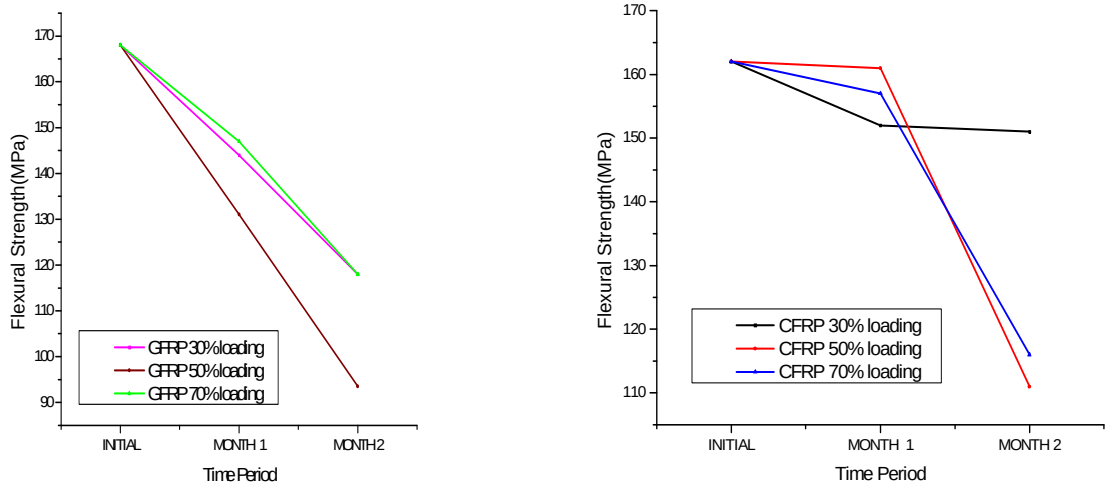


a) b)

**Fig. 5.11:** Graph for ultimate flexural strength of a) GFRP laminates b) CFRP laminates

The trend of decrease in ultimate flexural strength of GFRP and CFRP were shown in Fig. 5.11. The flexural strength reduction in bath T2 was nearly same after one month with few exceptions. Noticeable change in strength was seen after two months, ranging from 25 to 45% mainly where as the reduction in one month seems to be between 10to 25% mainly in case of GFRP and for CFRP % decrease in second month ranges between 10 to 30%. The reason for decrease in ultimate flexural strength and change in percentage flexural strength seems to be the continuous degradation done by hygrothermal load which affected the epoxy and fibre strength.

The flexural strength of 50% UFL GFRP specimen reduced more when compared to other loaded specimen. The 30% UFL and 70% UFL specimen have almost same reduction in flexural strength after two months.

The flexural strength of 30% UFL CFRP specimen reduction is almost same after one month. The 50% UFL specimen has more reduction in flexural strength.

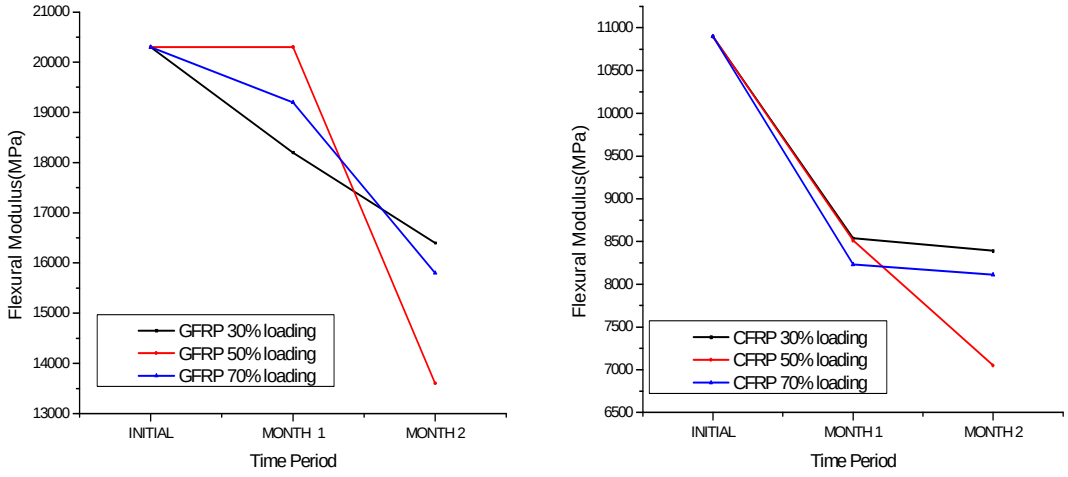


a) b)

**Fig. 5.12**: Graph for ultimate flexural modulus of a) GFRP laminates b) CFRP laminate

The flexural modulus with time is decreasing in all specimen. The 50% UFL GFRP specimen has flexural modulus almost same up to one month and sudden drop in flexural modulus is observed from the Fig. 5.12 which was depicted using the Table 8.1.the flexural modulus of 50% UFL CFRP specimen had reduced as shown in Fig. 5.12.

### 5.1.2.3. Bending test results of natural degradation specimen for two months

**5.1.2.3.1.** Bending graphs of specimen loaded at 30%UFL

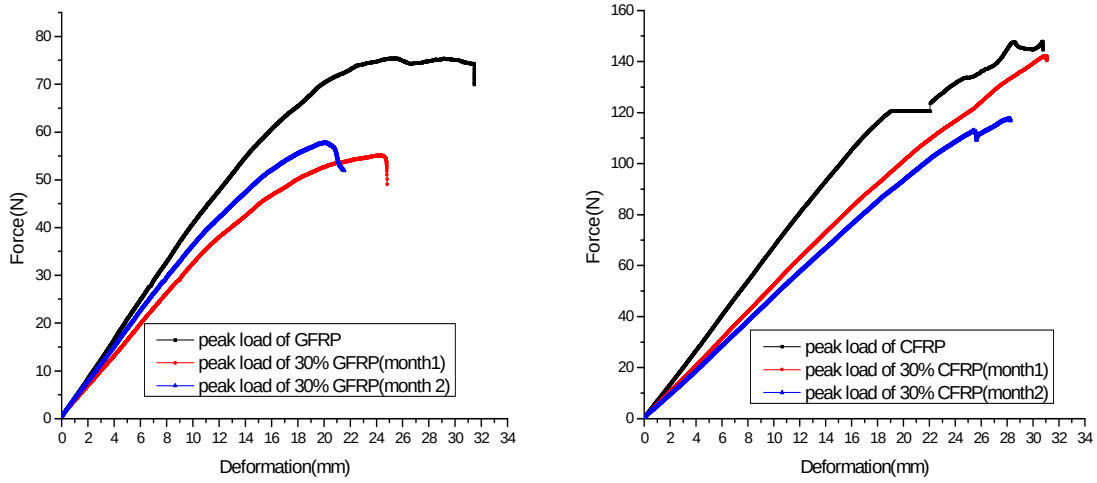


a) b)

**Fig. 5.13:** Peak load graph of a) GFRP 30% UFL b) CFRP 30% UFL

**5.1.2.3.2.** Bending graphs of specimen loaded at 50%UFL

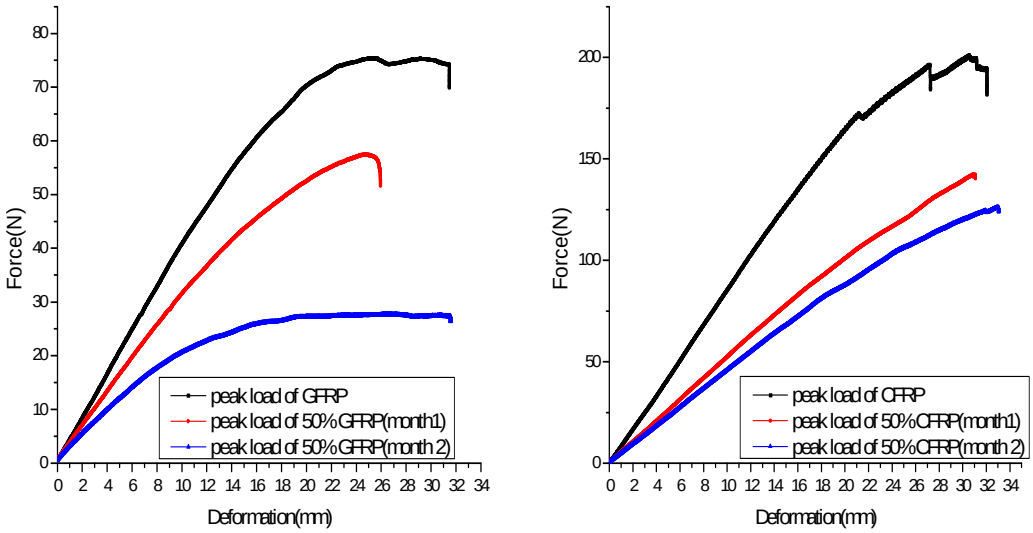


a) b)

**Fig. 5.14**: Peak load graph of a) GFRP 50% UFL b) CFRP 50% UFL

**5.1.2.3.3.** Bending graphs of specimen loaded at 70%UFL

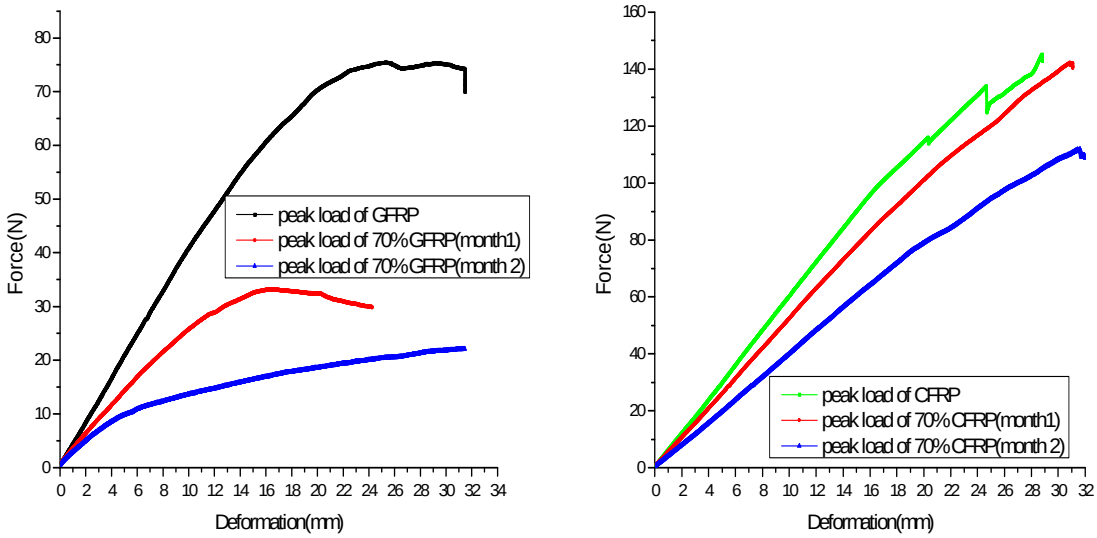


a) b)

**Fig. 5.15:** Peak load graph of a) GFRP 70% UFL b) CFRP70% UFL

### 5.1.2.3.4. Bending graphs of specimen at without load

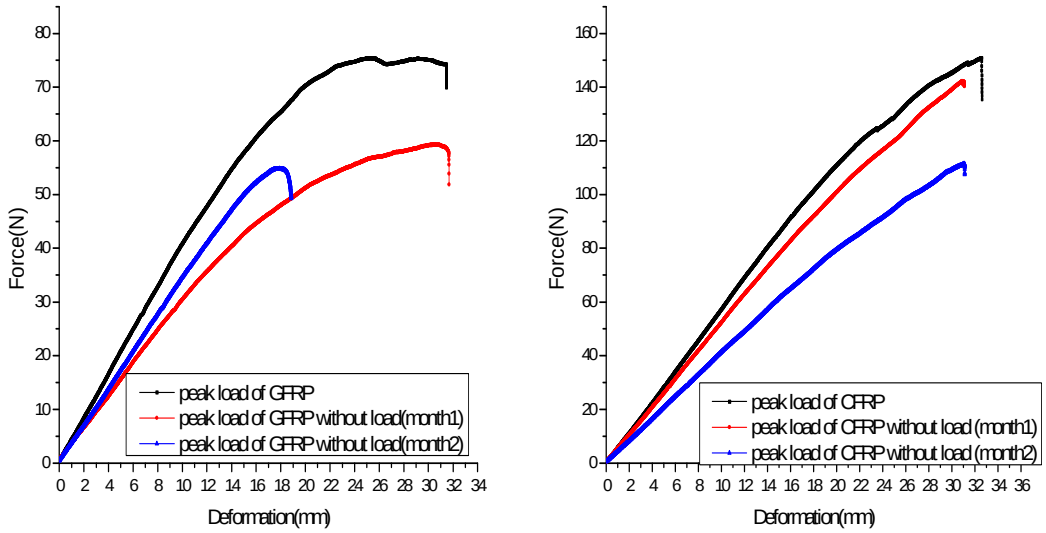


a) b)

**Fig. 5.16**: Peak load graph of a) without load GFRP b) without load CFRP

From the Fig. 5.13, Fig. 5.14, Fig. 5.15 and Fig. 5.16 we came to know that the peak loads of GFRP and CFRP laminates composites were decreasing from first month to second month. When compared with initial, second month specimen have considerable decrease. It was noticed that degradation of specimen kept at room temperature was less when compared to thermally aged specimen. The flexural strength and flexural modulus of laminated composites after and before natural treatment had been decreased as shown in the Table 5.3.

**Table 5.3:** Percentage Decrease in Flexural Strength of GFRP at Various Loads

| Specimen name | Flexural load(N) | Flexural strength(MPa) | Flexural modulus(MPa) | % Decrease in strength |
|---|---|---|---|---|
| initial GFRP | 75.4 | 168 | 20300 | 0 |
| GFRP 30% loading(month 1) | 55.1 | 128 | 18000 | 23.81 |
| GFRP 30% loading(month 2) | 57.7 | 122 | 15700 | 27.4 |
| GFRP 50% Loading(Month1) | 57.4 | 128 | 15600 | 23.81 |
| GFRP 50% loading(month 2) | 27.7 | 61.6 | 10800 | 63.3 |
| GFRP 70% loading(month 1) | 33.2 | 73.7 | 13000 | 56.13 |
| GFRP 70% loading(month 2) | 22.1 | 49.2 | 7900 | 70.7 |
| GFRP without load(month 1) | 59.3 | 132 | 14800 | 21.4 |
| GFRP without load(month 2) | 54.8 | 122 | 16800 | 27.4 |

**Table 5.4**: Percentage decrease in flexural strength of CFRP at various loads

| Specimen name | Flexural load(N) | Flexural strength(MPa) | Flexural Modulus(MPa) | %Decrease in strength |
|---|---|---|---|---|
| initial CFRP | 151 | 162 | 10900 | 0 |
| CFRP 30% loading(month1) | 148.0 | 159 | 9200 | 1.85 |
| CFRP 30% loading(month2) | 117.7 | 126 | 7530 | 22.2 |
| CFRP 50% loading(month1) | 140.2 | 150 | 8334 | 7.41 |
| CFRP 50% loading(month2) | 126.1 | 135 | 7410 | 16.7 |
| CFRP 70% loading(month1) | 145.1 | 156 | 9610 | 3.7 |
| CFRP 70% loading(month2) | 111.8 | 120 | 6350 | 25.93 |
| CFRP without load(month1) | 142.2 | 151 | 8540 | 6.79 |
| CFRP without load(month2) | 111.6 | 120 | 6610 | 25.93 |

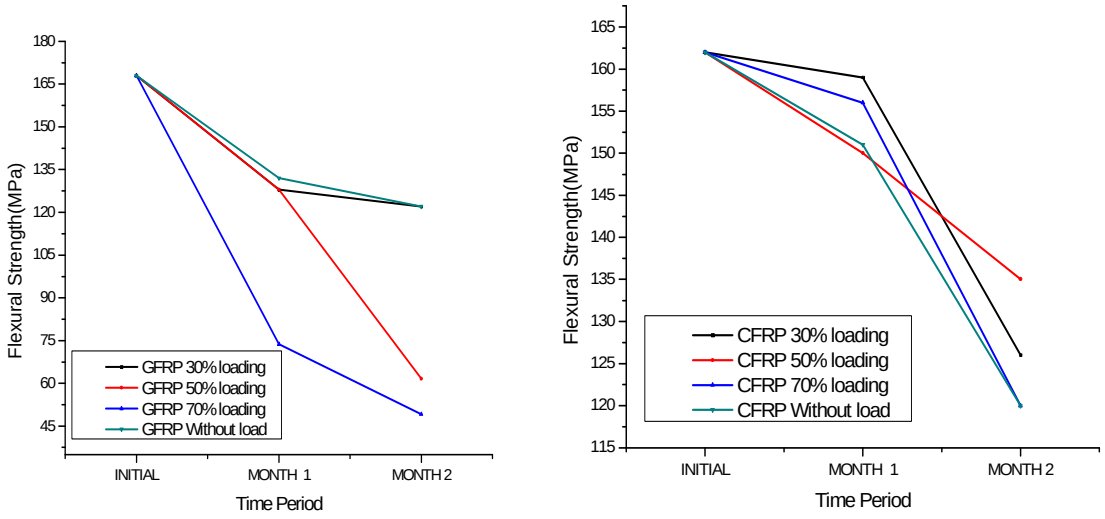


a) b)

**Fig. 5.17**: Graph for ultimate flexural strength of a) GFRP laminates b) CFRP laminates

The trend of decrease in ultimate flexural strength was shown in Fig.5.17 and Fig. 5.18. The flexural strength reduction in T5 tank seems to be nearly same after one month with few exceptions. But when comparing the reduction of strength after one month with respect to reduction after two months there was noticeable change ranging from 10 to 25% mainly for one month where as the reduction in two months seems to be between 25 to 45% in GFRP and 17 to 25% in case of CFRP mainly. The reason for decrease in ultimate flexural strength and change in percentage flexural strength seems to be the continuous degradation done by hygrothermal load which affected the epoxy and fibre strength.

The decrease in flexural strength of 30% UFL and without load GFRP specimen is almost same after two months where as the reduction in flexural strength of CFRP specimen were almost same and decrease is regular.

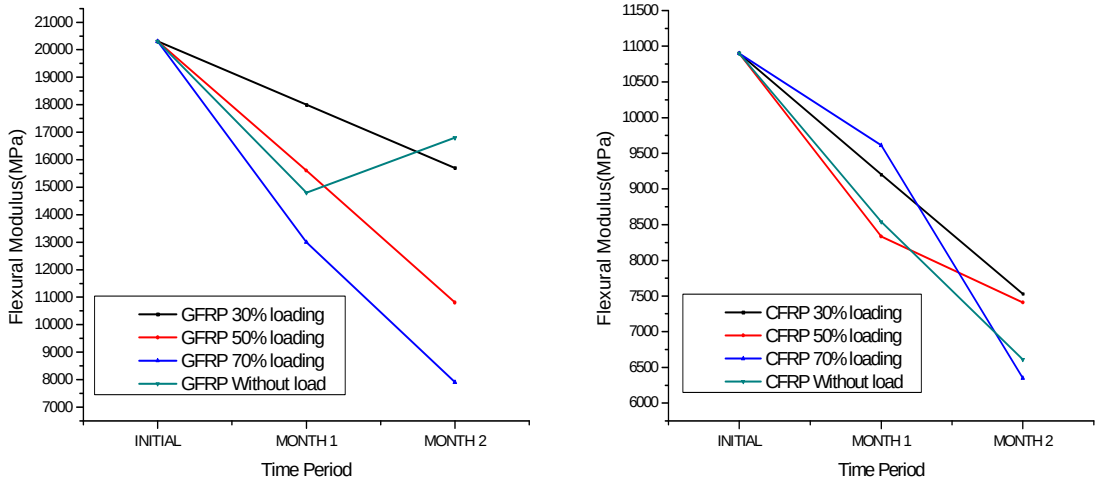


a) b)

**Fig. 5.18**: Graph for ultimate flexural modulus of a) GFRP laminates b) CFRP laminates

The flexural modulus of GFRP without loaded specimen decreased up to one month and increased after one month as shown in Fig. 5.18.but all other loaded specimen flexural modulus is decreasing regularly. The CFRP specimen has sudden reduction in flexural modulus after one month as shown in Fig. 5.18.

### 5.1.2.3.5. Percentage weight gain results of laminated bending composites

The weight gain graphs of GFRP and CFRP laminates were depicted using table 5.5.

**Table 5.5:** Percentage weight gain in GFRP laminated specimen

| Time period | GFRP 30%loading | GFRP without load | GFRP 70%loading | GFRP 50%loading |
|---|---|---|---|---|
| 3 | 9.58 | 9.78 | 9.48 | 9.25 |
| 6 | 10.51 | 10.57 | 9.26 | 10.00 |
| 9 | 11.13 | 10.60 | 11.97 | 9.88 |
| 10 | 9.14 | 8.88 | 8.95 | 10.29 |
| 12 | 12.17 | 12.97 | 13.43 | 11.50 |
| 20 | 14.37 | 16.81 | 14.22 | 14.69 |
| 30 | 14.01 | 16.34 | 17.20 | 17.65 |
| 40 | 16.58 | 16.85 | 19.35 | 18.11 |
| 50 | 14.15 | 20.06 | 21.62 | 18.22 |

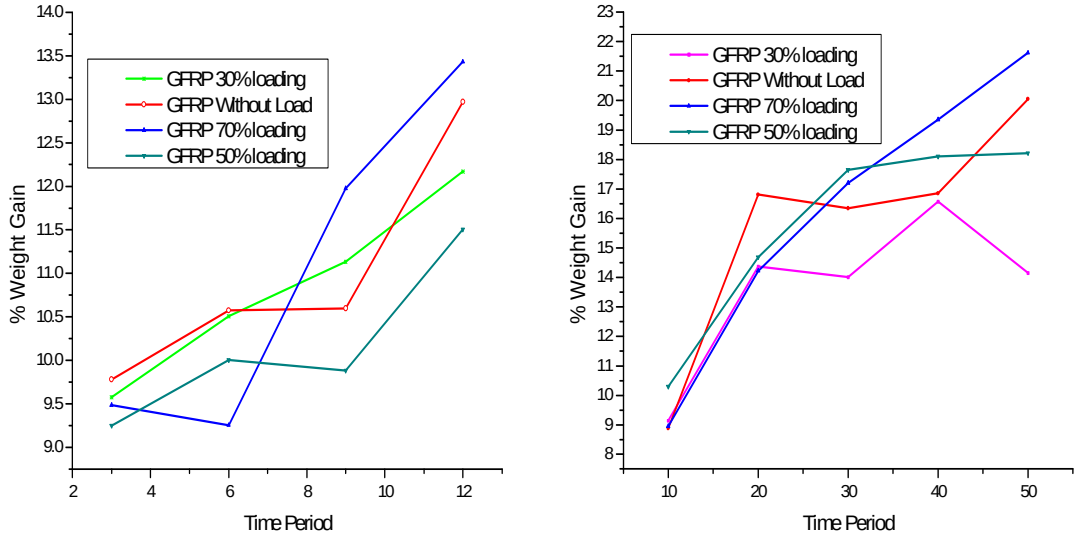


a) b)

**Fig. 5.19**: Percentage weight gain of GFRP laminates a) three days interval b) ten days interval

The percentage weight gain of GFRP and CFRP specimen were increasing as shown in Fig5.19.the percentage weight gain of 70 % UFL GFRP specimen has increased after six days as shown in the Fig. 5.19(a).The percentage weight gain of 30% UFL GFRP specimen after 40 days has decreased and the 50% UFL specimen weight gain is almost linear after 30 days as shown in Fig. 5.19(b).

**Table 5.6:** Percentage weight gain in CFRP laminated specimen

| Time period | CFRP 30%loading | CFRP 50%loading | CFRP 70%loading | CFRP without load |
|---|---|---|---|---|
| 3 | 4.39 | 3.71 | 3.88 | 3.80 |
| 6 | 3.48 | 3.25 | 3.55 | 3.00 |
| 9 | 3.80 | 4.04 | 4.80 | 3.98 |
| 10 | 4.26 | 4.51 | 4.44 | 4.10 |
| 12 | 4.75 | 4.08 | 5.91 | 3.94 |
| 20 | 6.05 | 7.09 | 4.83 | 4.83 |
| 30 | 8.34 | 8.53 | 7.87 | 7.07 |
| 40 | 9.45 | 10.89 | 9.46 | 8.39 |
| 50 | 7.22 | 11.51 | 10.16 | 11.58 |

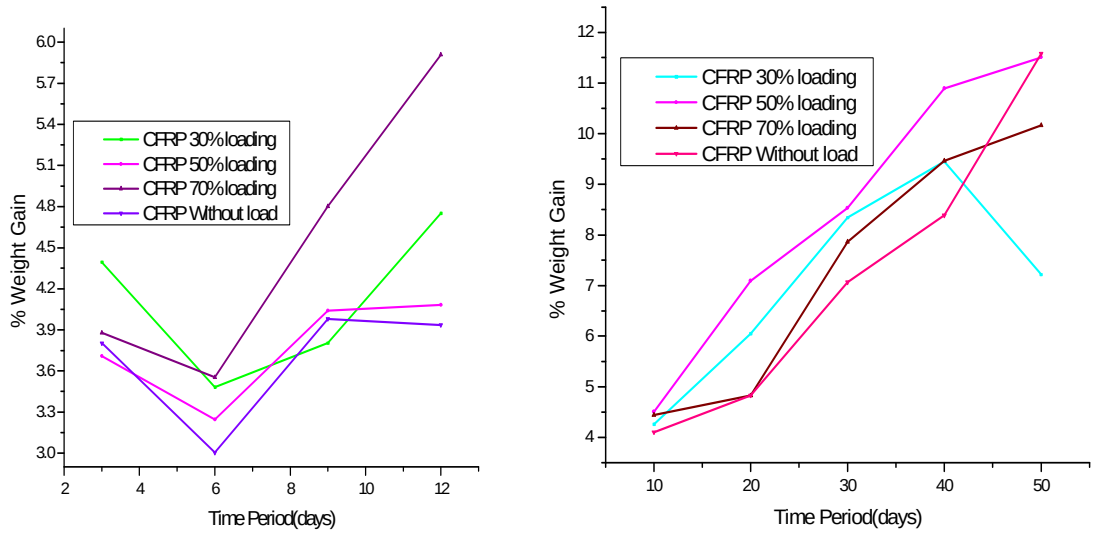


a) b)

**Fig. 5.20:** percentage weight gain of CFRP laminates at a) three days interval b) ten days interval

The above Fig. 5.20 shows percentage weight gain of CFRP specimen at consecutive three days time periods and for specimen at ten days interval.

The percentage weight gain (of moisture) was compared for various loads. It could be easily noticed that in water tanks the percentage weight gain is increasing with respect to time indicating that more moisture is absorbed after two months comparing to first month in almost all the specimen with few exceptions incase of GFRP specimen. The moisture absorption of CFRP specimen is comparatively low so more time is required for CFRP specimen to degrade more as of GFRP.There was marginal increase in weight gain of specimen at 45°c temperature as compared to specimen at normal conditions. The reason for increase in percentage weight gain is obvious that with time the pores of epoxy will loosen due to given hygrothermal load giving way to moisture.

The percentage weight gain after 9days for without loaded and 50% UFL CFRP specimen is linear. The 70% UFL CFRP specimen has sudden increase in percentage weight gain after 6days as shown in Fig. 5.20(a). The 30% UFL CFRP specimen has sudden decrease in percentage weight gain after 40days as shown in Fig. 5.20(b).

### 5.1.2.3.6. Moisture diffusivity results of laminated bending specimen

**Table 5.7:** Moisture diffusivity in GFRP laminated specimen

| Time period | GFRP 30%loading | GFRP without load | GFRP 70%loading | GFRP 50%loading |
|---|---|---|---|---|
| 3 | 0.0113 | 0.0112 | 0.0110 | 0.0109 |
| 6 | 0.0055 | 0.0056 | 0.0055 | 0.0055 |
| 9 | 0.0036 | 0.0037 | 0.0037 | 0.0036 |
| 10 | 0.0063 | 0.0060 | 0.0059 | 0.0061 |
| 12 | 0.0027 | 0.0028 | 0.0027 | 0.0027 |
| 20 | 0.0018 | 0.0014 | 0.0016 | 0.0017 |
| 30 | 0.0011 | 0.0012 | 0.0010 | 0.0010 |
| 40 | 0.0009 | 0.0009 | 0.0009 | 0.0008 |
| 50 | 0.0014 | 0.0012 | 0.0013 | 0.0014 |

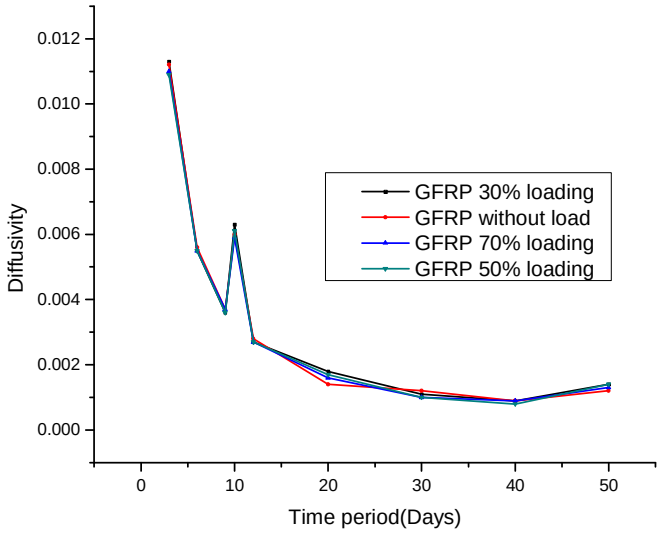


**Fig. 5.21:** Graph for moisture diffusivity of GFRP laminates w.r.t time

**Table 5.8:** Moisture diffusivity in CFRP laminated specimen

| Time period | CFRP 30%loading | CFRP 50%loading | CFRP 70%loading | CFRP without load |
|---|---|---|---|---|
| 3 | 0.007 | 0.020 | 0.018 | 0.020 |
| 6 | 0.022 | 0.010 | 0.009 | 0.010 |
| 9 | 0.011 | 0.007 | 0.006 | 0.007 |
| 10 | 0.006 | 0.006 | 0.008 | 0.008 |
| 12 | 0.005 | 0.005 | 0.005 | 0.005 |
| 20 | 0.001 | 0.001 | 0.001 | 0.002 |
| 30 | 0.001 | 0.001 | 0.001 | 0.001 |
| 40 | 0.001 | 0.001 | 0.001 | 0.001 |
| 50 | 0.002 | 0.001 | 0.001 | 0.001 |

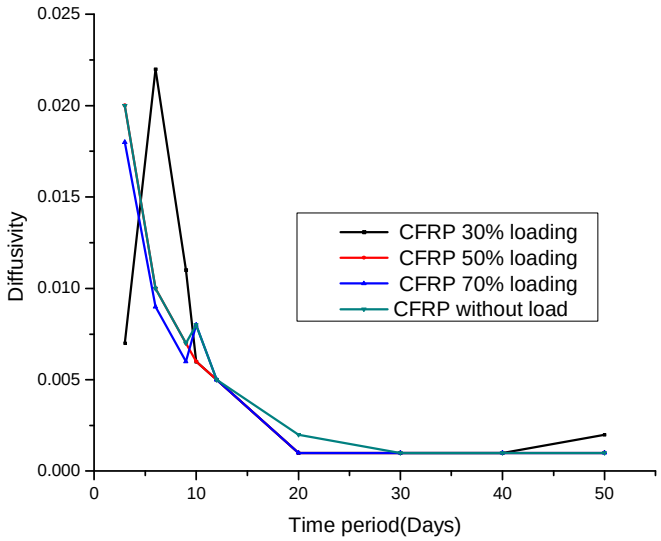


**Fig. 5.22:** Graph for moisture diffusivity of CFRP laminates w.r.t time

The moisture diffusivity was compared for various loads, it could be easily noticed that in water tank (T2) the moisture diffusivity is decreasing with respect to time indicating that more moisture is absorbed after two months comparing to first month in almost all the specimen with few exceptions. The reason for decrease in moisture diffusivity is obvious that with time percentage weight gain of specimen increases for given hygrothermal load giving way to moisture. The moisture diffusivity decrease in case of GFRP specimen was almost same as shown in Fig. 5.21. The range of moisture diffusivity values of CFRP specimen were low compared to GFRP as shown in Fig.5.22.

### 5.1.2.3.7. LCR meter results of laminated specimen

**Table 5.9:** Capacitance results in GFRP laminated specimen

| Time period | GFRP 30%loading | GFRP without load | GFRP 70%loading | GFRP 50%loading |
|---|---|---|---|---|
| 3 | 1.78E-11 | 2.08E-11 | 2.58E-11 | 2.90E-11 |
| 6 | 4.38E-11 | 2.59E-11 | 3.45E-11 | 3.35E-11 |
| 9 | 4.61E-11 | 2.63E-11 | 3.60E-11 | 3.60E-11 |
| 10 | 8.85E-11 | 3.42E-11 | 4.62E-11 | 3.73E-11 |
| 12 | 8.92E-11 | 3.58E-11 | 6.19E-11 | 3.99E-11 |
| 20 | 8.97E-11 | 3.69E-11 | 7.11E-11 | 5.31E-11 |
| 25 | 9.00E-11 | 4.79E-11 | 7.16E-11 | 6.12E-11 |
| 30 | 9.20E-11 | 6.95E-11 | 7.67E-11 | 7.04E-11 |
| 40 | 9.30E-11 | 7.52E-11 | 8.36E-11 | 7.74E-11 |
| 50 | 9.52E-11 | 9.13E-11 | 8.56E-11 | 8.51E-11 |

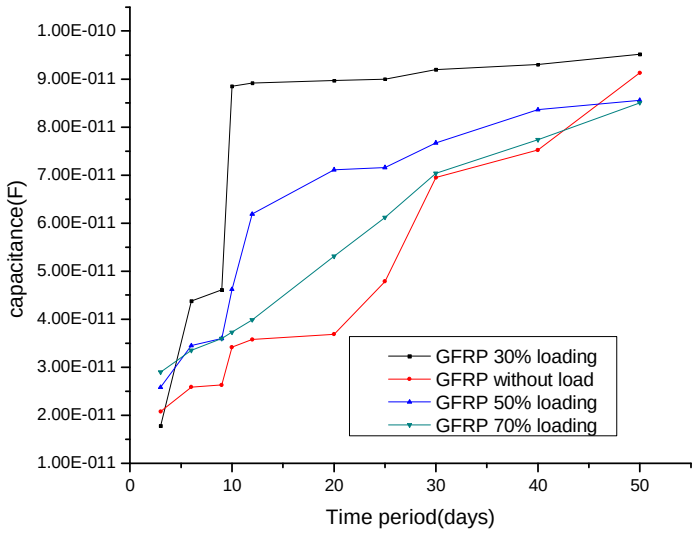


**Fig. 5.23**: Graph for capacitance of GFRP laminates w.r.t time

**Table 5.10:** Capacitance results in CFRP laminated specimen

| Time period | CFRP 30%loading | CFRP 50%loading | CFRP 70%loading | CFRP without load |
|---|---|---|---|---|
| 3 | 1.03E-12 | 1.86E-12 | 3.40E-12 | 4.20E-13 |
| 6 | 2.04E-12 | 2.28E-12 | 3.60E-12 | 1.20E-12 |
| 9 | 2.60E-12 | 4.20E-12 | 4.36E-12 | 6.20E-12 |
| 10 | 4.82E-12 | 4.98E-12 | 5.30E-12 | 1.32E-11 |
| 12 | 5.10E-12 | 5.70E-12 | 7.40E-12 | 1.40E-11 |
| 20 | 5.70E-12 | 7.90E-12 | 9.80E-12 | 1.54E-11 |
| 25 | 1.24E-11 | 9.00E-12 | 1.86E-11 | 1.93E-11 |
| 30 | 1.75E-11 | 2.22E-11 | 2.89E-11 | 2.27E-11 |
| 40 | 1.94E-11 | 2.37E-11 | 4.63E-11 | 5.47E-11 |
| 50 | 3.50E-11 | 5.93E-10 | 5.58E-11 | 6.95E-11 |

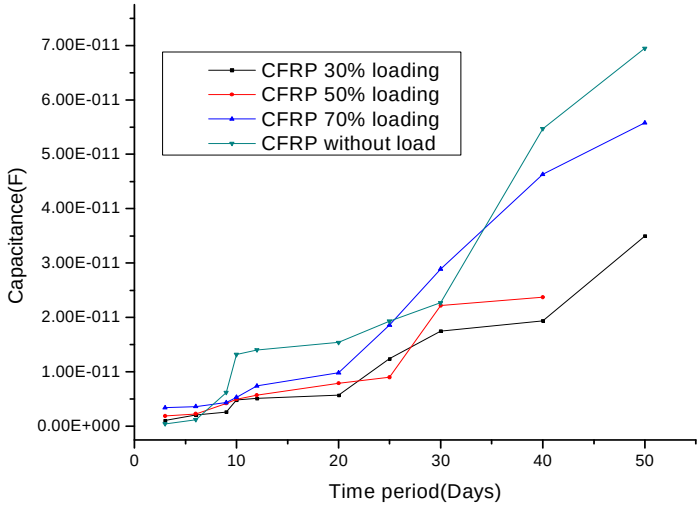


**Fig. 5.24:** Graph for capacitance of CFRP laminates w.r.t time

The capacitance was compared for various loaded specimen, it could be easily noticed that in water tanks the capacitance is increasing with respect to time indicating degradation of fibre. There was marginal increase in capacitance of specimen up to 40days in GFRP laminates and 50days in case of CFRP laminates at 45°C temperature. The reason for increase in capacitance is that with time the %weight gain increases due to given hygrothermal load giving way to moisture. The capacitance of 30% loaded GFRP specimen has attained saturation before other specimen as shown in Fig. 5.24. The capacitance value of CFRP specimen started increasing after one month as CFRP specimen started gaining weight as shown in Fig.5.24.

## 5.1.3. Tensile test results of laminated specimen

### 5.1.3.1. Initial testing graphs of tensile specimen before experiment

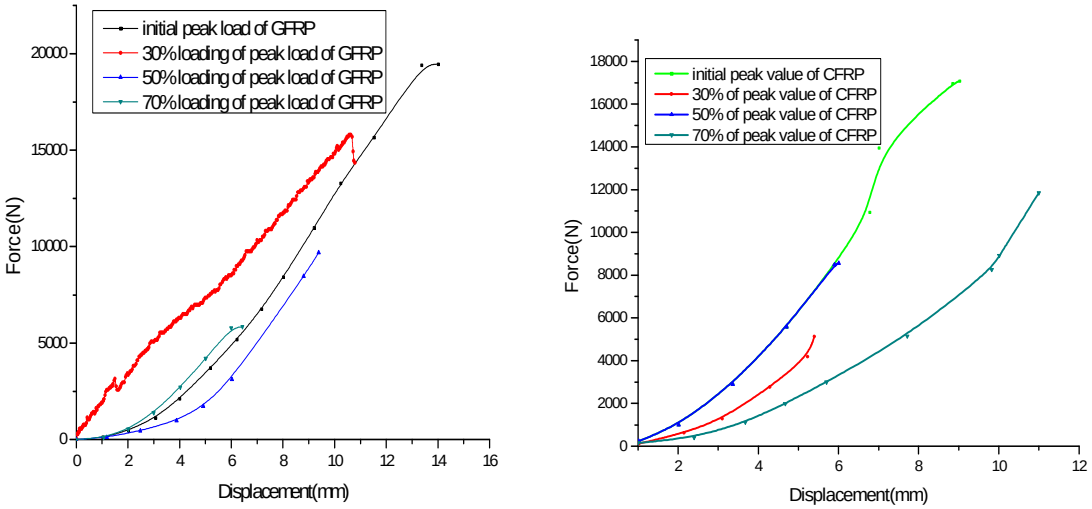


a) b)

**Fig. 5.25:** initial graphs of **a)** GFRP at various loads b**)** CFRP at various loads

The initial peak loads values of both GFRP and CFRP were used to calculate strength degradation of specimen after hygrothermal treatment. The peak loads shown in 70% UTL, 50%UTL, 30% UTL graphs were pre-stretched specimen loads as shown in Fig.5.25.

### 5.1.3.2. Tensile test Results of water tank ($T_{2)}$ of two months

**5.1.3.2.1.** Tensile graphs of specimen loaded at 30%UTL

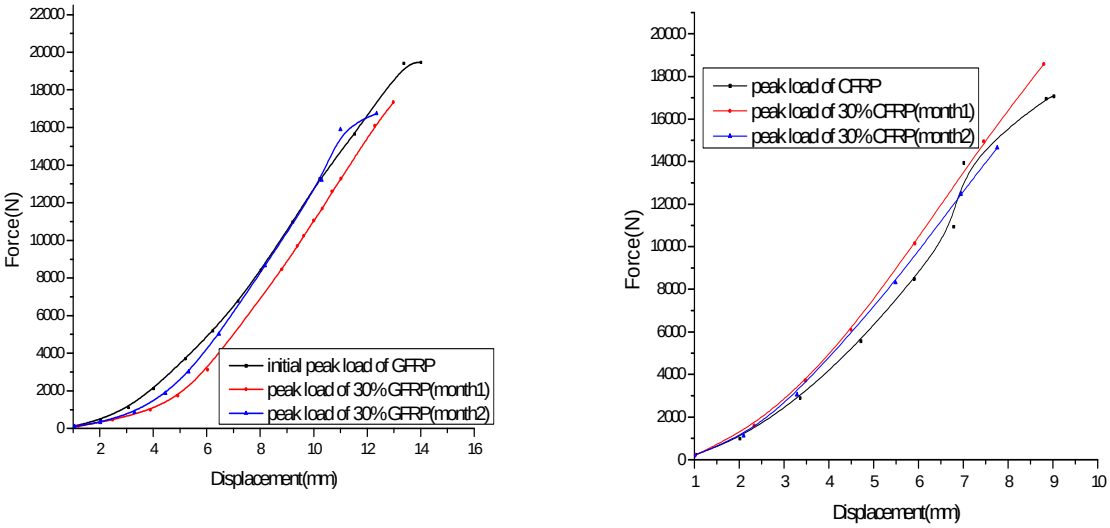


a) b)

**Fig. 5.26:** Peak load graphs of a) GFRP 30% UTL b) CFRP 30% UTL

**5.1.3.2.2.** Tensile graphs of specimen loaded at 50%UTL

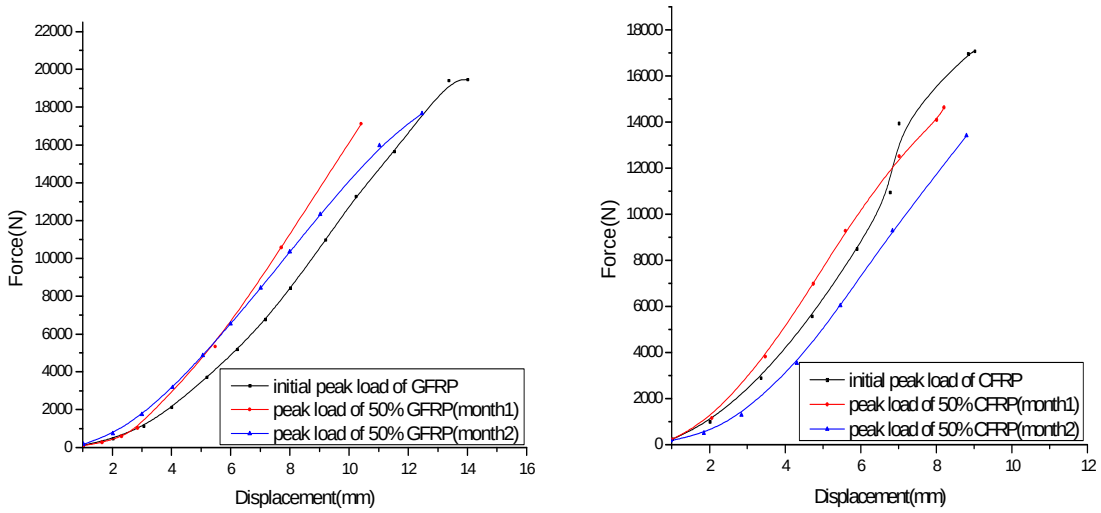


a) b)

**Fig. 5.27:** Peak load graphs of a) GFRP 50% UTL b) CFRP 50% UTL

**5.1.3.2.3.** Tensile graphs of specimen loaded at 70%UTL

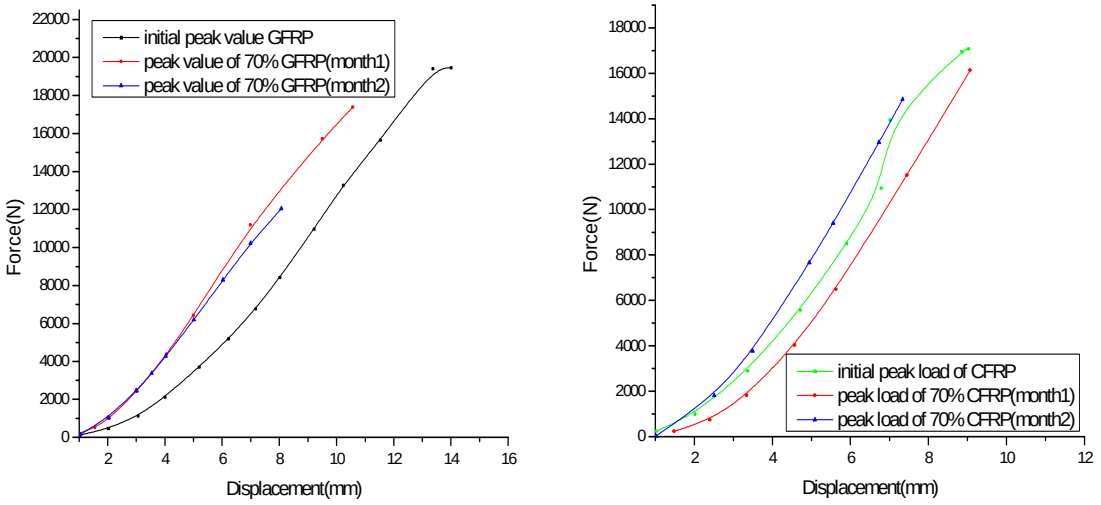


a) b)

**Fig. 5.28:** Peak load graph of a) GFRP 70% UTL b) CFRP 70% UTL

From the Fig. 5.26, Fig. 5.27 and Fig. 5.28. it was observed that the peak load of GFRP and CFRP laminates composites were decreasing from first month to second month. When compared with initial, second month specimen have considerable decrease. The tensile

strength and tensile modulus of laminated composites after and before hygrothermal treatment had been decreased as shown in the Table 5.11 and Table 5.12.

**Table 5.11:** Percentage decrease in Tensile strength of GFRP at various loads

| Specimen name | peak load(N) | Tensile strength(MPa) | Tensile modulus(MPa) | % Decrease in strength |
|---|---|---|---|---|
| initial GFRP | 19460 | 432.5 | 871.5 | 0 |
| GFRP 30% loading(month1) | 17140 | 380.9 | 631.2 | 13.6 |
| GFRP 30% loading(month2) | 16810 | 373.5 | 514.9 | 15.1 |
| GFRP 50% loading(month1) | 19330 | 429.6 | 827 | 0.67 |
| GFRP 50% loading(month2) | 18600 | 413.4 | 648 | 4.4 |
| GFRP 70% loading(month1) | 17420 | 387 | 854 | 10.5 |
| GFRP 70% loading(month2) | 12220 | 271.5 | 814.1 | 37.2 |

**Table 5.12:** Percentage decrease in Tensile strength of CFRP at various loads

| Specimen name | peak load(N) | Tensile strength(MPa) | Tensile modulus(MPa) | % Decrease in strength |
|---|---|---|---|---|
| initial CFRP | 17080 | 263 | 679 | 0 |
| CFRP 30% loading(month1) | 16583 | 256 | 631 | 2.7 |
| CFRP 30% loading(month2) | 14660 | 226 | 545 | 14.1 |
| CFRP 50% loading(month1) | 14770 | 227.9 | 645 | 13.35 |
| CFRP 50% loading(month2) | 13430 | 207 | 505 | 21.3 |
| CFRP 70% loading(month1) | 16997 | 262 | 654 | 0.38 |
| CFRP 70% loading(month2) | 14880 | 230 | 639.5 | 12.6 |

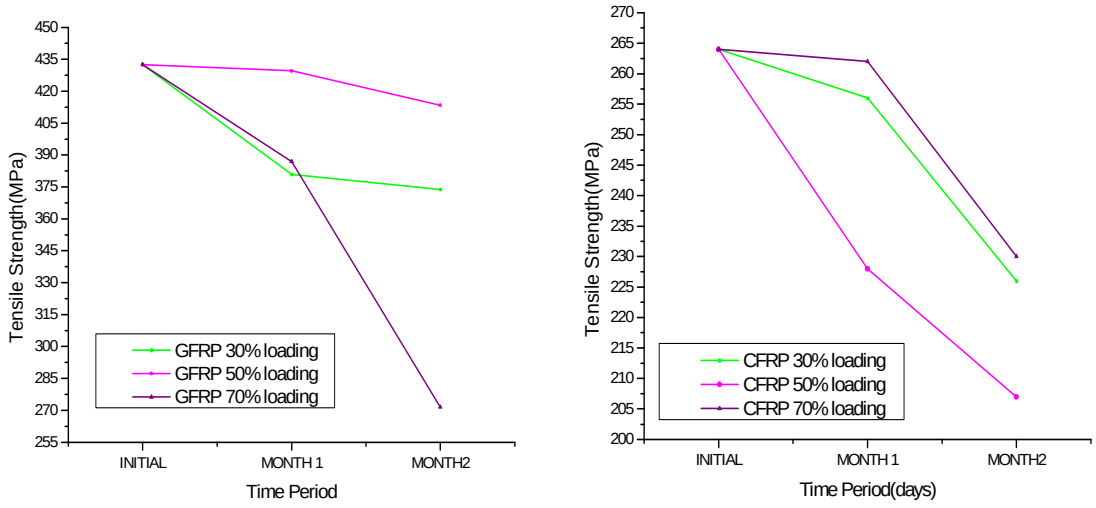


a) b)

**Fig. 5.29:** Graphs for ultimate tensile strength of a) GFRP laminates b) CFRP laminates

Form the Fig.5.29 we came to know that the tensile strength of laminated specimen was decreasing with time. The tensile strength of 70% UTL GFRP decreased after one month where as 30% UTL and 50% UTL GFRP specimen decreased up to one month and is almost same after one month as shown in Fig.5.29(a).

The CFRP Graph shown in Fig.5.29 (b) shows that the tensile strength is almost same up to one month has started decreasing after one month as CFRP specimen started degrading.

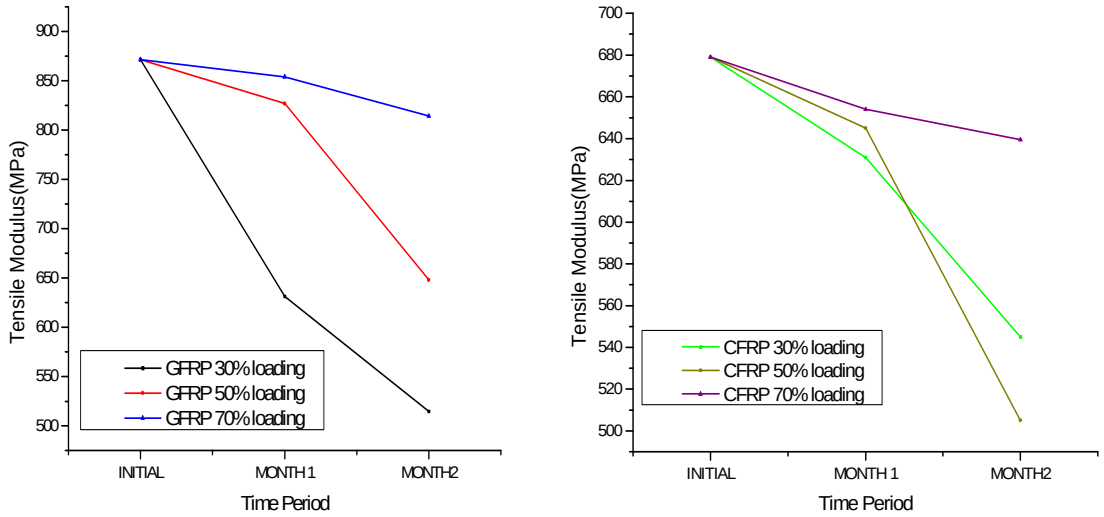


a) b)

**Fig. 5.30:** Graphs for ultimate tensile modulus of a) GFRP laminates b) CFRP laminates

The tensile modulus of GFRP and CFRP specimen were decreasing from one month to second month with some exceptions. The 70% UTL GFRP specimen has tensile modulus almost same after one month as shown in the Fig. 5.30(a).
The tensile modulus of CFRP specimen was decreasing after one month with an exception of 70% UTL CFRP specimen. The 70% UTL CFRP specimen has tensile modulus almost same after one month as shown in the Fig. 5.30(b).

### 5.1.3.3. Tensile test results of natural degradation specimen for two months

The following graphs depict the degradation of GFRP and CFRP specimen. The peak loads of initial specimen their mechanical properties were discussed in Fig 5.25.after one month and two months exposure of specimen in water at room temperature the behavior of laminated specimen was depicted in Fig.5.31, Fig. 5.32, Fig. 5.33, Fig. 5.34.

**5.1.3.3.1.** Tensile graphs of specimen loaded at 30%UTL

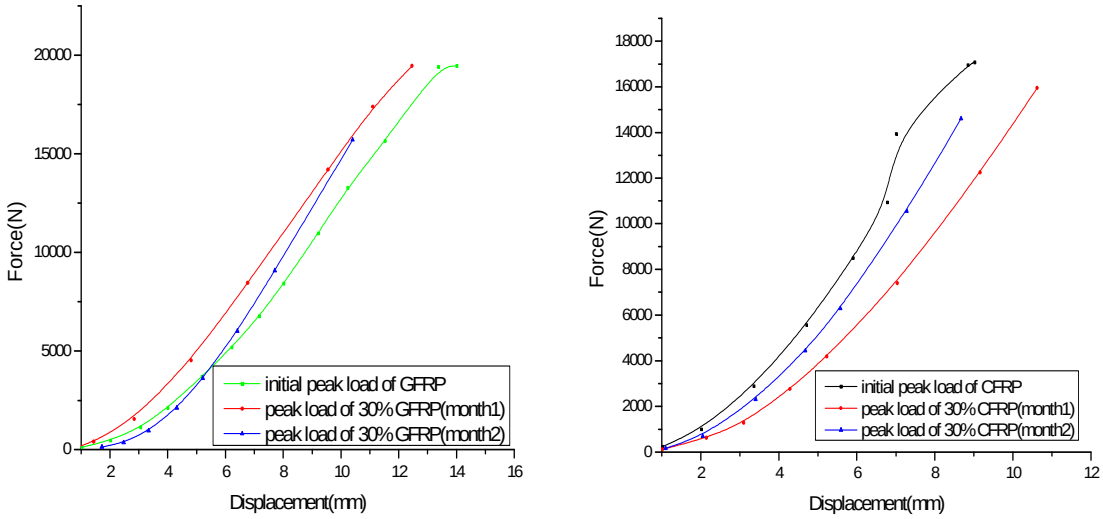


a) b)

**Fig. 5.31:** Peak load graphs of a) GFRP 30% UTL b) CFRP 30% UTL

**5.1.3.3.2.** Tensile graphs of specimen loaded at 50%UTL

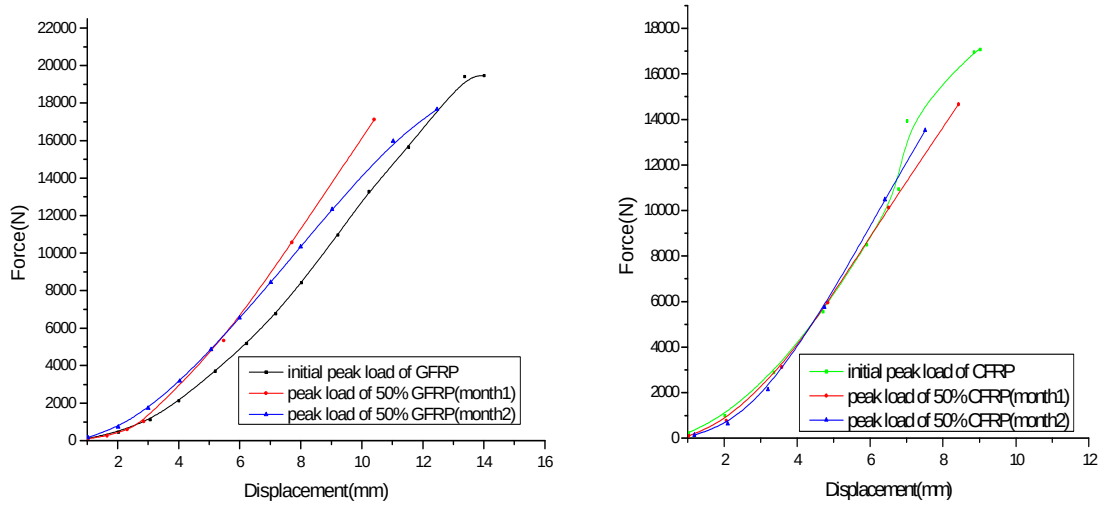


a) b)

**Fig. 5.32:** Peak load graph of a) GFRP 50% UTL b) CFRP 50% UTL

**5.1.3.3.3.** Tensile graphs of specimen loaded at 70%UTL

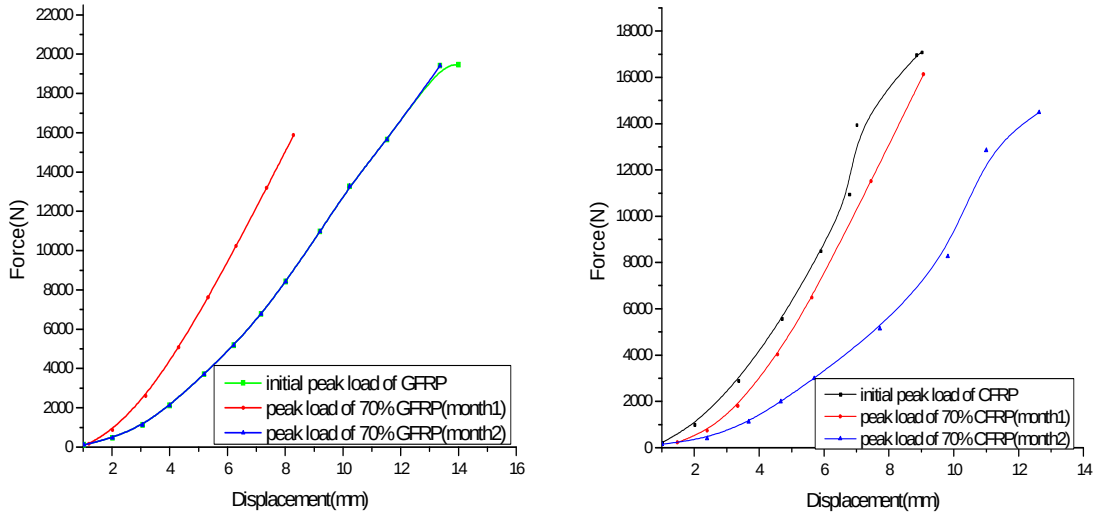


a) b)

**Fig. 5.33:** Peak load graph of a) GFRP 70% UTL b) CFRP 70% UTL

**5.1.3.3.4**. Tensile graphs of specimen without loaded

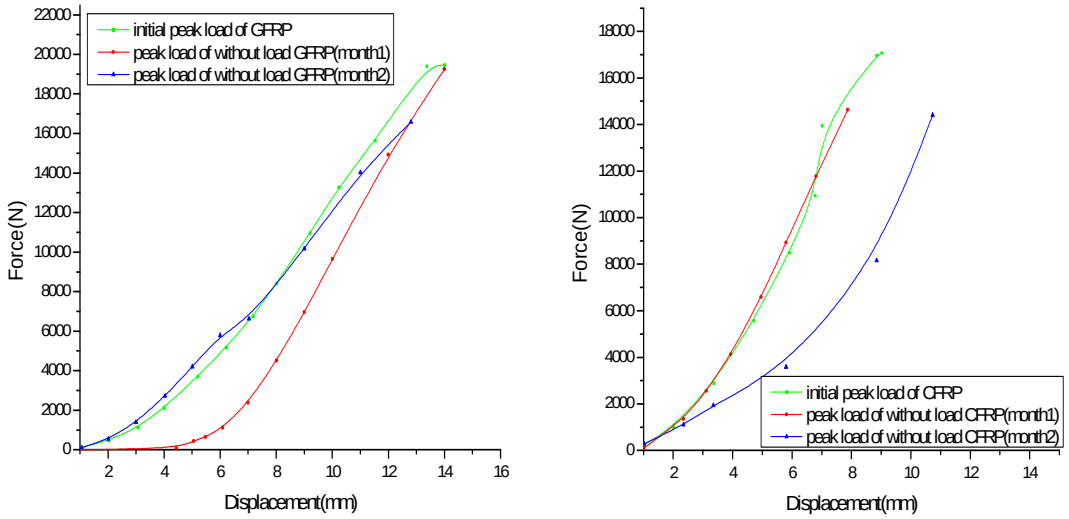


a) b)

**Fig. 5.34:** Peak load graph of a) without load GFRP b) without load CFRP

From the above Fig. 5.31, Fig. 5.32, Fig. 5.23 and Fig. 5.24, we came to know that the peak load of GFRP and CFRP laminates composites was decreasing from first month to second month. When compared with initial specimen second month specimen have considerable

decrease in strength. The tensile strength and tensile modulus of laminated composites after and before natural treatment had been decreased as shown in the Table 5.13 and Table 5.14.

**Table 5.13:** Percentage decrease in tensile strength of GFRP at various loads

| Specimen name | Peak load(N) | Tensile strength (MPa) | Tensile modulus (MPa) | %Decrease in strength |
|---|---|---|---|---|
| initial GFRP | 19460 | 432.5 | 871.5 | 0 |
| GFRP 30% loading(month1) | 19450 | 431 | 724 | 0.35 |
| GFRP 30% loading(month2) | 15706 | 349 | 651 | 19.3 |
| GFRP 50% loading(month1) | 17840 | 396.4 | 736.6 | 8.35 |
| GFRP 50% loading(month2) | 17118 | 380.42 | 670.5 | 12 |
| GFRP 70% loading(month1) | 19420 | 431.5 | 771.8 | 0.23 |
| GFRP 70% loading(month2) | 15878 | 353 | 619.3 | 18.4 |
| GFRP without load(month1) | 19255 | 428 | 846.9 | 1.04 |
| GFRP without load(month2) | 16600 | 368.9 | 681.4 | 8.41 |

**Table 5.14:** Percentage decrease in tensile strength of GFRP at various loads

| Specimen name | Peak load (N) | Tensile strength (MPa) | Tensile modulus (MPa) | %Decrease in strength |
|---|---|---|---|---|
| initial CFRP | 17080 | 263 | 679 | 0 |
| CFRP 30% loading(month1) | 15970 | 246 | 513 | 6.46 |
| CFRP 30% loading(month2) | 14240 | 220 | 463 | 16.35 |
| CFRP 50% loading(month1) | 14830 | 229 | 679 | 12.93 |
| CFRP 50% loading(month2) | 13720 | 212 | 626 | 19.4 |
| CFRP 70% loading(month1) | 16320 | 251.9 | 560.9 | 4.2 |
| CFRP 70% loading(month2) | 14550 | 224.6 | 344.5 | 14.5 |
| CFRP without load(month1) | 14740 | 227.4 | 584.5 | 13.54 |
| CFRP without load(month2) | 14650 | 226 | 438 | 14.1 |

The tensile strength values shown in the Table 5.13 and Table 5.14 were depicted graphically to know the behavior of the curves of GFRP and CFRP laminated composites as shown in Fig 5.35.

The tensile modulus values shown in Table 5.13 and Table 5.14 were depicted graphically to know the behavior of the curves of GFRP and CFRP laminated composites as shown in Fig. 5.36.

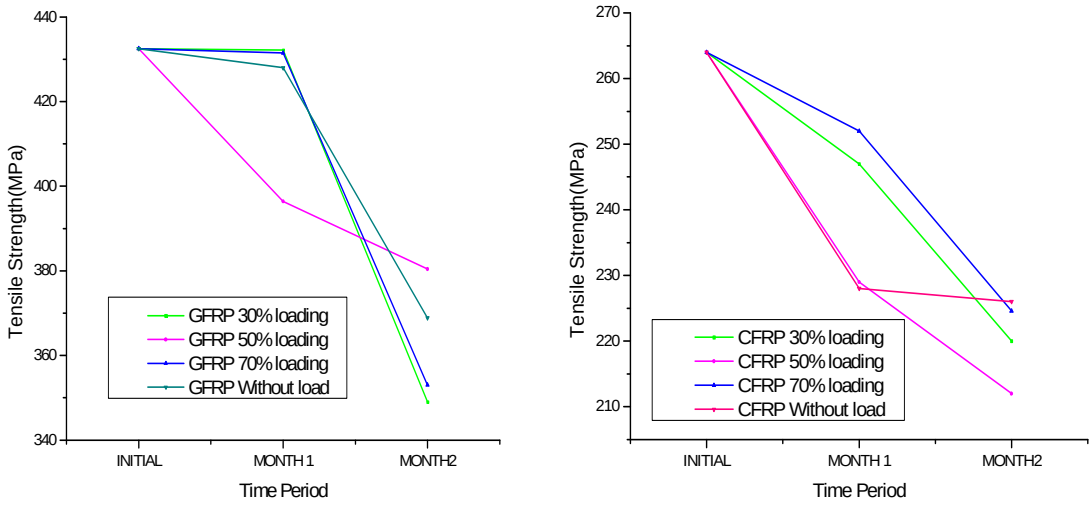


a) b)

**Fig. 5.35:** Graphs for ultimate tensile strength of a) GFRP laminates b) CFRP laminate

The trends of decrease in ultimate Tensile strength were shown in Fig.5.35. The tensile strength reduction in T5 tanks seems to be nearly same after one month and two months with few exceptions. But when comparing the reduction in two tanks after one month with respect to reduction in two months there is noticeable change as we had seen that after one month the reduction is ranging from 10 to 25% mainly where as the reduction in two month seems to be between 25 to 45% mainly. The reason for decrease in ultimate tensile strength and change in percentage tensile strength seems to be the continuous degradation done by hygrothermal load which affected the epoxy and fibre strength. The CFRP without loaded specimen has tensile strength almost same after one month as shown in Fig. 5.35(b).the GFRP specimen were almost decreasing after one month as shown in Fig. 5.35(a).

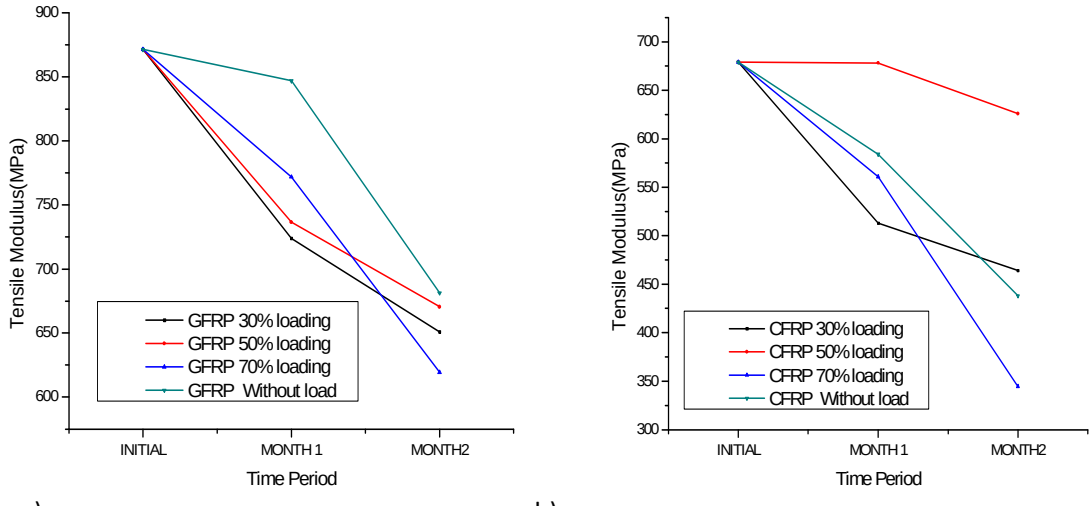


a) b)

**Fig. 5.36:** Graphs for ultimate tensile modulus of a) GFRP laminates b) CFRP laminate

The tensile modulus of 30% UTL and 50% UTL CFRP specimen is almost same after one month. The decrease in 70% UTL and without load specimen were more when compared to other loadings as shown in Fig. 5.36(b).The tensile modulus of GFRP specimen were decreasing after one month as shown in Fig. 5.36(a).

### 5.1.3.4. Results and discussions of percentage weight gain of laminated composites

**Table 5.15: P**ercentage weight gain in GFRP laminated specimen

| Time period | GFRP 30%loading | GFRP without load | GFRP 70%loading | GFRP 50%loading |
|---|---|---|---|---|
| 3 | 4.994 | 3.689 | 4.282 | 6.729 |
| 6 | 5.088 | 4.033 | 4.309 | 7.485 |
| 9 | 6.198 | 5.214 | 4.855 | 9.069 |
| 10 | 3.853 | 4.031 | 4.460 | 4.814 |
| 12 | 6.055 | 5.298 | 6.495 | 10.335 |
| 20 | 8.414 | 3.760 | 4.946 | 4.890 |
| 30 | 9.763 | 6.700 | 7.967 | 9.293 |
| 40 | 10.215 | 6.898 | 8.539 | 11.192 |
| 50 | 11.614 | 6.996 | 14.193 | 11.199 |

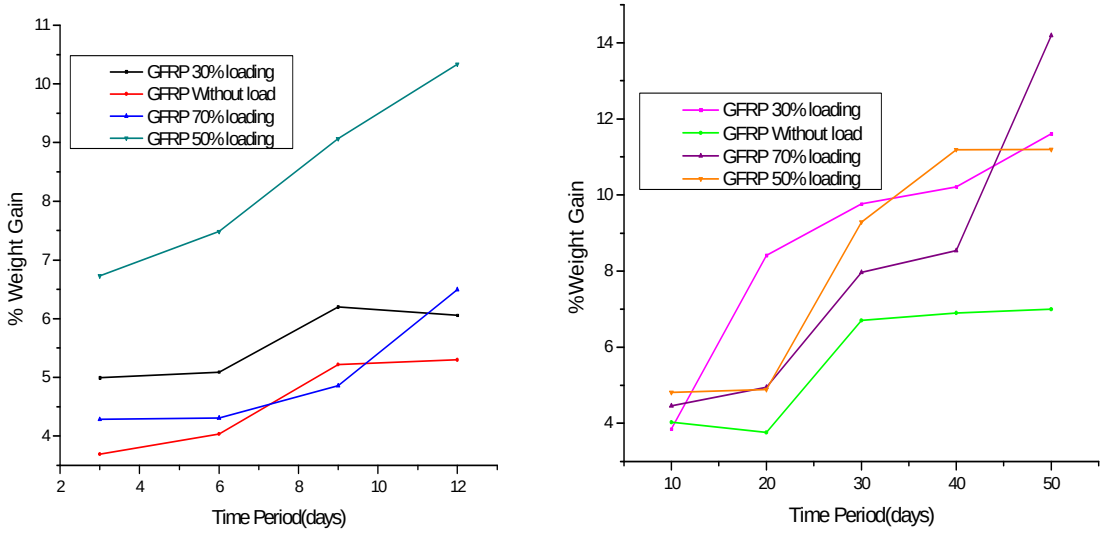


a) b)

**Fig. 5.37:** Graphs for percentage weight gain of GFRP laminates at a) three days interval b) ten days interval

The percentage decrease in weight gain of GFRP specimen at consecutive 3 days was depicted in Fig. 5.37(a) using the Table 5.15.the weight gain of 30% UTL GFRP specimen is almost same after 9 days as shown in Fig. 5.37(a).

The percentage decrease in weight gain of GFRP specimen at consecutive 10 days is depicted in Fig.5.37 (b).The without loaded specimen weight gain is almost same after 30 days as shown in Fig. 5.37(b).

**Table 5.16**: Percentage weight gain in CFRP laminated specimen

| **Time period** | **CFRP 30%loading** | **CFRP 50%loading** | **CFRP 70%loading** | **CFRP without load** |
|---|---|---|---|---|
| 3 | 1.91 | 1.96 | 2.12 | 2.45 |
| 6 | 2.42 | 2.28 | 2.78 | 2.41 |
| 9 | 4.18 | 3.29 | 4.20 | 4.00 |
| 10 | 2.03 | 3.40 | 2.37 | 2.22 |
| 12 | 4.55 | 4.01 | 4.01 | 4.65 |
| 20 | 3.68 | 4.02 | 3.31 | 2.34 |
| 30 | 3.73 | 5.09 | 3.73 | 4.30 |
| 40 | 6.45 | 6.56 | 4.95 | 5.83 |
| 50 | 7.82 | 8.02 | 6.12 | 8.37 |

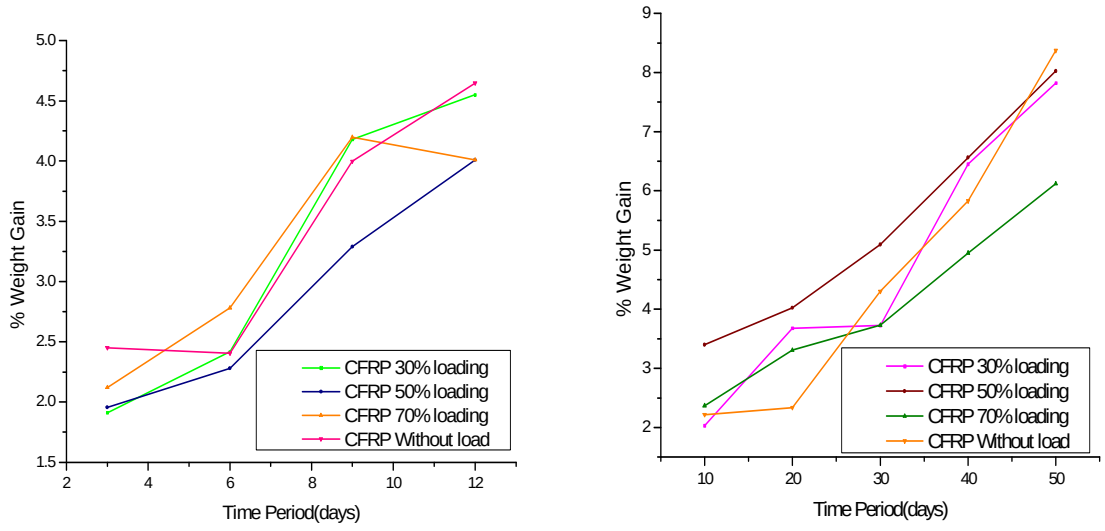


a) b)

**Fig. 5.38:** Graphs of percentage weight gain of CFRP laminates at a) three days interval b) Ten days interval

The percentage weight gain (of moisture) was compared for various loads using the Table 5.16. It could be easily noticed that in water tanks the percentage weight gain is increasing with respect to time indicating that more moisture is absorbed after two months comparing to first month in almost all the specimen with few exceptions. The reason for increase in percentage weight gain is obvious that with time the pores of epoxy will loosen due to given hygrothermal load giving way to moisture. The 70% UTL CFRP specimen has decrease in percentage weight gain after 9 days as shown in Fig. 5.38(a).the CFRP specimen at consecutive 10 days has percentage weight gain increase after 20 days as shown in Fig. 5.38(b). The 30% UTL CFRP specimen has percentage weight gain almost same up to 30days and sudden increase has occurred after 30 days.

### 5.1.3.5. Moisture diffusivity results of laminated specimen

**Table 5.17:** Moisture diffusivity in GFRP laminated specimen

| Time period | GFRP 30%loading | GFRP without load | GFRP 70%loading | GFRP 50%loading |
|---|---|---|---|---|
| 3 | 0.1065 | 0.1066 | 0.1025 | 0.1250 |
| 6 | 0.0532 | 0.0533 | 0.0512 | 0.0625 |
| 9 | 0.0355 | 0.0355 | 0.0342 | 0.0417 |
| 10 | 0.0335 | 0.0390 | 0.0414 | 0.0411 |
| 12 | 0.0266 | 0.0266 | 0.0256 | 0.0312 |
| 20 | 0.0189 | 0.0195 | 0.0159 | 0.0144 |
| 30 | 0.0147 | 0.0128 | 0.0124 | 0.0148 |
| 40 | 0.0071 | 0.0101 | 0.0091 | 0.0091 |
| 50 | 0.0158 | 0.0127 | 0.0112 | 0.0162 |

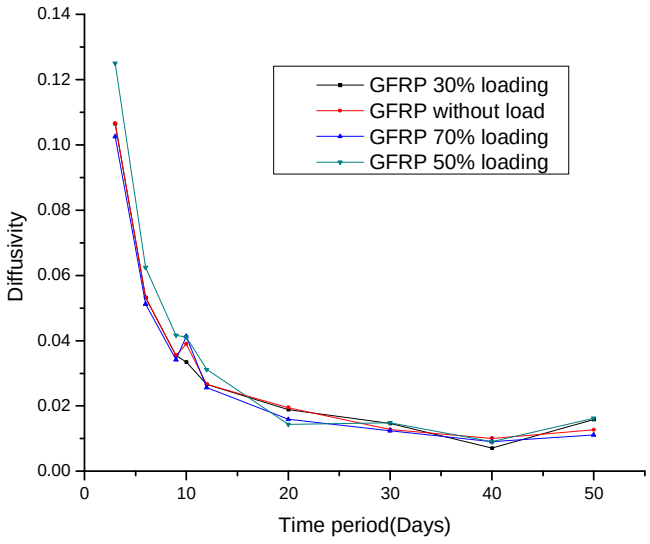


**Fig. 5.39:** Comparison of moisture diffusivity of CFRP laminates

**Table 5.18:** Moisture diffusivity in CFRP laminated specimen

| Time period | CFRP 30%loading | CFRP 50%loading | CFRP 70%loading | CFRP without load |
|---|---|---|---|---|
| 3 | 0.1679 | 0.2369 | 0.1695 | 0.1545 |
| 6 | 0.0839 | 0.1185 | 0.0848 | 0.0772 |
| 9 | 0.0560 | 0.0790 | 0.0565 | 0.0515 |
| 10 | 0.0535 | 0.0366 | 0.0550 | 0.0378 |
| 12 | 0.0420 | 0.0592 | 0.0592 | 0.0386 |
| 20 | 0.0187 | 0.0217 | 0.0309 | 0.0403 |
| 30 | 0.0179 | 0.0186 | 0.0262 | 0.0187 |
| 40 | 0.0054 | 0.0065 | 0.0066 | 0.0067 |
| 50 | 0.0114 | 0.0127 | 0.0125 | 0.0117 |

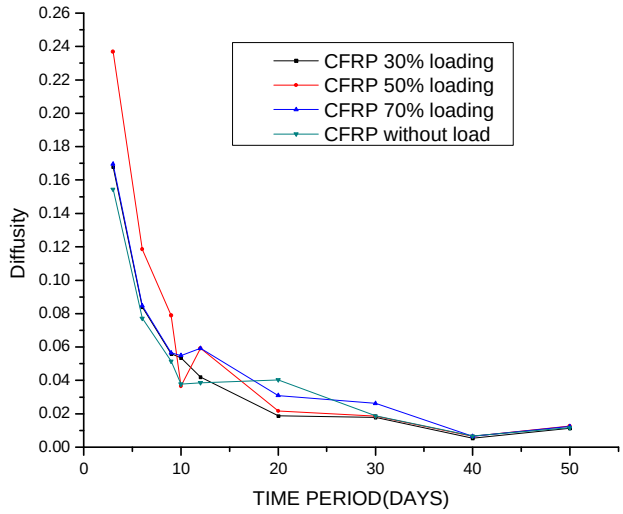


**Fig. 5.40:** Comparison of Moisture diffusivity of CFRP laminates

The moisture diffusivity was compared for various loads, it could be easily noticed that in water tank the percentage weight gain is increasing with respect to time indicating that more moisture is absorbed after two months comparing to first month in almost all the specimen with few exceptions. The reason for decrease in moisture diffusivity is obvious that with time the pores of epoxy will loosen due to given hygrothermal load giving way to moisture.

The CFRP specimen have apparent moisture diffusivity range more when compared to GFRP specimen because the percentage increase in weight gain of CFRP specimen is slow as compared. The moisture diffusivity of 50% UTL CFRP specimen starts from 0.24.The apparent moisture diffusivity for all CFRP specimen after 30 days is nearly same as shown in

Fig. 5.40. The GFRP specimen apparent moisture diffusivity decrease is almost same as shown in Fig. 5.39.

### 5.1.3.6. LCR Meter results of laminated specimen

**Table 5.19: C**apacitance in GFRP laminated specimen

| Time period | GFRP 30%loading | GFRP without load | GFRP70%loading | GFRP 50%loading |
|---|---|---|---|---|
| 3 | 1.52E-12 | 1.78-11 | 1.46E-12 | 1.51E-11 |
| 6 | 6.58E-12 | 2.30E-12 | 1.36E-11 | 1.72E-11 |
| 9 | 1.78E-11 | 2.56E-11 | 1.41E-11 | 2.11E-11 |
| 10 | 2.15E-11 | 3.03E-11 | 1.69E-11 | 2.11E-11 |
| 12 | 3.43E-11 | 3.34E-11 | 2.32E-11 | 2.65E-11 |
| 20 | 4.13E-11 | 3.60E-11 | 3.75E-11 | 3.14E-11 |
| 25 | 7.85E-11 | 3.67E-11 | 3.94E-11 | 4.80E-11 |
| 30 | 8.33E-11 | 7.01E-11 | 6.81E-11 | 5.97E-11 |
| 40 | 8.92E-11 | 7.34E-11 | 7.32E-11 | 6.73E-11 |
| 50 | 9.20E-11 | 8.16E-11 | 7.43E-11 | 9.02E-11 |

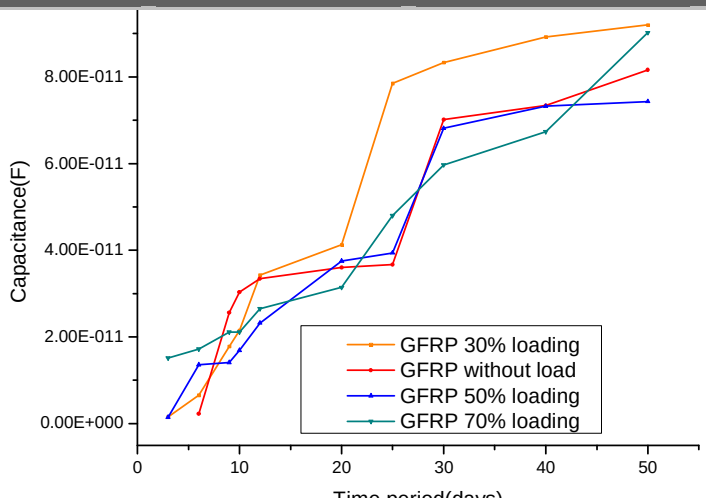


**Fig 5.41:** Graph for capacitance of GFRP laminates w.r.t. time

**Table 5.20:** Capacitance in CFRP laminated specimen

| Time period | CFRP 30%loading | CFRP 50%loading | CFRP 70%loading | CFRP without load |
|---|---|---|---|---|
| 3 | 7.60E-13 | 7.80E-13 | 1.20E-12 | 4.20E-13 |
| 6 | 8.70E-13 | 8.50E-13 | 1.34E-12 | 1.89E-12 |
| 9 | 1.20E-12 | 1.30E-12 | 1.46E-12 | 1.90E-12 |
| 10 | 1.35E-12 | 1.85E-12 | 1.60E-12 | 2.00E-12 |
| 12 | 1.52E-12 | 1.97E-12 | 1.66E-12 | 2.28E-12 |
| 20 | 2.70E-12 | 2.30E-12 | 1.68E-12 | 2.40E-12 |
| 25 | 8.96E-12 | 3.40E-12 | 5.96E-12 | 2.90E-12 |
| 30 | 1.32E-11 | 4.75E-12 | 1.80E-11 | 3.63E-12 |
| 40 | 2.57E-11 | 7.02E-12 | 2.29E-11 | 1.68E-11 |
| 50 | 6.28E-11 | 1.20E-11 | 7.98E-11 | 6.03E-11 |

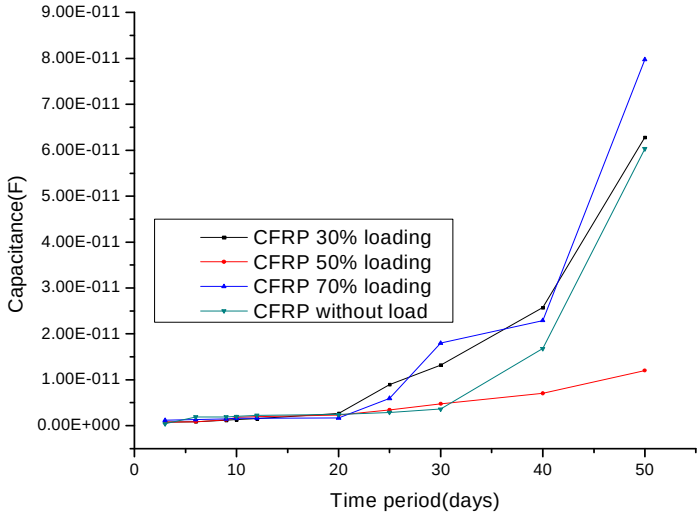


**Fig. 5.42:** Graph for capacitance of CFRP laminates w.r.t. time

The capacitance graphs of laminated composites depict using the Table 5.19. and Table 5.20.The capacitance was compared for various loaded specimen, it could be easily noticed that in water tank $T_2$ the capacitance is increasing with respect to time indicating degradation of fibre. There was marginal increase in capacitance of specimen up to 40 days in GFRP laminates and 50 days in case of CFRP laminates at 45°C temperature as shown in Fig. 5.41 and Fig. 5.42. The reason for increase in capacitance is that with time the pores of epoxy will loosen due to given hygrothermal load giving way to moisture. The capacitance increase started after one month in case of CFRP specimen, so a sudden raise was observed in the graph after 30 days.

The capacitance of all GFRP specimen are nearly same after 30 days except 70% UTL graph as shown in Fig. 5.41.the CFRP figure shows almost linear increase of capacitance up to 20 days as shown in Fig. 5.42.

## 5.1.4. Results of pure epoxy specimen

### 5.1.4.1. Percentage weight gain results of pure epoxy specimen

**Table 5.21:** Percentage weight gain results of pure epoxy specimen

| Time period | Temperature 45°C | Temperature 55°C | Natural temperature |
|---|---|---|---|
| 3 | 3.35 | 2.47 | 2.77 |
| 6 | 4.56 | 6.78 | 4.54 |
| 9 | 11.47 | 9.90 | 9.86 |
| 12 | 12.46 | 11.31 | 11.72 |

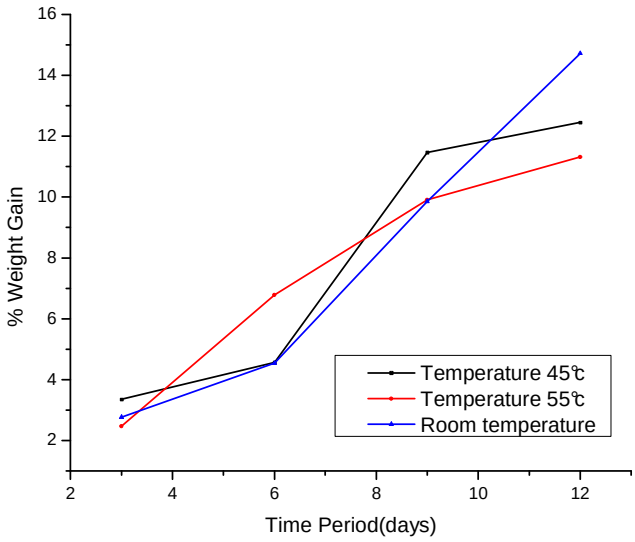


**Fig. 5.43:** Graph for percentage weight gain of epoxy specimen

The percentage weight gain was compared for various conditions from the Table 5.21, it could be easily noticed that in water tanks the percentage weight gain is increasing with respect to time indicating that more moisture is absorbed after 9 days in almost all the specimen with few exceptions. There was marginal increase in weight gain of specimen at 45°C temperature as compared to specimen at room temperature as shown in Fig. 5.43. The reason for increase in percentage weight gain is obvious that with time the pores of epoxy will loosen due to given hygrothermal load giving way to moisture.

### 5.1.4.2. Moisture diffusivity results of pure epoxy specimen

**Table 5.22:** Moisture diffusivity in pure epoxy specimen

| Time period | Temperature 45°C | Temperature 55°C | Natural temperature |
|---|---|---|---|
| 3 | 0.0033 | 0.0052 | 0.0053 |
| 6 | 0.0023 | 0.0032 | 0.0039 |
| 9 | 0.0020 | 0.0026 | 0.0027 |
| 12 | 0.0011 | 0.0009 | 0.0011 |

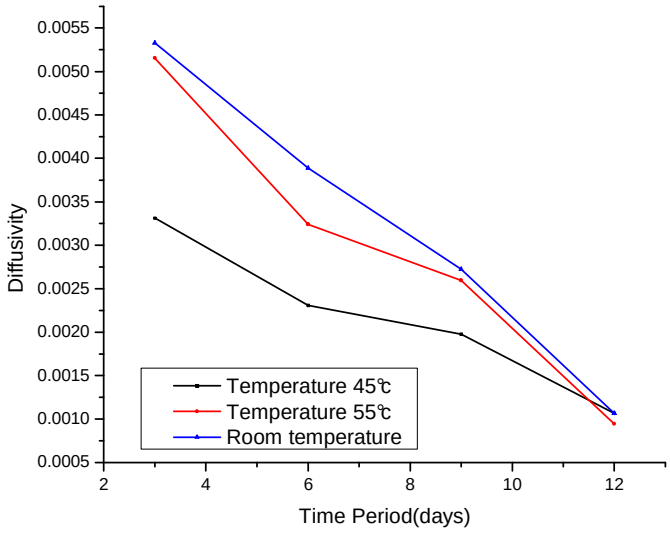


**Fig 5.44:** Comparison of moisture diffusivity of epoxy specimen

The Moisture diffusivity was compared for various conditions, it could be easily noticed that in water tanks the moisture diffusivity is decreasing with respect to time indicating degradation fibre as shown in the Fig. 5.44 depicted using the Table 5.22. There was marginal decrease in moisture diffusivity of specimen at 55°c temperature as compared to specimen at room temperature as shown in Fig. 5.44. The reason for decrease in moisture diffusivity is obvious that with time the pores of epoxy will loosen due to given hygrothermal load giving way to moisture.

### 5.1.4.3. LCR Meter results of pure epoxy specimen

The capacitance of epoxy specimen at various conditions was shown in the Table 5.23 and graphs are depicted using this Table 5.23.

**Table 5.23:** Capacitance results in pure epoxy specimen

| Time period | Temperature 45°C | Temperature 55°C | Natural temperature |
|---|---|---|---|
| 3 | 2.80E-13 | 6.00E-14 | 8.00E-13 |
| 6 | 5.00E-13 | 7.56E-13 | 6.35E-13 |
| 9 | 7.06E-12 | 6.76E-12 | 7.40E-12 |
| 12 | 7.50E-12 | 7.20E-12 | 7.42E-12 |

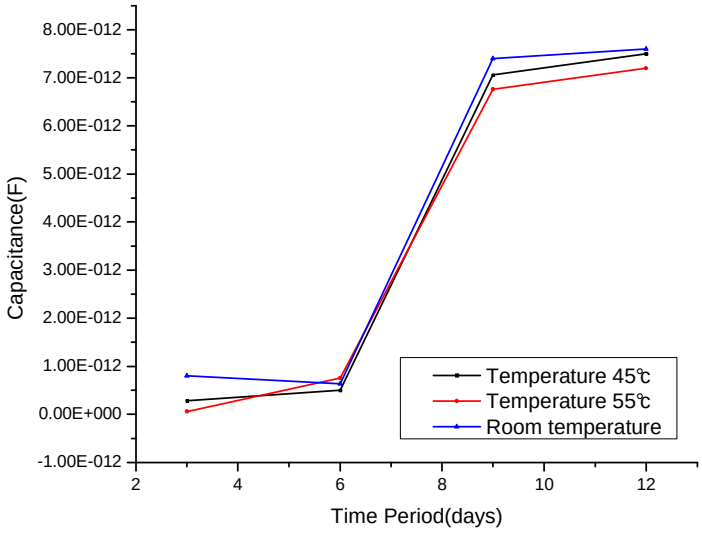


**Fig. 5.45:** Comparison of capacitance of epoxy specimen

The capacitance was compared for various conditions, it could be easily noticed that in water tanks the capacitance is increasing with respect to time indicating degradation fibre as shown in the Fig. 5.45. There was marginal increase in capacitance of specimen at 45°C temperature as compared to specimen at room temperature as shown in the Fig. 5.45. The reason for increase in capacitance is that with time the pores of epoxy will loosen due to given hygrothermal load giving way to moisture.

## 5.2. Microscopic Behavior

The parameters discussed here are Micro hardness, SEM images, percentage area fraction and circularity at 45$^{o}$C.

### 5.2.1. Microscopic Mode of failure

The SEM images for the GFRP and CFRP laminated composite specimen taken at 2000X magnification from their cut-cross-section and cut-longitudinal-section at the start of testing, before exposure to hygrothermal loads show a fibre epoxy composite with fibres densely embedded in epoxy matrix with epoxy surrounding completely the fibres which maintain their circularity and suggest good strength. The SEM image of cut-longitudinal section show cylindrical unbroken long fibres with no damage was shown in Fig. 5.46 and Fig. 5.47.

### 5.2.2. SEM results of laminated specimen

**5.2.2.1.** SEM results of bending specimen
**5.2.2.1.1.** SEM images before start of the experiment

The SEM images shown below were of undamaged fibres and epoxy surrounding the surface of fibres completely, which maintain the circularity

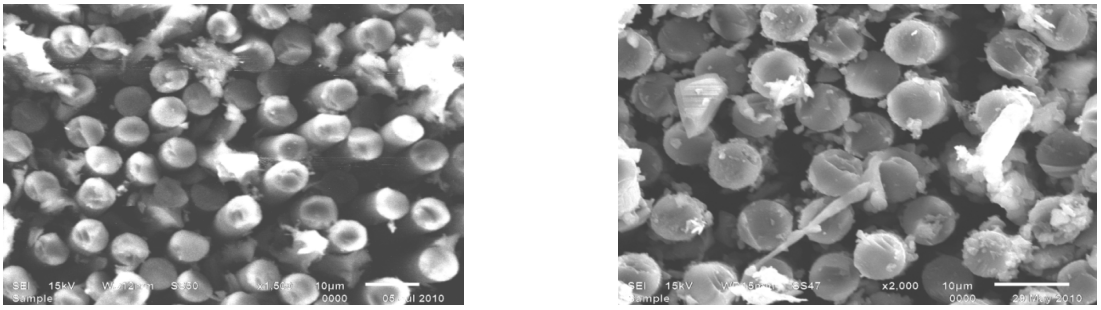

a) b)

**Fig. 5.46:**a) CFRP cross-section b) GFRP cross-section

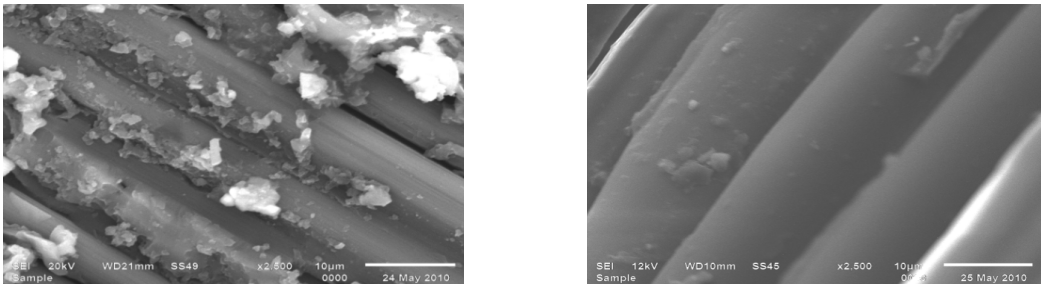

a) b)

**Fig. 5.47**:a) CFRP longitudinal section b) GFRP longitudinal section

**5.2.2.1.2.** SEM images after one month

The SEM images of specimen which were subjected to bending load after one month are shown in Fig. 5.48. The undamaged fibre and lumping of epoxy is clearly visible, the lumping of epoxy is due to hardening by absorption of water in case of GFRP specimen. While the CFRP Specimen had little lumping of epoxy in one month due to less amount of absorption of water as discussed earlier.

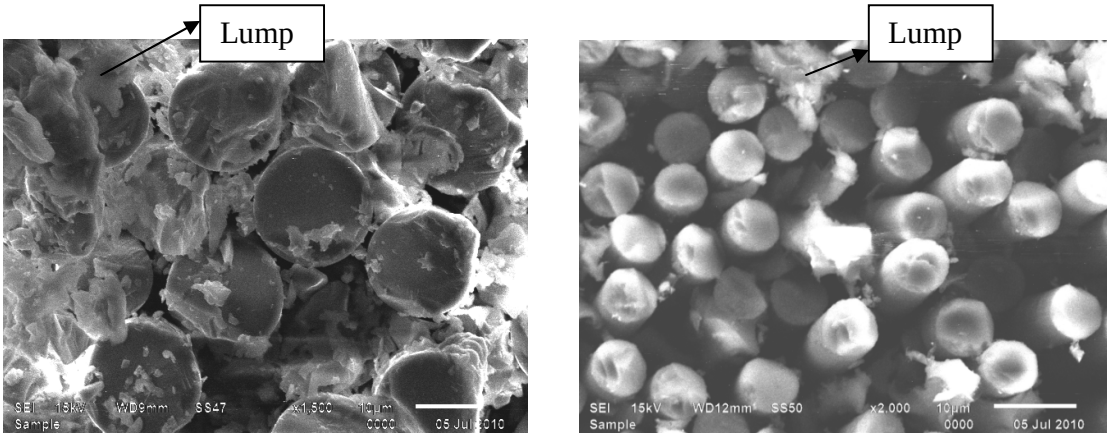


a) b)

**Fig. 5.48**: a) GFRP cross-section b) CFRP cross-section

**5.2.2.1.3.** SEM images after two months

After two months fibre degradation is observed and flaking of epoxy is also clearly visible due to hardening of epoxy by absorption of water in GFRP specimen. The epoxy lumping had taken place in CFRP specimen with little damage to fibre, extensive voids between the fibres, lumping of epoxy matrix is shown in Fig 5.49(b), as epoxy has dissolved away from surface protruding undamaged fibres are visible in CFRP and damaged fibres in GFRP as shown in Fig. 5.49.

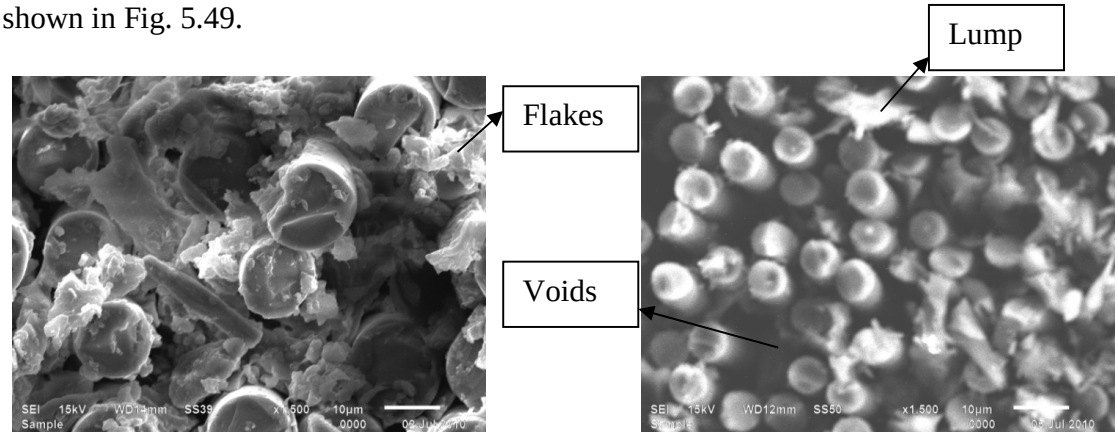


a) b)

**Fig. 5.49**: a) GFRP cross-section b)CFRP cross-section

### 5.2.2.2. SEM results of tensile specimen

**5.2.2.2.1.** SEM images before start of the experiment

The SEM images shown below are undamaged fibres and epoxy surrounding the surface of fibres completely, which maintain the circularity as shown in Fig 5.50 and Fig. 5.51.

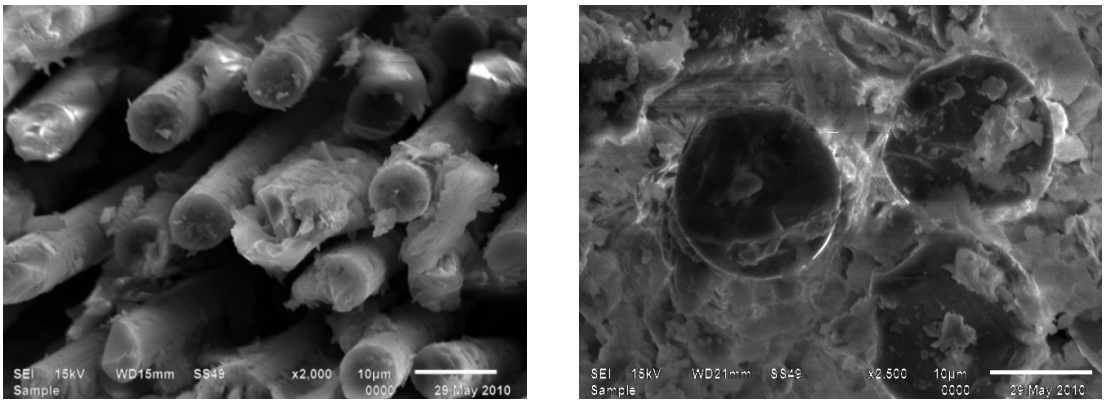


a) b)

**Fig. 5.50**:a) CFRP cross-section b) GFRP cross-section

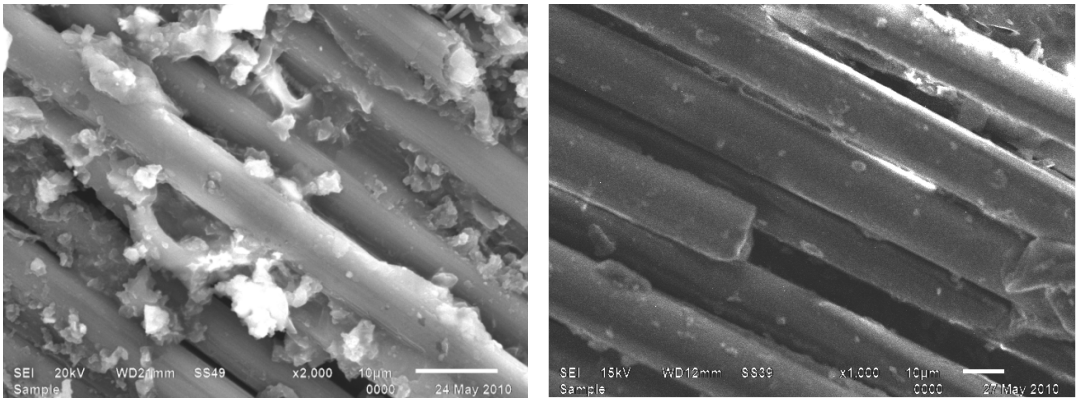


a) b)

**Fig. 5.51**:a) CFRP longitudinal section b) GFRP longitudinal section

**5.2.2.2.2.** SEM images after one month

The SEM images of specimen which were subjected to tensile load after one month are shown in Fig. 5.52. The damaged fibre and lumping of epoxy is clearly visible, the flaking of epoxy has occurred due to hardening of epoxy by absorption of water in case of GFRP specimen as shown in Fig. 5.52(a). While the CFRP Specimen had lumping of epoxy after one month but no damage to the fibre as shown in Fig. 5.52(b).

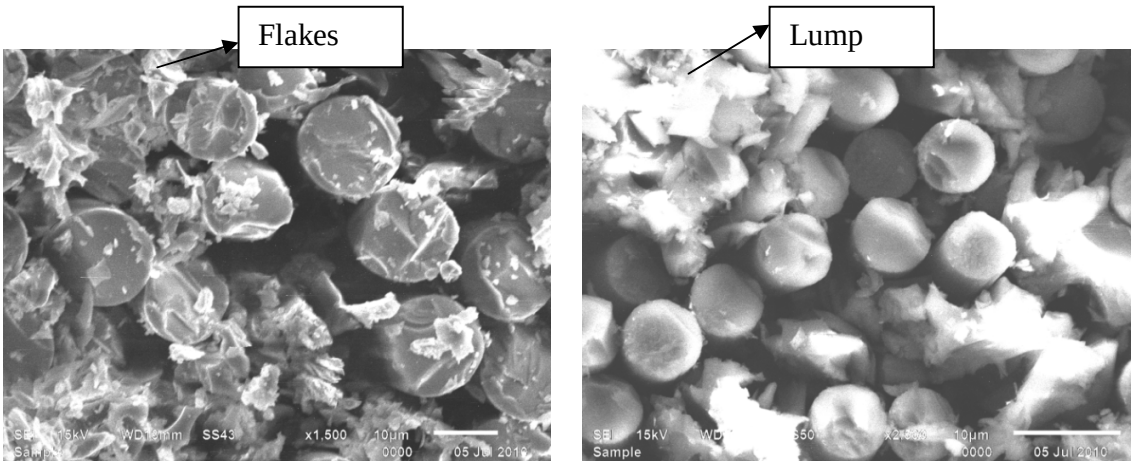


a) b)

**Fig. 5.52**: a) GFRP cross-section b) CFRP cross-section

**5.2.2.2.3.** SEM images after two months

After two months fibre failure is observed and flaking of epoxy is also clearly visible due to hardening by absorption of water in GFRP and CFRP specimen. Flaking of epoxy matrix is shown in Fig. 5.53 as epoxy has dissolved away from surface protruding undamaged fibres are visible in CFRP and damaged fibres in GFRP.

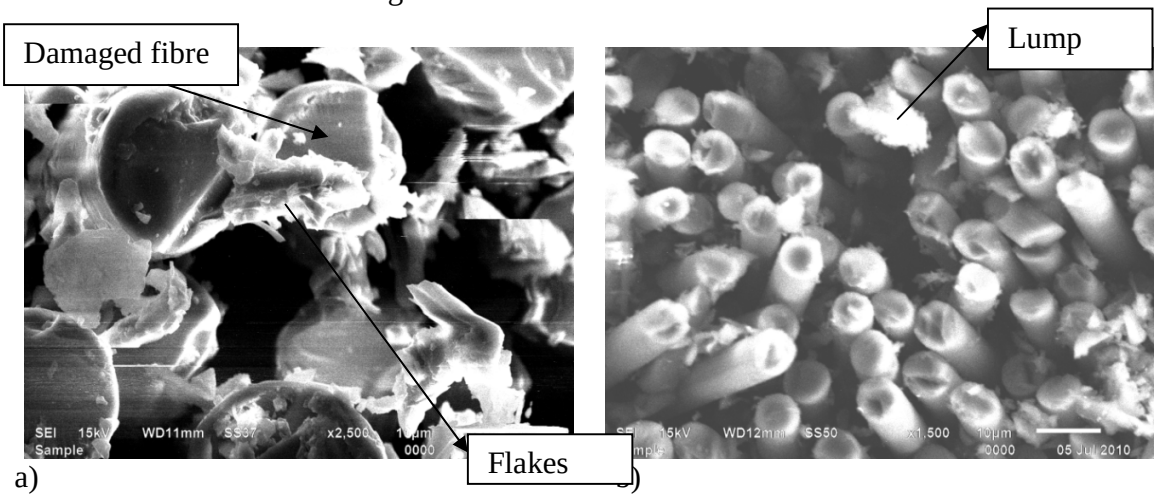


a) b)

**Fig. 5.53**: a) GFRP cross-section b)CFRP cross-section

The fibre was compared for various conditions it could be easily noticed that in water tank the percentage weight gain is increasing with respect to time indicating that more moisture is absorbed in almost all the specimen with few exceptions. Because of this the fibre surface is eaten up by epoxy with respect to time as shown in above Fig.5.53.

## 5.2.3. Image analysis by “IMAGE-J” analyzer software

The analysis of SEM specimen was done in order to compare the area fraction of both epoxy as well as the fibre. The commercially available software Image-J was used for analysis of images. Image-J is open source software developed by national institute of health and considered as powerful tool for image analysis. Few representative images after analysis by software are shown in figures below.

**Procedure followed for analysis of the SEM images is explained below**:

1. The image to be analyzed was opened in the software.
2. A line was drawn parallel to the 20µm line (shown on SEM images) using the Set Scale option. That distance was set equivalent to number of pixel (automatically counted by software).
3. Now as the scale was set a line was drawn across fibre edges to measure the length of fibre.
4. To calculate the area fraction, first image was converted to RGB colour (we could choose from various colour options, here we had used Red/Green colour to fill the areas of SEM image)
5. After applying above option the colour of image would change (from the grey scale to chosen Red/Green), in which red colour indicated the fibre area, green indicated epoxy and black was for voids. These areas were selected automatically by software according to the image contrast.
6. Using the process option from the software select binary and make the image as binary image.
7. To calculate the area fraction first tick the option of measure area fraction in set measurement menu. To measure the area fraction, the option Analyze →Measure was used. Area to be measured was selected by making a window around it and above mentioned. Analyze option showed the results in a tabular form.

### 5.2.3.1. Results for bending test laminated specimen

The SEM images were converted to Image J images as shown from Fig. 5.54 - Fig. 5.65.

**5.2.3.1.1**. SEM and image j images before start of the experiment

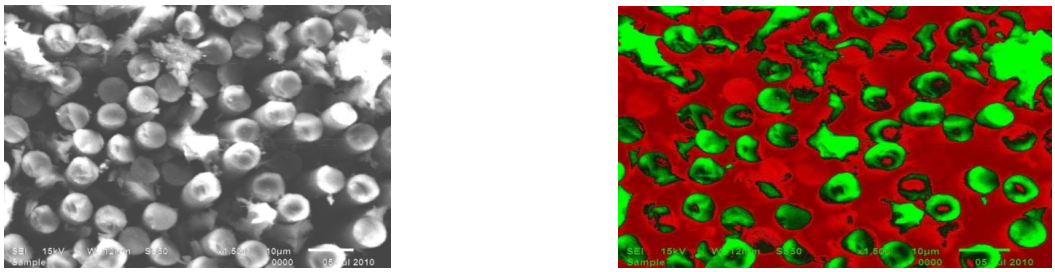

a) b)

**Fig. 5.54**: CFRP a) SEM image b) Image J analyser image before experimentation

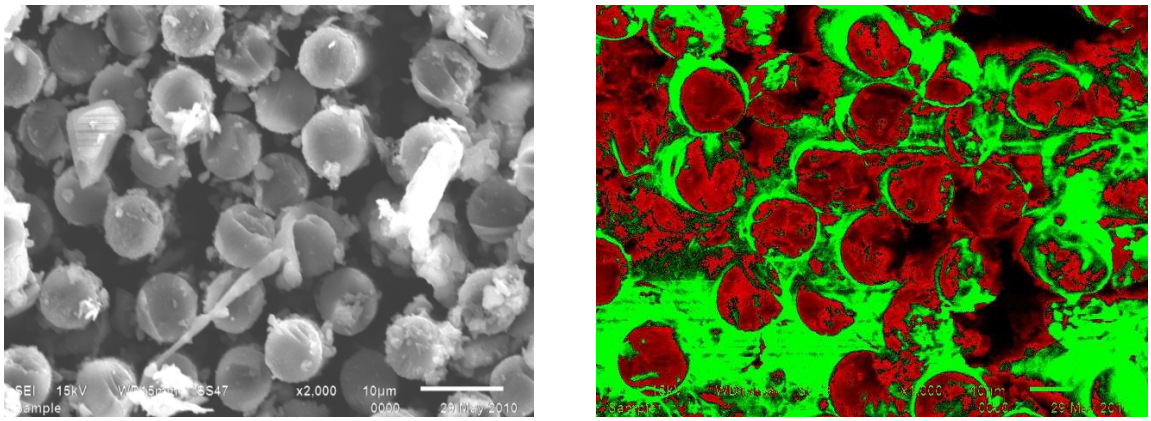


a) b)

**Fig. 5.55**:GFRP a) SEM image b) Image J analyser image before start of experiment

**5.2.3.1.2.** SEM images after one month

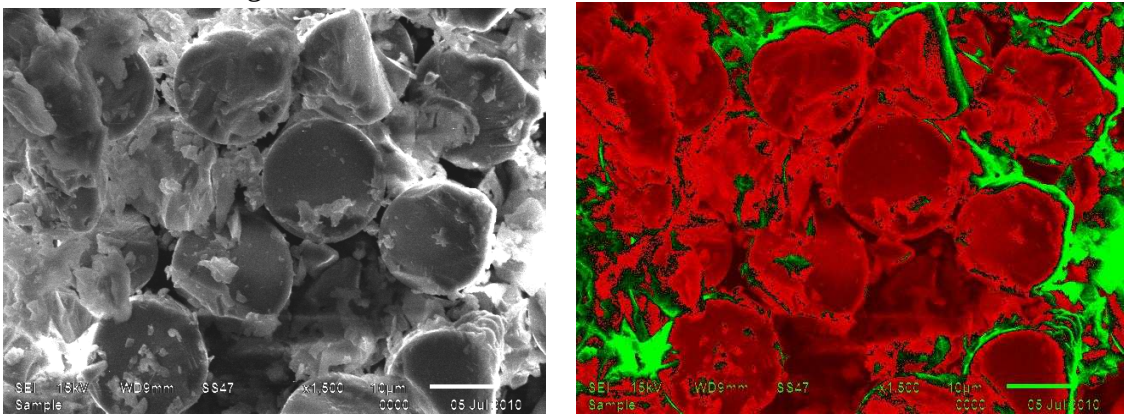


a) b)

**Fig. 5.56**:GFRP a) SEM image b) Image J analyser image after one month

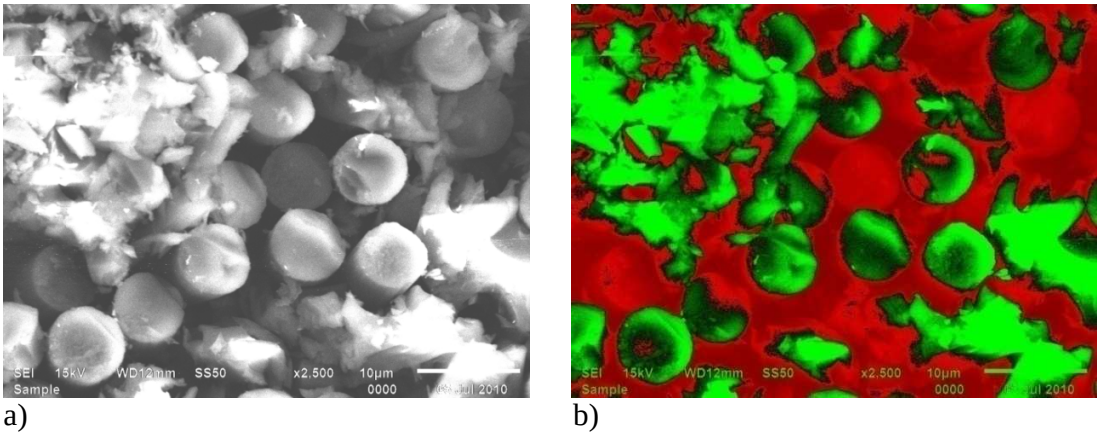


a) b)

**Fig. 5.57:**CFRP a) SEM image b) Image J analyser image after one month

**5.2.3.1.3.** SEM images after two months

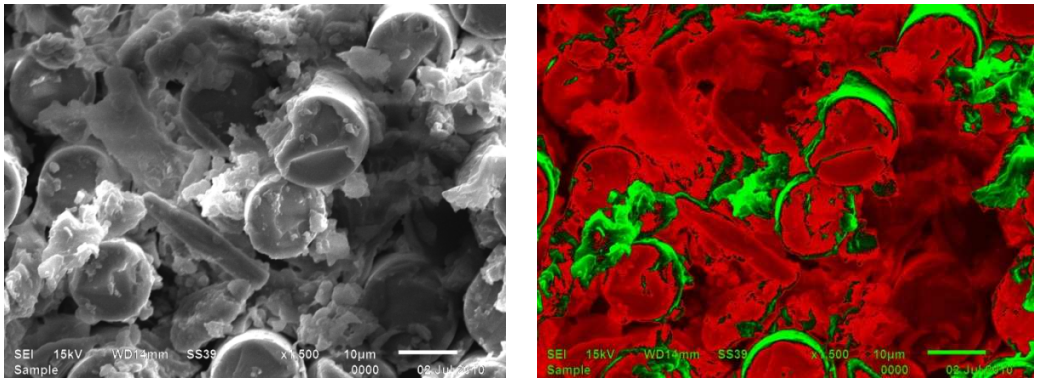

a) b)

**Fig. 5.58:**GFRP a) SEM image b) Image J analyser image after two months

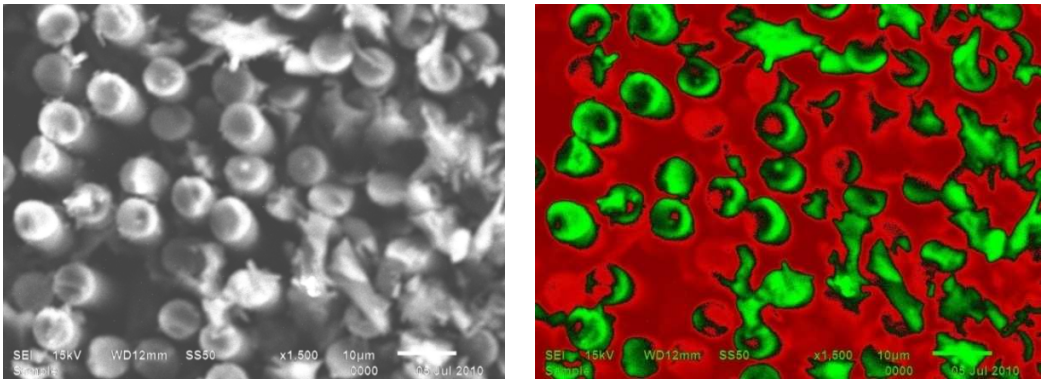

a) b)

**Fig. 5.59:**CFRP a) SEM image b) Image J analyser image after two months

**5.2.3.2. SEM results of tensile test of laminated specimen**

**5.2.3.2.1.** SEM images before start of the experiment

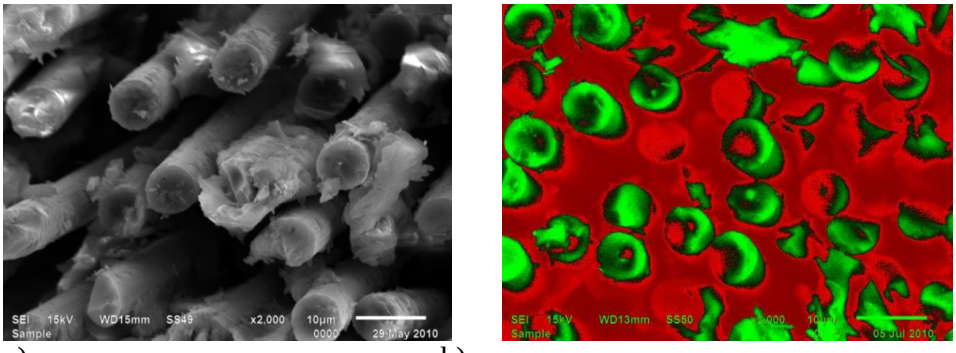

a) b)

**Fig. 5.60:**CFRP a) SEM image b) Image J analyser image before experimentation

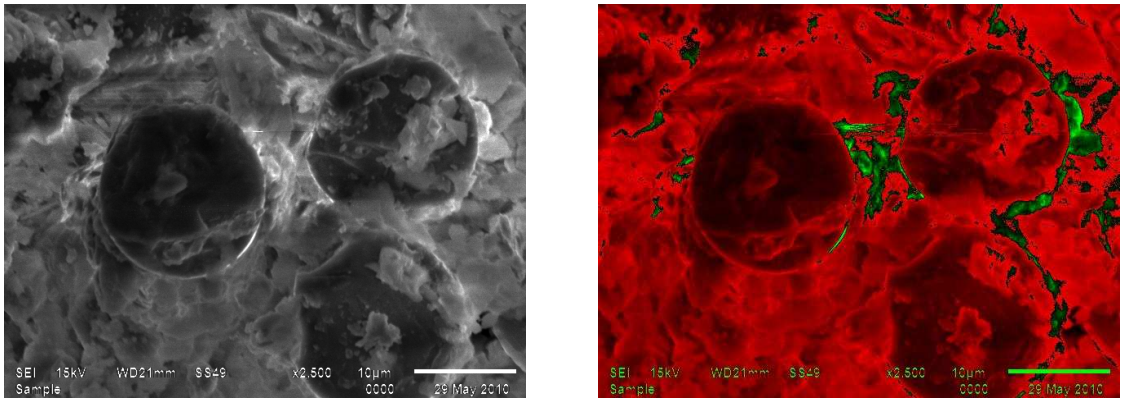

a) b)

**Fig. 5.61:**GFRP a) SEM image b) Image J analyser Image before experimentation

**5.2.3.2.2.** SEM images after one month

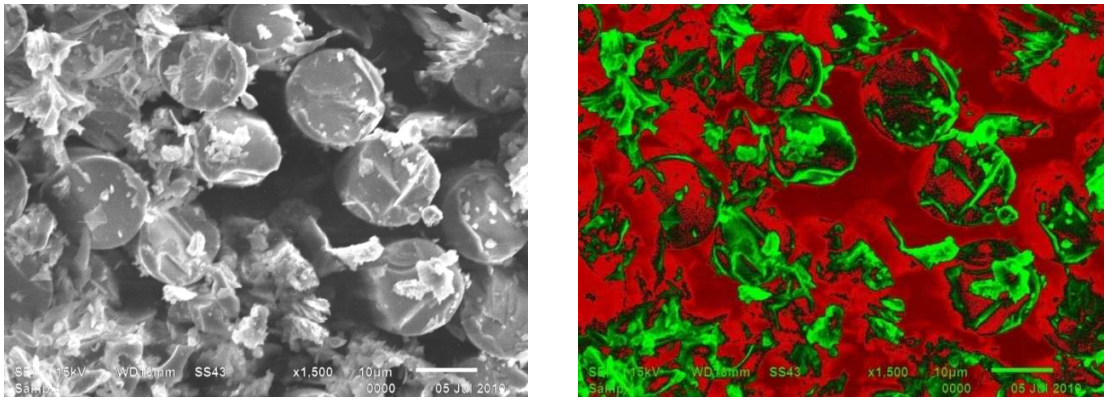

a) b)

**Fig. 5.62**:GFRP a) SEM image b) Image J analyser image after one month

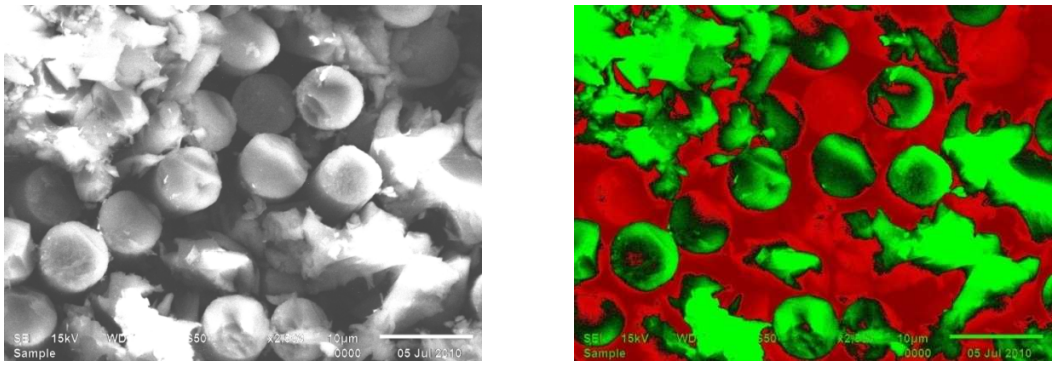

a) b)

**Fig. 5.63:**CFRP a) SEM image b) Image J analyser image after one month

**5.2.3.2.3**. SEM images after two months

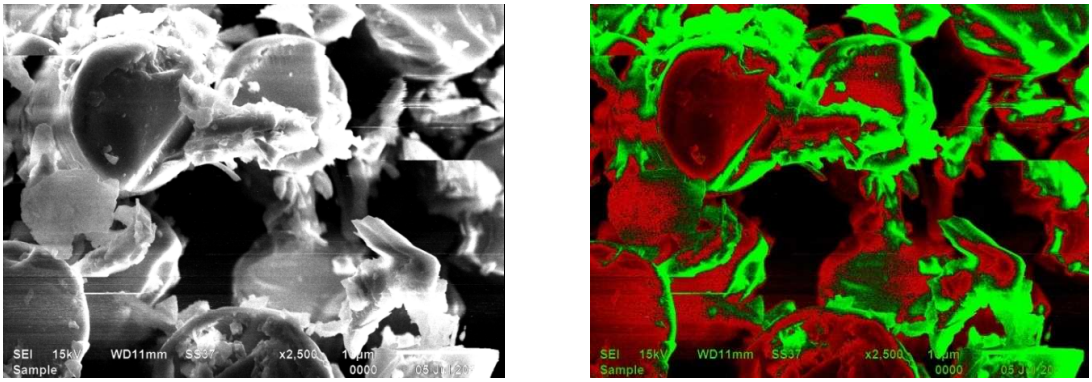

a) b)

**Fig. 5.64:**GFRP a) SEM image b) Image J analyser image after two months

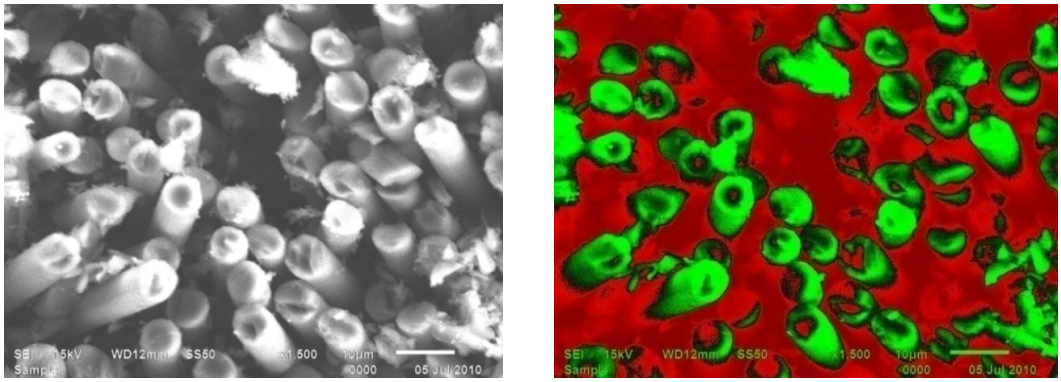

a) b)

**Fig. 5.65:** CFRP a) SEM image b) Image J analyser image after two months

## 5.2.3.3. Percentage Area fraction and circularity results by Image Analysis

### 5.2.3.3.1. Results of percentage area fraction

The graphs of percentage area fraction are depicted using the Table 5.24 and Table 5.25.

**Table 8.24:** Percentage Area fraction for bending specimen

| Time period | %Area fraction of fibre(GFRP) | %Area fraction of Fibre(CFRP) | % Area fraction of Epoxy(GFRP) | % Area fraction of Epoxy(CFRP) |
|---|---|---|---|---|
| initial | 69.2 | 68.8 | 30.8 | 31.2 |
| 30%loading (month 1) | 67.3 | 64.1 | 32.7 | 35.9 |
| 30%loading (month 2) | 67.8 | 57.8 | 42.2 | 42.2 |
| 50%loading (month1) | 67.3 | 60.7 | 32.7 | 39.3 |
| 50%loading (month2) | 60.9 | 51.3 | 39.1 | 48.7 |
| 70% loading (month1) | 66.2 | 62.6 | 33.8 | 37.4 |
| 70% loading (month2) | 65.8 | 63 | 34.2 | 37 |

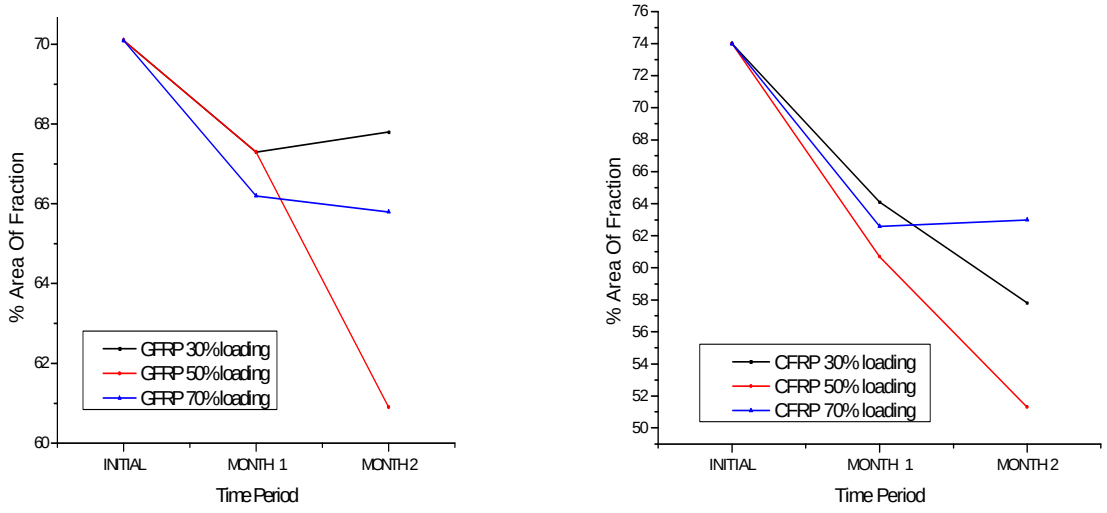


**a)** **b)**

**Fig. 5.66:** Graphs for percentage Area fraction of fibre GFRP and CFRP laminates

**Table 5.25:** Percentage Area fraction for tensile specimen

| Time period | %Area fraction of fibre(GFRP) | %Area fraction of Fibre(CFRP) | % Area fraction of Epoxy(GFRP) | % Area fraction Epoxy(CFRP) |
|---|---|---|---|---|
| initial | 74.3 | 69.6 | 25.7 | 30.4 |
| 30%loading (month 1) | 67.8 | 64.1 | 35.9 | 35.9 |
| 30%loading (month 2) | 66.7 | 63 | 33.3 | 37 |
| 50%loading (month1) | 60.9 | 63 | 39.1 | 37 |
| 50%loading (month2) | 58.2 | 60.7 | 41.8 | 39.3 |
| 70% loading (month1) | 68.8 | 69.6 | 31.2 | 30.4 |
| 70% loading (month2) | 51.5 | 67 | 48.5 | 33 |

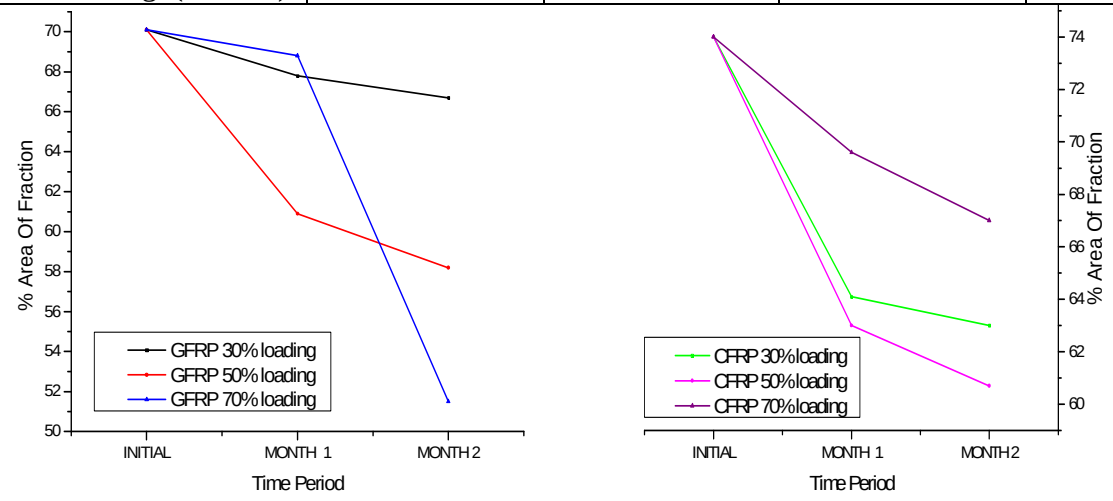


**a)** **b)**

**Fig. 5.67:** Graphs for percentage Area fraction of a) GFRP laminates b) CFRP laminates

The GFRP bending specimen percentage area fraction for 50% UFL GFRP specimen was decreasing as shown in Fig 5.66(a).The 70% UFL CFRP bending specimen percentage area fraction is almost same after one month as shown in Fig 5.66(b).

The GFRP tensile specimen percentage area fraction for 70% UTL GFRP specimen is decreasing after one month and is almost same in other loaded specimen as shown in Fig 5.67(a).Incase of CFRP tensile specimen percentage area fraction is almost same after one month as shown in Fig. 5.67(b).

### 5.2.3.3.3. Results of Circularity

**Table 5.26:** Circularity results for various bending specimen

| Time period | Circularity(GFRP) | Circularity(CFRP) |
|---|---|---|
| initial | 1 | 1 |
| 30%loading (month 1) | 0.906 | 0.933 |
| 30%loading (month 2) | 0.897 | 0.923 |
| 50%loading (month1) | 0.927 | 0.92 |
| 50%loading (month2) | 0.889 | 0.916 |
| 70% loading (month1) | 0.91 | 0.929 |
| 70% loading (month2) | 0.892 | 0.904 |

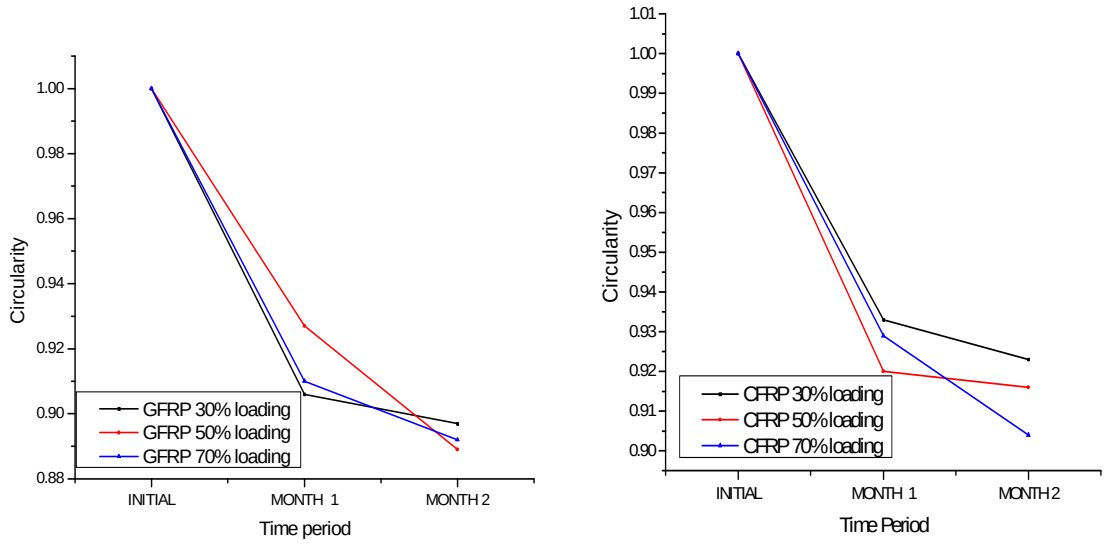


a) b)

**Fig. 5.68:** Graphs for circularity of fibre a) GFRP laminates b) CFRP laminates

**Table 5.27:** Circularity results for various tensile specimen

| Time period | Circularity(GFRP) | Circularity(CFRP) |
|---|---|---|
| initial | 1 | 1 |
| 30%loading (month 1) | 0.933 | 0.926 |
| 30%loading (month 2) | 0.923 | 0.912 |
| 50%loading (month1) | 0.92 | 0.934 |
| 50%loading (month2) | 0.916 | 0.922 |
| 70% loading(month1) | 0.929 | 0.928 |
| 70% loading(month2) | 0.904 | 0.923 |

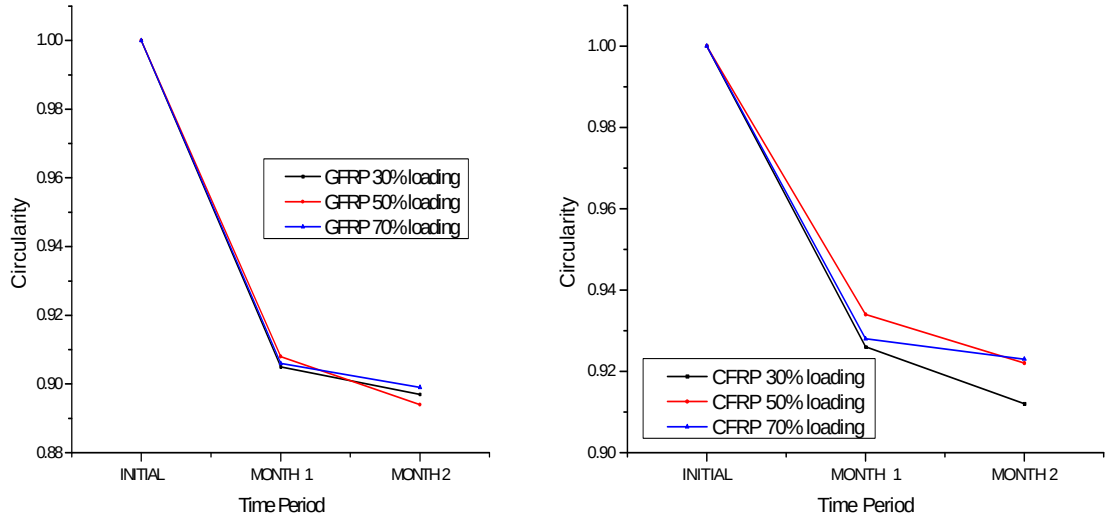


**a)** **b)**

**Fig. 5.69:** Graphs for circularity of fibre a) GFRP laminates b) CFRP laminate

The area fraction of specimen is compared in for epoxy and for fibres. From comparison of epoxy fractions it is clearly seen that it is increasing with time as there is considerable increase after two month compared to one month. But the trend is seen to be opposite in fibre fraction comparison. Here the fibre fraction is increasing in first month and decreased in second month. All the specimen loaded at different value shows the same trend when compared between one and two month. The reason for such a trend seems to be that fibre in total area is degrading with heat and moisture attack and epoxy seems to have expanded with above effect which obviously leaves more area for epoxy as compared to fibre. The circularity of fibres was decreasing when compared to initial. But the circularity of fibre is almost same for CFRP specimen as shown in Fig. 5.69.

### 5.2.5. Micro hardness test results of laminated specimen

**5.2.5.1.** Micro hardness test results of bending specimen

**Table 5.28:** Micro hardness results in GFRP laminated specimen

| Time period | GFRP 30% loading | GFRP Without load | GFRP 70%loading | GFRP 50% loading |
|---|---|---|---|---|
| 3 | 14.75 | 13.78 | 15.71 | 12.85 |
| 6 | 12.81 | 12.56 | 13.63 | 12.79 |
| 9 | 11.95 | 11.92 | 12.97 | 11.60 |
| 10 | 11.12 | 11.42 | 12.24 | 11.10 |
| 12 | 10.42 | 10.84 | 11.55 | 10.88 |
| 20 | 10.34 | 10.60 | 10.93 | 9.74 |
| 25 | 10.16 | 10.03 | 10.44 | 9.70 |
| 30 | 9.96 | 9.69 | 9.66 | 9.58 |
| 40 | 9.66 | 9.55 | 9.42 | 9.01 |
| 50 | 8.22 | 9.36 | 8.63 | 8.91 |

**Table 5.29:** Micro hardness results in CFRP laminated specimen

| Time period | CFRP 30%loading | CFRP 50%loading | CFRP 70%loading | CFRP without load |
|---|---|---|---|---|
| 3 | 14.53 | 15.84 | 12.84 | 12.79 |
| 6 | 11.70 | 10.66 | 11.91 | 12.22 |
| 9 | 11.35 | 10.63 | 11.46 | 12.07 |
| 10 | 10.66 | 10.51 | 11.25 | 11.23 |
| 12 | 10.59 | 14.50 | 11.15 | 10.94 |
| 20 | 10.44 | 10.31 | 10.84 | 10.37 |
| 25 | 9.41 | 10.27 | 9.90 | 9.96 |
| 30 | 9.39 | 9.38 | 9.48 | 8.75 |
| 40 | 8.94 | 8.49 | 9.33 | 8.69 |
| 50 | 8.40 | 7.11 | 9.07 | 8.60 |

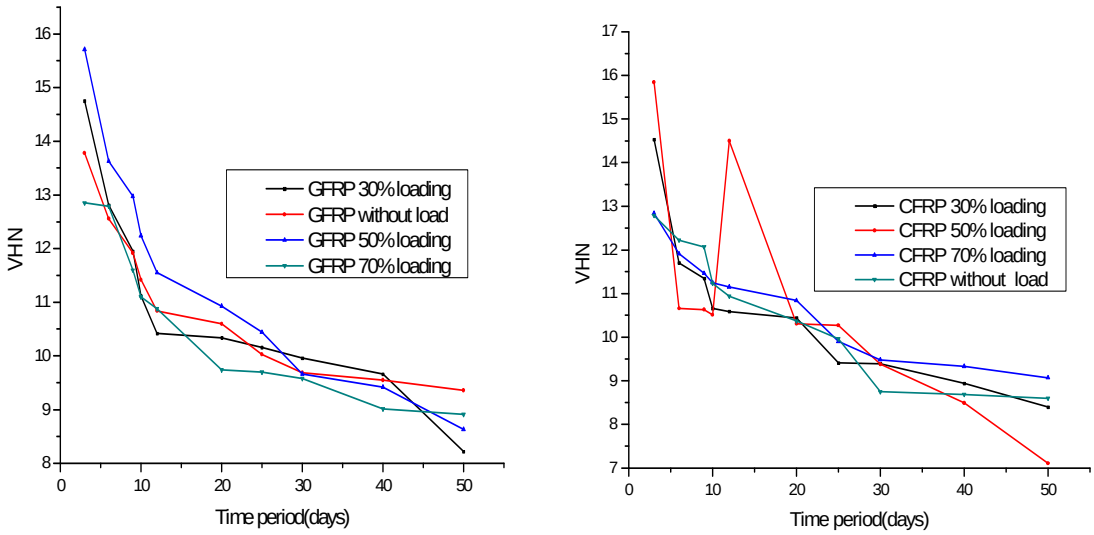


**a)** **b)**

**Fig. 5.70:** Comparison of micro hardness of a) GFRP laminates b) CFRP laminates

The Micro hardness readings of GFRP and CFRP laminated specimen decreased when compared to initial reading before hygrothermal treatment due to hardening of epoxy with absorption of water as shown in Fig. 5.70 which depicted using the Table 5.28 and Table 5.29. The micro hardness of GFRP specimen is same at the end of exposure duration.

**5.2.5.2.** Micro hardness test results of tensile specimen

**Table 5.30: Micro hardness in GFRP laminated specimen**

| Time period | GFRP 30% loading | GFRP without load | GFRP 70%loading | GFRP 50% loading |
|---|---|---|---|---|
| 3 | 16.72 | 12.42 | 14.31 | 16.38 |
| 6 | 11.78 | 11.72 | 12.89 | 13.92 |
| 9 | 11.60 | 11.06 | 11.52 | 12.42 |
| 10 | 11.43 | 10.55 | 11.11 | 11.66 |
| 12 | 11.09 | 10.34 | 10.96 | 11.10 |
| 20 | 10.44 | 10.16 | 10.23 | 10.92 |
| 25 | 9.66 | 9.75 | 9.43 | 10.37 |
| 30 | 9.64 | 9.46 | 9.39 | 9.70 |
| 40 | 9.52 | 9.46 | 9.36 | 9.60 |
| 50 | 7.88 | 9.43 | 8.93 | 9.38 |

**Table 5.31:** Micro hardness in CFRP laminated specimen

| Time period | CFRP 30% loading | CFRP 50% loading | CFRP 70% loading | CFRP without load |
|---|---|---|---|---|
| 3 | 15.98 | 12.26 | 14.75 | 11.85 |
| 6 | 15.16 | 12.22 | 12.02 | 11.43 |
| 9 | 13.22 | 12.15 | 10.68 | 10.81 |
| 10 | 12.82 | 11.72 | 10.07 | 10.06 |
| 12 | 11.72 | 9.80 | 9.77 | 9.47 |
| 20 | 10.36 | 9.70 | 9.32 | 9.46 |
| 25 | 9.18 | 9.66 | 9.00 | 9.04 |
| 30 | 9.13 | 9.36 | 8.79 | 8.75 |
| 40 | 9.08 | 8.60 | 8.56 | 8.55 |
| 50 | 8.53 | 8.41 | 8.15 | 8.54 |

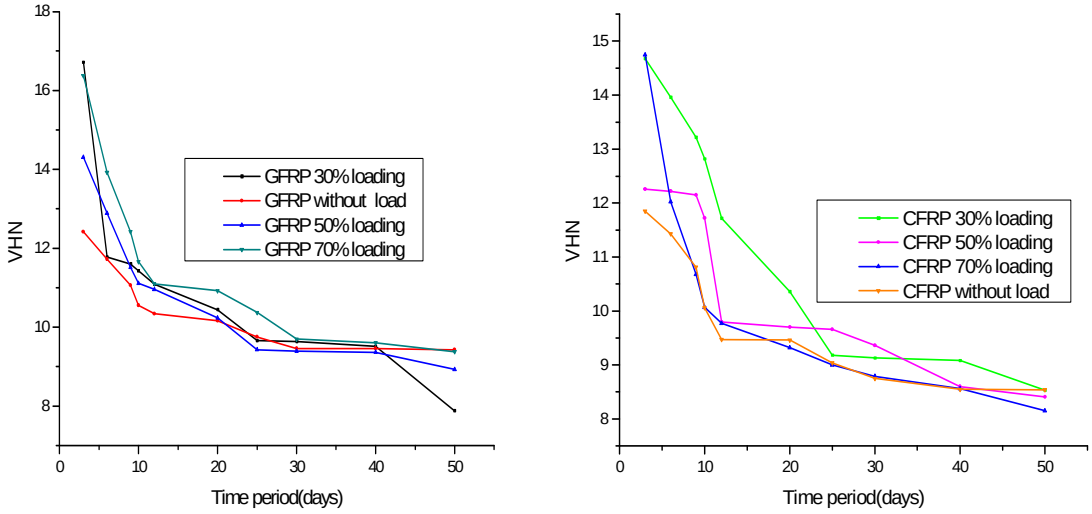


**a)** **b)**

**Fig. 5.71:** Comparison of micro hardness of a) GFRP laminates b) CFRP laminates

The Micro hardness of GFRP and CFRP laminated specimen decreased when compared to initial reading before hygrothermal treatment due to hardening of epoxy with absorption of water as shown in Fig. 5.71 which was depicted using the Table 5.30 and Table 5.31. The hardness graph of GFRP specimen is almost same at the end as saturation is attained. But CFRP specimen has not attained saturation as the absorption of moisture for CFRP specimen is slow as compared to GFRP.

### 5.2.5.3. Micro hardness test results of pure epoxy specimen

**Table 5.32:** Micro hardness in epoxy specimen

| Time period | Temperature 45°c | Temperature 55°c | Room temperature |
|---|---|---|---|
| 3 | 1.91E+00 | 1.99E+00 | 1.94E+00 |
| 6 | 1.90E+00 | 1.68E+00 | 1.85E+00 |
| 9 | 1.78E+00 | 1.57E+00 | 1.65E+00 |
| 12 | 1.62E+00 | 1.53E+00 | 1.51E+00 |

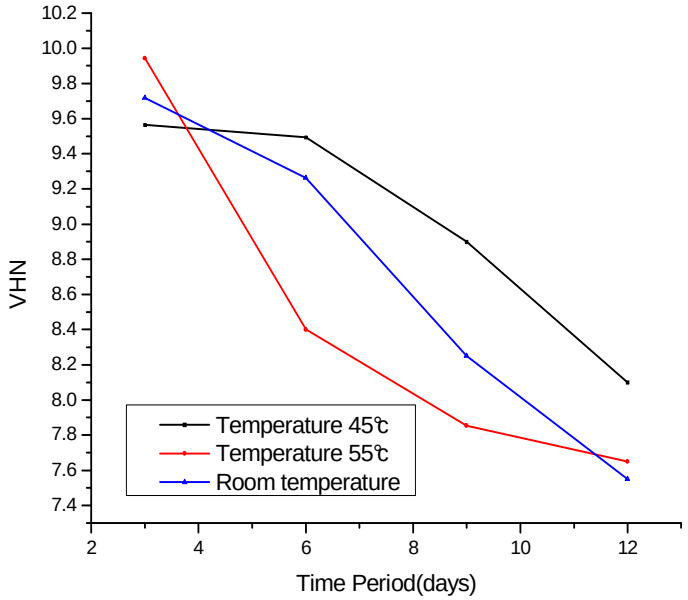


**Fig. 5.72:** Comparison of micro hardness of epoxy specimen w.r.t. time

The Micro hardness readings of epoxy specimen were depicted using the Table 5.32. decreased when compared to initial reading before hygrothermal treatment due to hardening of epoxy with absorption of water a shown in Fig. 5.72.

## 5.2.6. Relationship between macroscopic and microscopic behavior

Parameters related in this were tensile strength, Flexural strength, percentage weight gain, capacitance with percentage area fraction of fibre and micro hardness.

### 5.2.6.1. For bending specimen

#### 5.2.6.1.1. Comparison of Flexural strength with Micro hardness

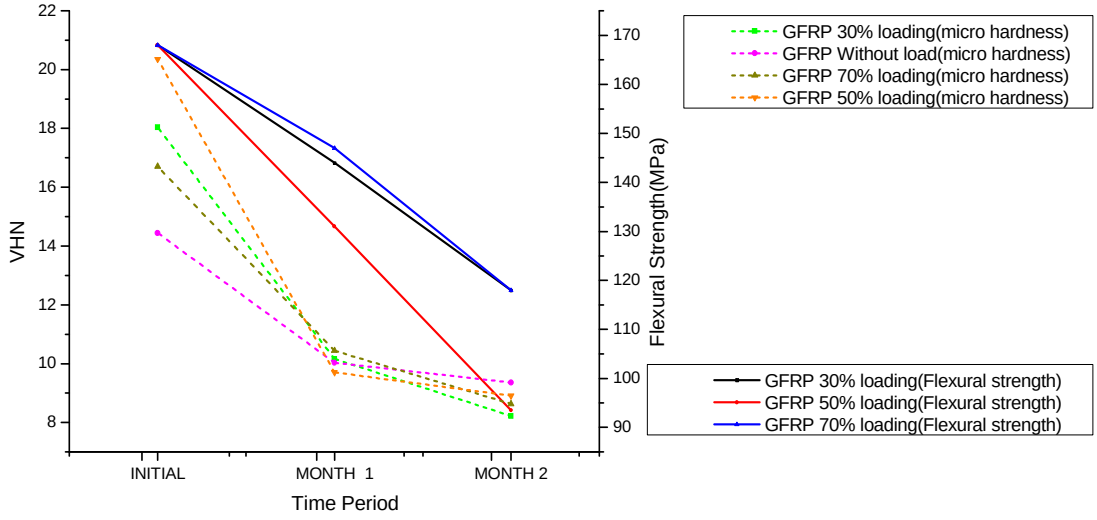


a)

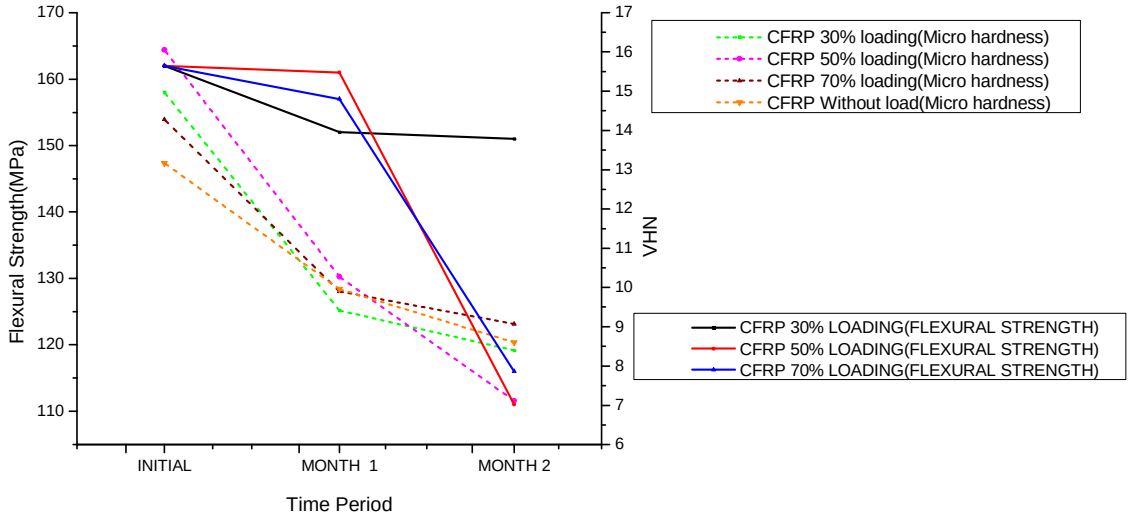


**b)**

**Fig. 5.73:** Comparison of micro hardness and flexural strength of a) GFRP laminates b) CFRP laminates

The reduction in flexural strength is considerably large in almost all the specimen immersed in water tank $T_2$ as compared to the initial specimen flexural strength. There was reduction in micro hardness with decrease in strength of the laminate as shown in Fig. 5.73. From the above graph CFRP 30% UFL specimen has flexural strength almost same after one month. With the decrease in strength of GFRP specimen the micro hardness values were decreasing as shown in Fig.5.73 (a).

### 5.2.6.1.2. Comparison of Flexural strength with percentage Area fraction of fibre

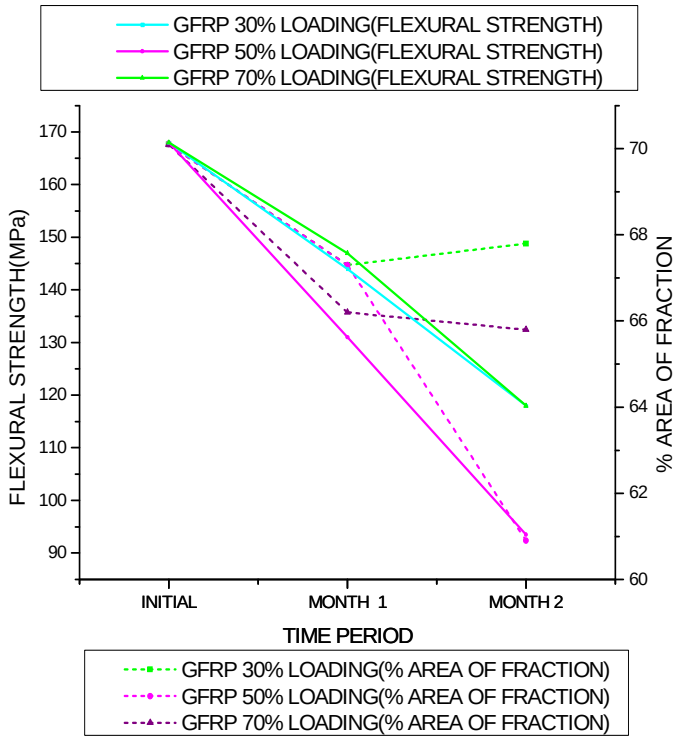


a)

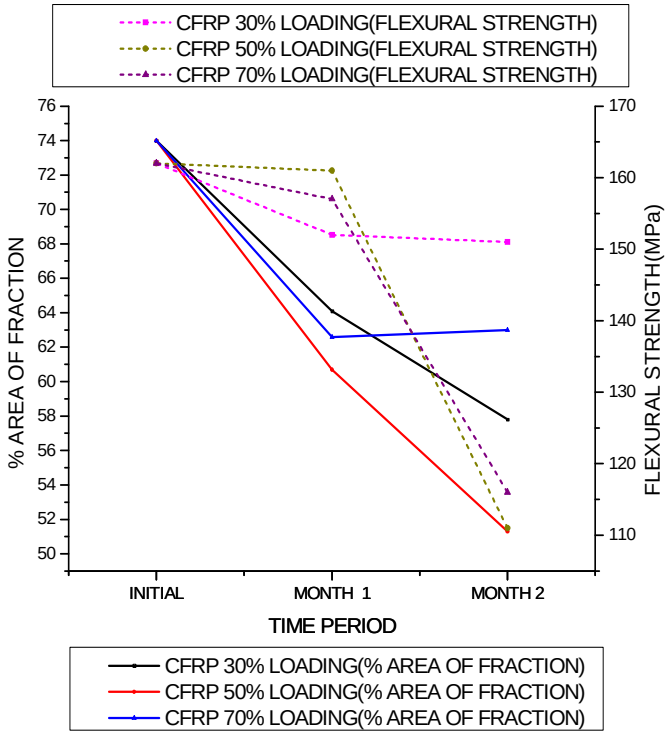


**b)**

**Fig. 5.74:** Comparison of percentage area fraction and flexural strength of a) GFRP laminate b) CFRP laminate

From the above Fig. 5.74 we can see that the flexural strength decrease caused fibre area fraction reduction as shown above. The flexural strength of 50% UFL GFRP specimen decreased more as a result percentage area fraction of fibre was decreased. During first month the flexural strength of specimen are relatively same as initial incase of CFRP specimen, GFRP specimen had more degradation as an affect the flexural strength decreased in first month and the area fraction fibre is also reducing. Maximum degradation had taken place in second month in both CFRP and GFRP specimen. The 30%UFL and 50% UFL GFRP specimen had almost same area fraction after one month.

### 5.2.6.1.3. Comparison of Flexural modulus with percentage Area fraction of fibre

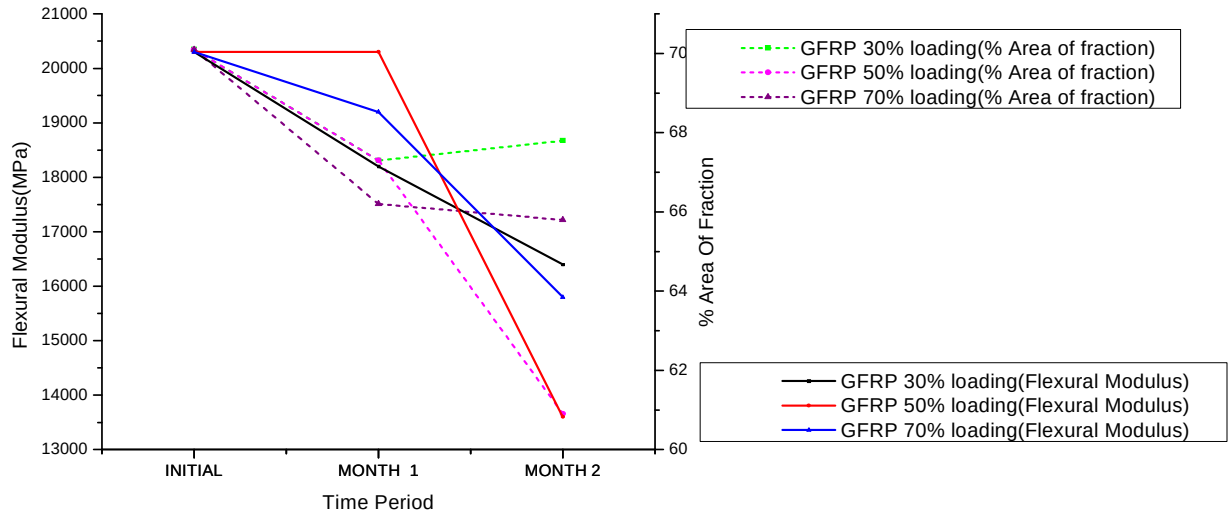


a)

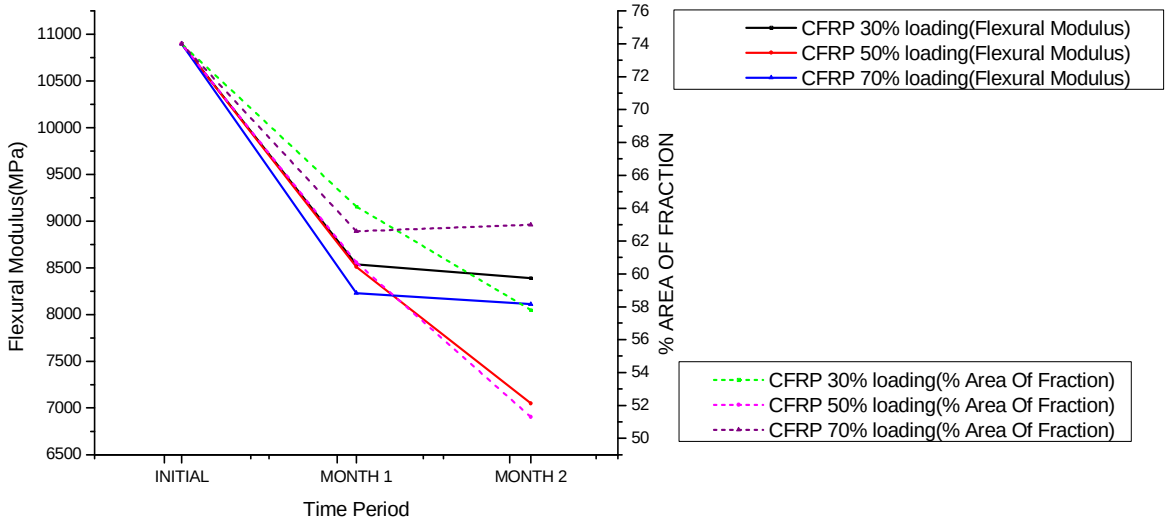


**b)**

**Fig. 5.75:** Comparison of Flexural modulus with percentage Area fraction of fibre of a) GFRP laminates b) CFRP laminate

In case of GFRP specimen the flexural modulus is linear up to first month and a sudden fall in the graph during the second month, where as the CFRP specimen had flexural modulus

less in first month when compared to initial and modulus decreased regularly. The area fraction of fibre decreased up to first month and almost same up to second month in case of CFRP specimen.

The 50% UFL CFRP specimen has decrease in flexural modulus after one month when compared to other specimen as shown in Fig. 5.75. The percentage area fraction of 50% UFL CFRP specimen is less as compared to other specimen.

### 5.2.6.1.3. Comparison of percentage Weight gain and percentage Area fraction of fibre

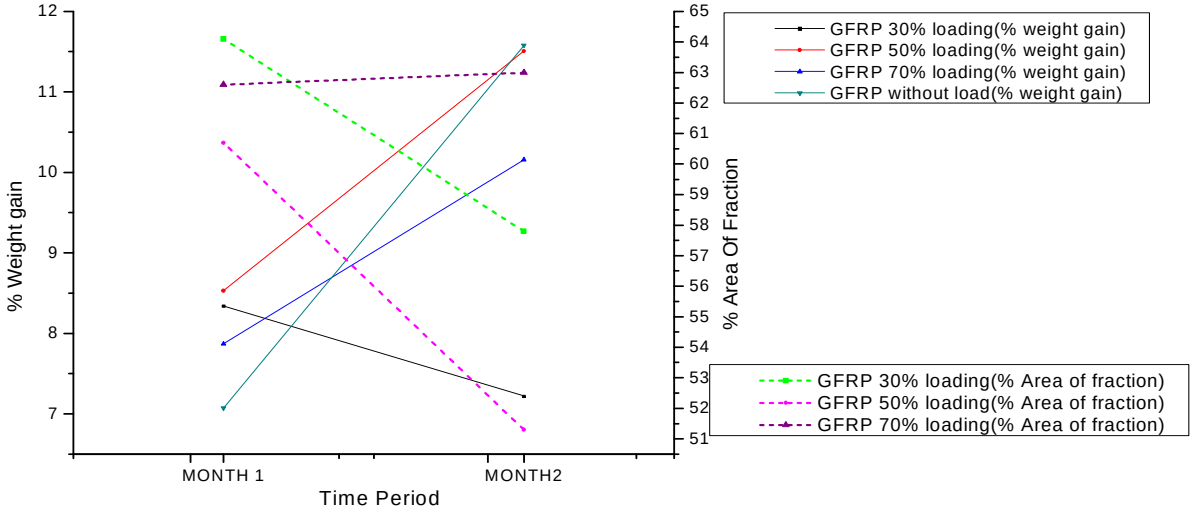


a)

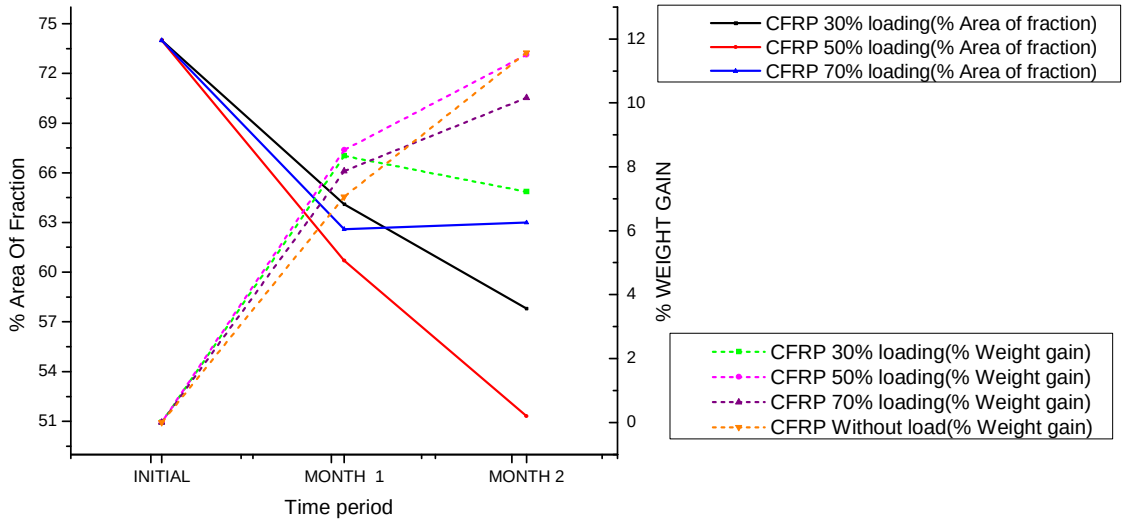


**b)**

**Fig. 5.76:** Comparison of percentage weight gain with percentage Area fraction of fibre of a) GFRP laminates b) CFRP laminates

From the Fig. 5.76 it is clearly shown that as percentage weight gain increases the percentage area fraction of fibre decreases due degradation of fibre, voids formation in the specimen. In case of 70% UFL specimen the area of fibre reduction is comparatively low in second month when compared to other specimen. The 70% UFL of CFRP and GFRP specimen percentage area fraction of fibre showed a liner graph after one month as shown in Fig. 5.76.

### 5.2.6.1.4. Comparison of %Weight gain and Micro hardness

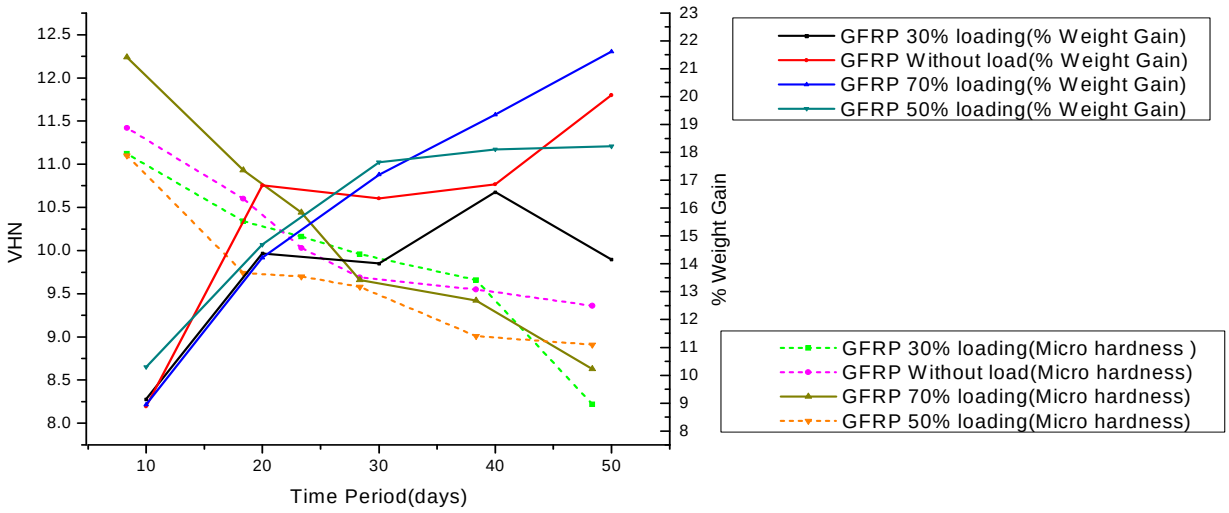


a)

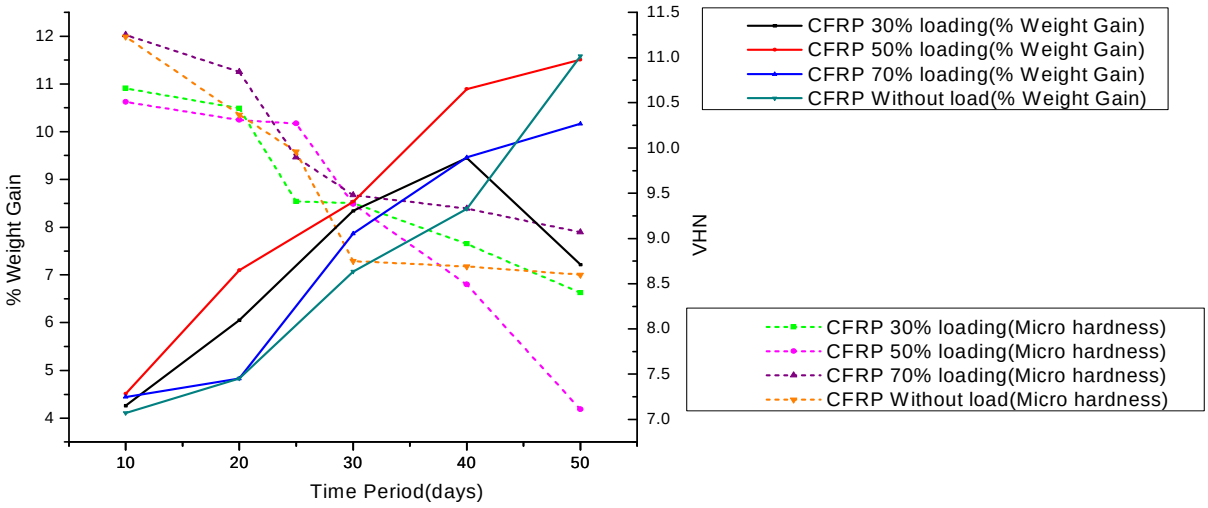


b)

**Fig. 5.78:** Comparison of percentage weight gain with Micro hardness of a) GFRP laminates b) CFRP laminates

From the Fig. 5.78 it is clearly shown that as percentage weight gain increases VHN of fibre decreases relatively due to water absorption through the pores of epoxy. The 30% UFL

specimen fall in the graph after 40 days in both GFRP and CFRP specimen. The 50% UFL specimen area fraction of fibre is less compared all other specimen.

### 5.2.6.1.6. Comparison of capacitance with Micro Hardness

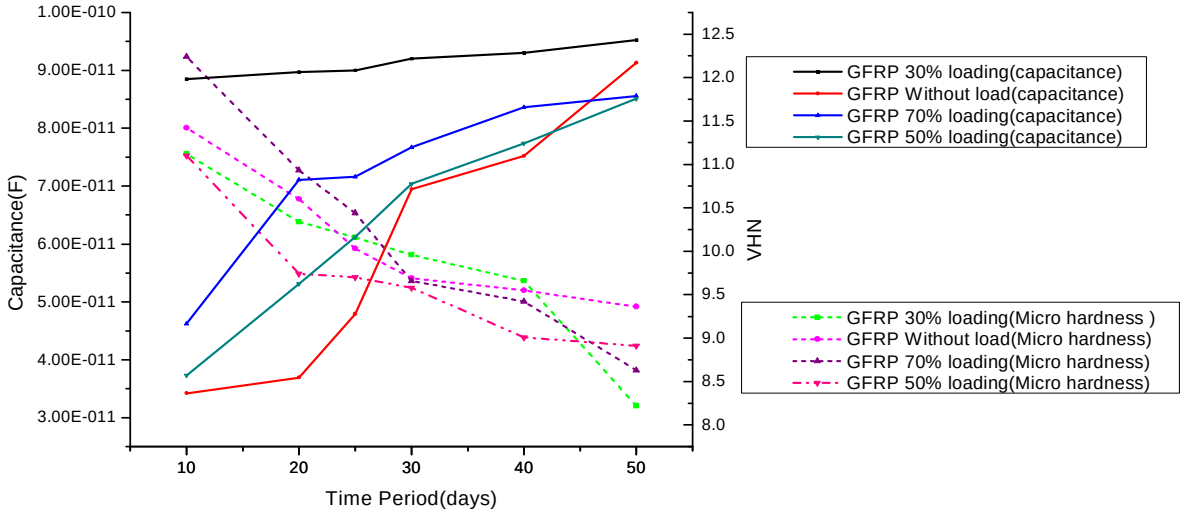


**Fig. 5.79:** Comparison of capacitance with Micro hardness of GFRP laminates

### 5.2.6.1.7. Comparison of capacitance with Micro hardness

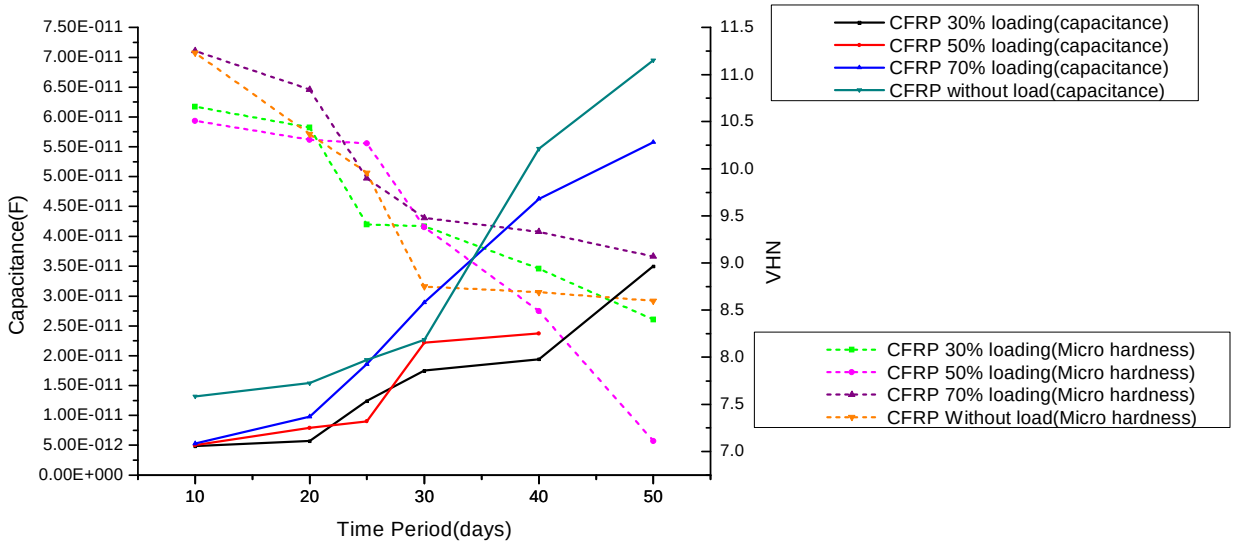


**Fig. 5.80:** Comparison of capacitance with Micro hardness of CFRP laminates

From the Fig. 5.80 it is clearly shown that as Capacitance increases, the Micro hardness of fibre decreases due degradation of fibre, voids formation in the specimen. The micro hardness was constant in all specimen but the hardness of 50% UFL CFRP specimen is decreasing after 50 days.so,saturation limit has not occurred for this specimen as moisture

absorption is slow for CFRP specimen. The 50%UFL GFRP specimen capacitance increased linearly as shown in Fig. 5.80.

### 5.2.6.1.8. Comparison of percentage capacitance increase with percentage Area fraction

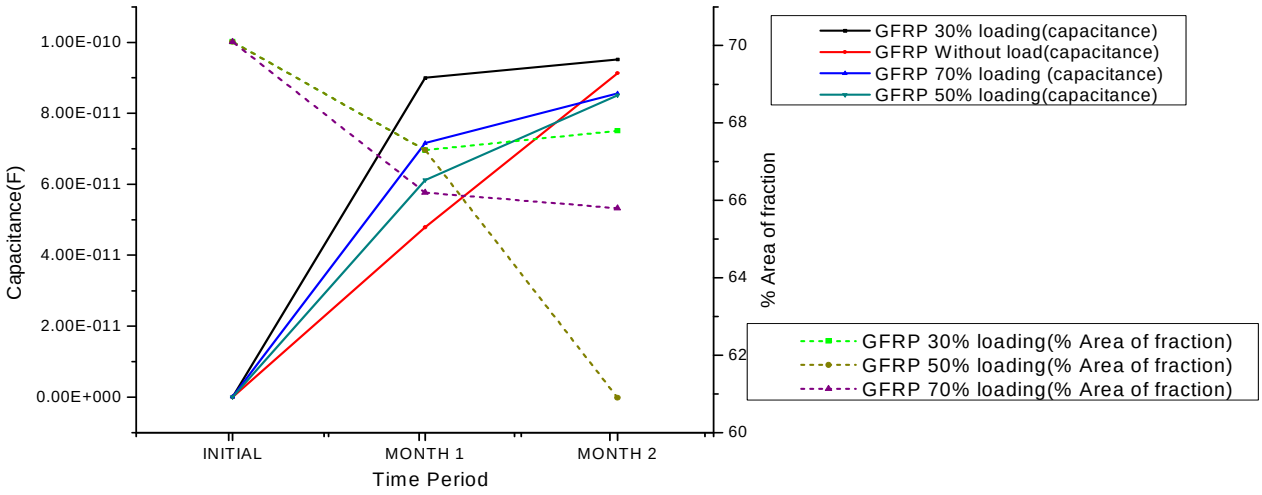


**Fig. 5.81:** Comparison of capacitance with percentage Area fraction of fibre of GFRP specimen

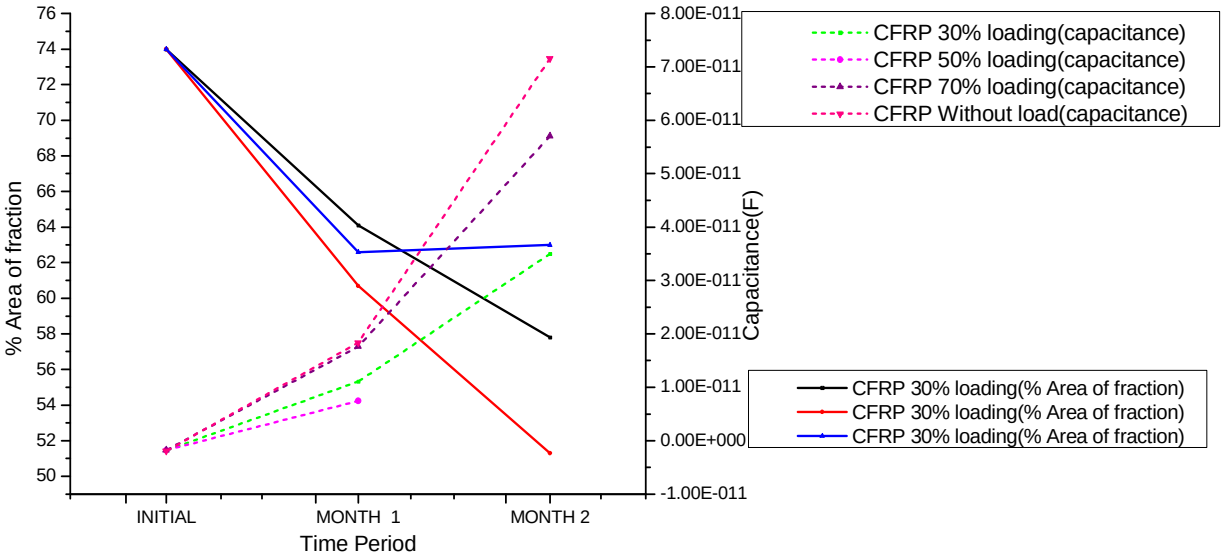


**Fig. 5.82:** Comparison of capacitance with percentage Area fraction of fibre of CFRP specimen

From the Fig. 5.82 and Fig. 5.81 it is clearly shown that as percentage capacitance increases the percentage area fraction of fibre decreases due degradation of fibre, voids formation in the specimen. In both the above figures it is clearly seen that the 50% UFL GFRP specimen

degradation is more comparatively all other specimen. The area fraction of CFRP specimen after one month is almost same as shown in Fig. 5.82.

## 5.2.6.2. For Tensile specimen

### 5.2.6.2.1. Comparison of tensile strength with Micro hardness

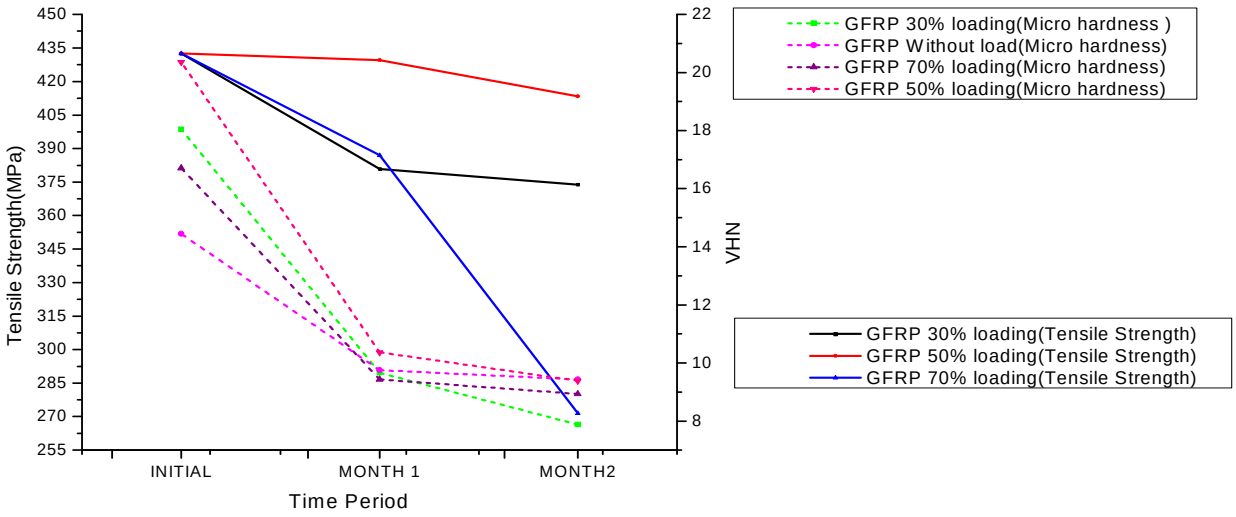


**Fig. 5.83:** Comparison of tensile strength with Micro hardness of various GFRP specimen

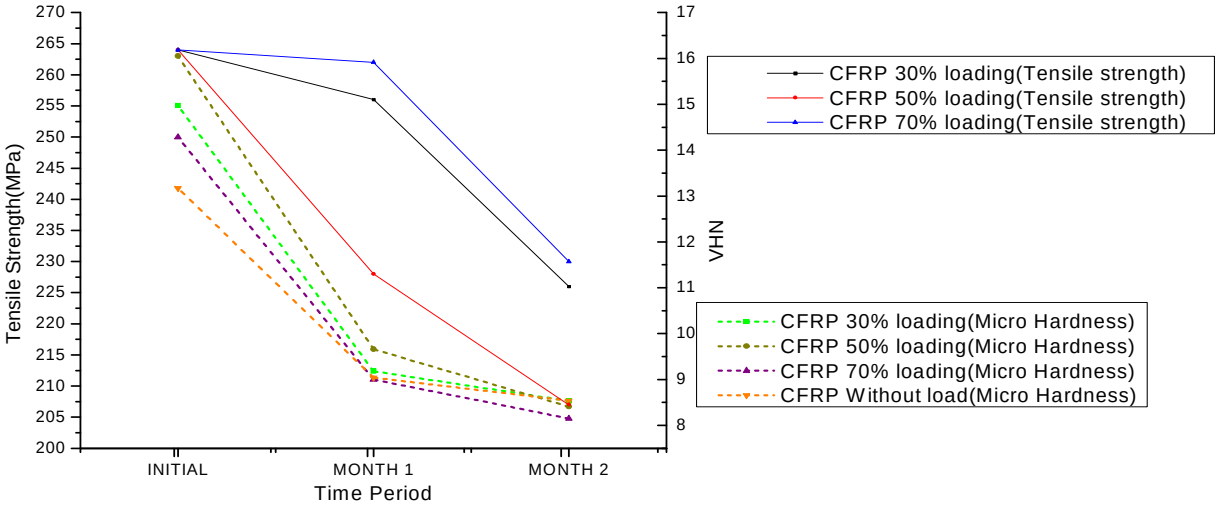


**Fig. 5.84:** Comparison of tensile strength with Micro hardness of various CFRP specimen

The reduction in tensile strength is considerably more in almost all the specimen immersed in water tank $T_2$ as compared to the initial specimen tensile strength. The reduction in micro hardness is also taking place as strength of the laminate is decreasing as shown in above Fig.

5.83 and Fig. 5.84. The 70% UTL GFRP specimen had sudden fall of tensile strength when compared to other specimen.

### 5.2.6.2.2. Comparison of tensile strength with percentage Area fraction

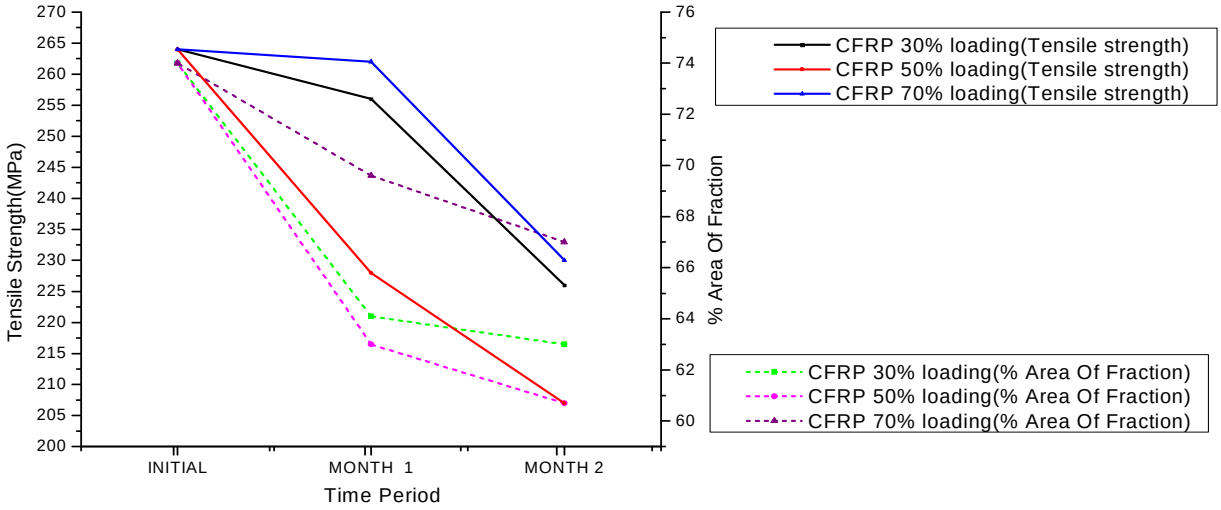


**Fig. 5.85:** Comparison of tensile strength with percentage area fraction of various CFRP specimen

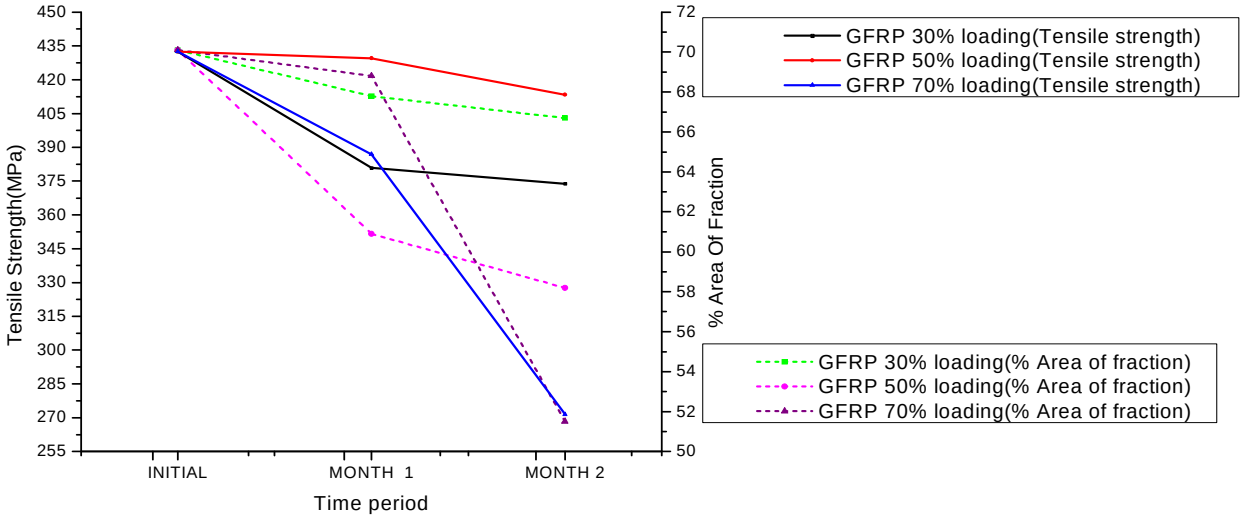


**Fig. 5.86:** Comparison of tensile strength with percentage area fraction of various GFRP specimen

From the above Fig 5.85 and Fig. 5.86 we can show how the tensile strength decrease causes fibre area fraction decrease as shown .the decrease in flexural strength of 70% UTL GFRP specimen and relative percentage area fraction of fibre had coincided, because as strength decreases the fibres get damaged and area fraction of fibre become very less.

### 5.2.6.2.3. Comparison of tensile Modulus with percentage Area fraction

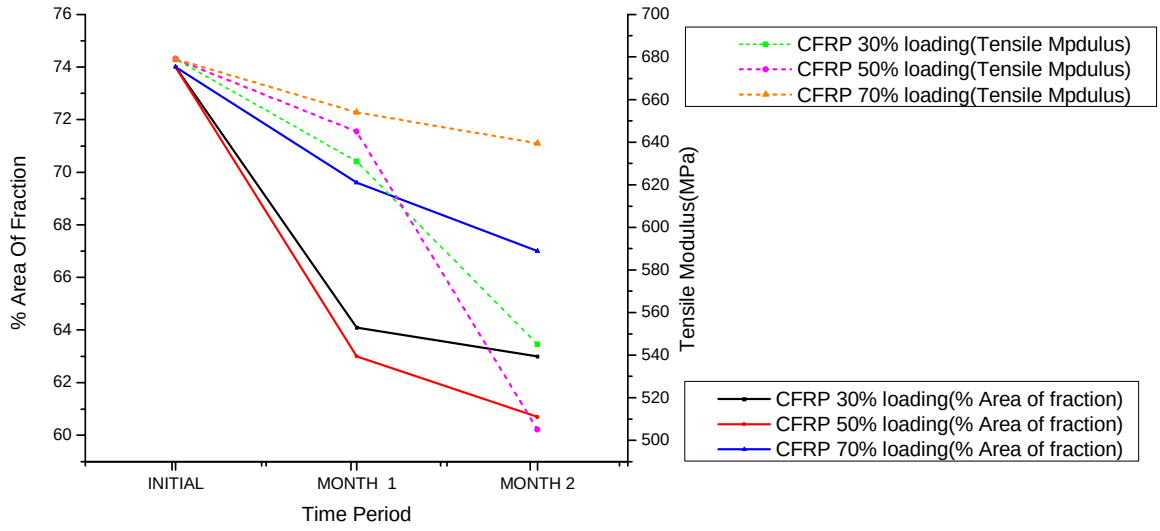


**Fig. 5.87:** Comparison of tensile modulus with percentage area fraction of various CFRP specimen

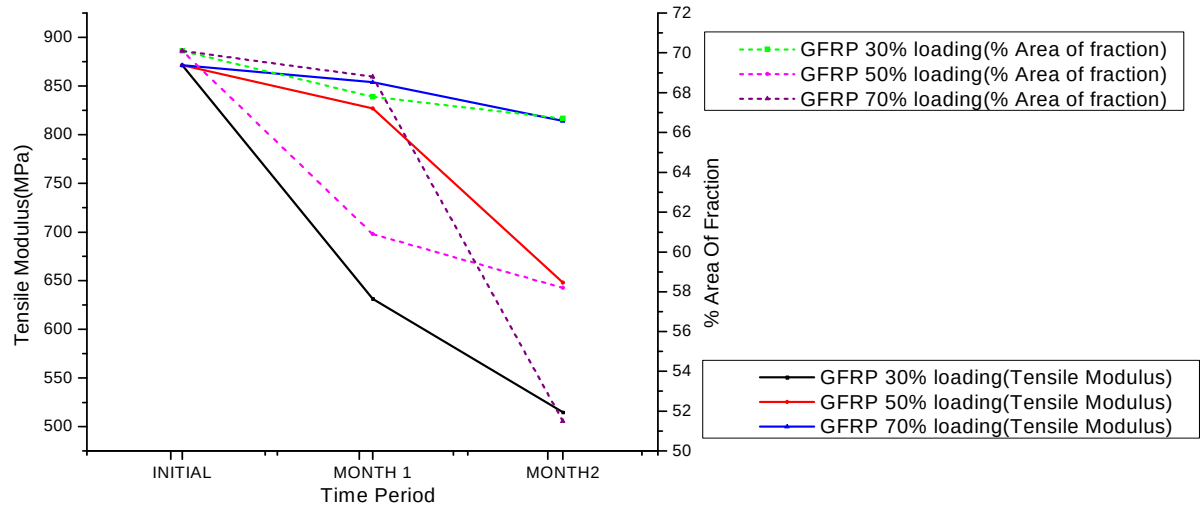


**Fig. 5.88:** Comparison of tensile modulus with percentage area fraction of various GFRP specimen

The tensile modulus of specimen were decreasing with time, the tensile modulus of 70% UTL GFRP is more and the relative area fraction is very less when compared to other specimen in second month. The 50% UTL CFRP specimen has sudden fall in value of tensile modulus after one month as shown in Fig. 5.87 and Fig. 5.88.

### 5.2.6.2.3. Comparison of percentage Weight gain with Micro hardness

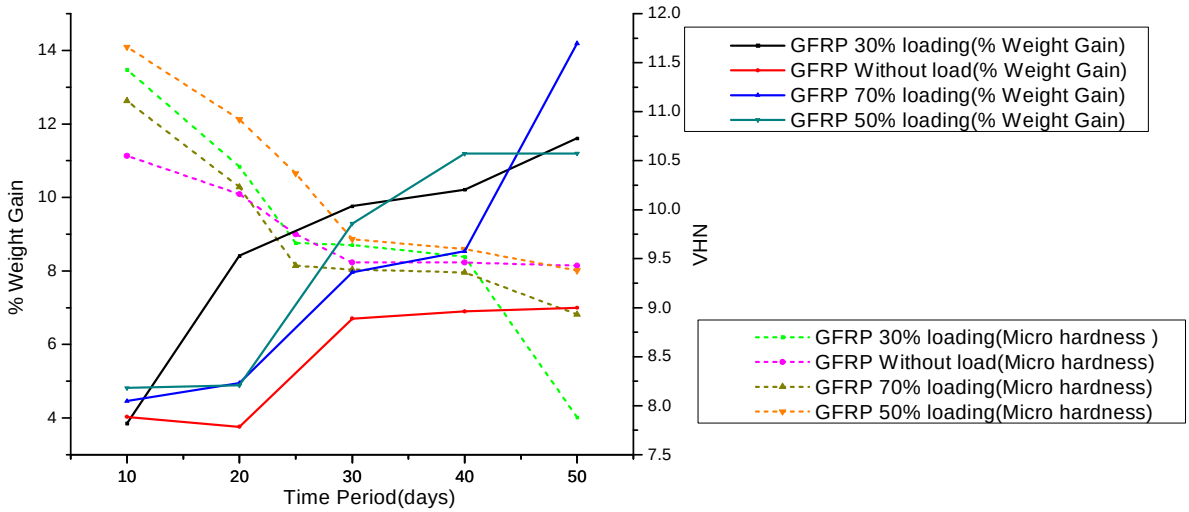


**Fig. 5.89:** Comparison of Micro hardness with percentage Weight gain of various GFRP specimen

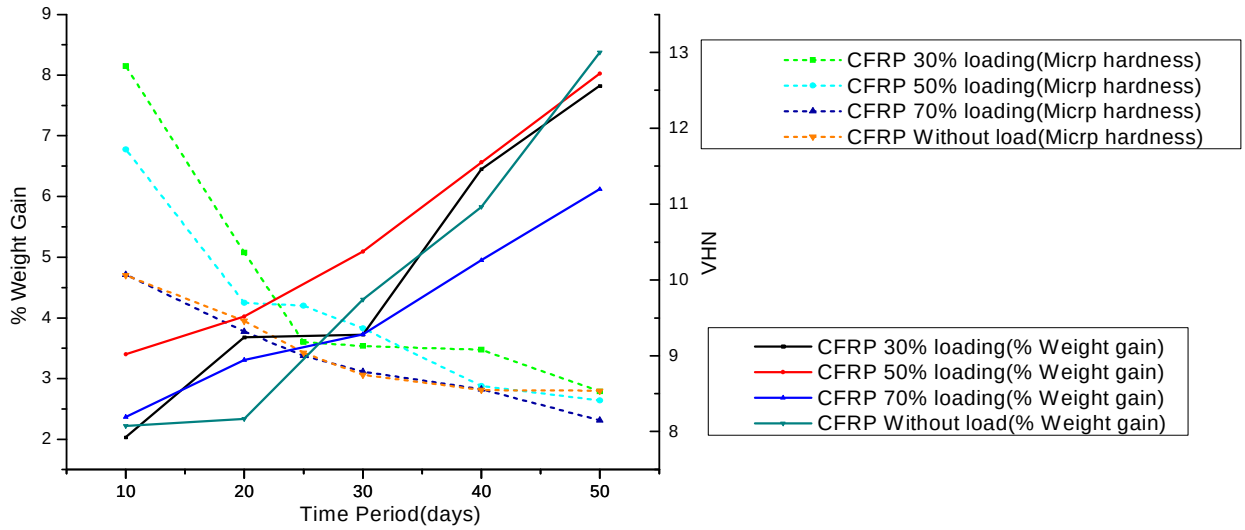


**Fig. 5.90:** Comparison of Micro hardness with percentage Weight gain of various CFRP specimen

From the Fig.5.89 and Fig. 5.90 it is clearly shown that as percentage weight gain increases with hardness decrease, due to water absorption through the pores of epoxy. When CFRP and GFRP specimen are compared all specimen of CFRP had not attained saturation as the water absorption is slow for CFRP specimen as shown in Fig.5.90. But most of the specimen of GFRP attained saturation. The 70% UTL GFRP specimen has not yet achieved saturation

as the curve is showing a regular increase in weight at regular intervals as shown in Fig. 5.89.

### 5.2.6.2.4. Comparison of percentage Weight gain with percentage Area fraction

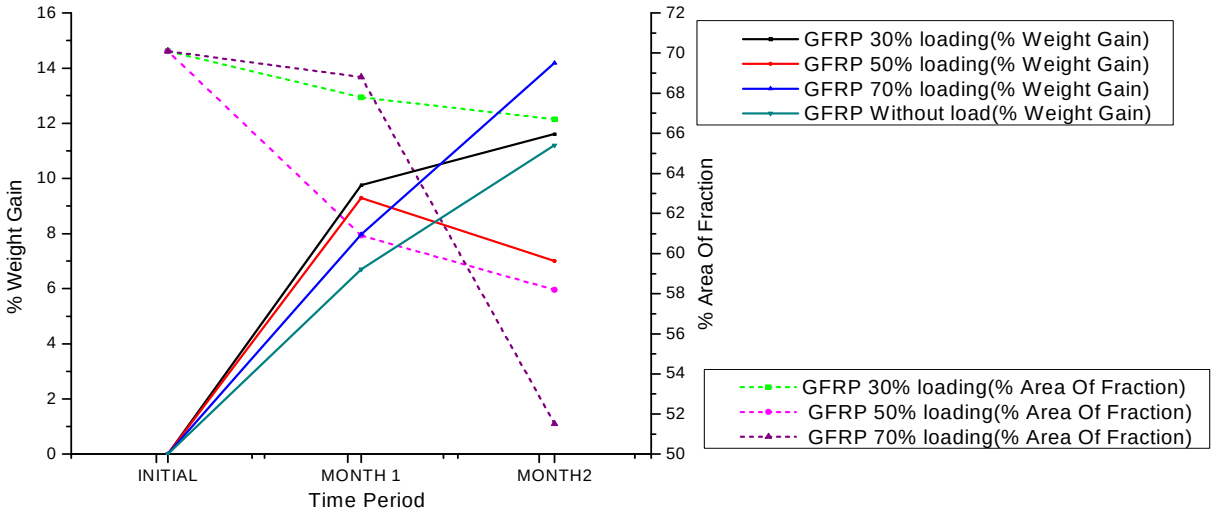


**Fig. 5.91:** Comparison of percentage Weight gain with percentage Area fraction of various GFRP specimen

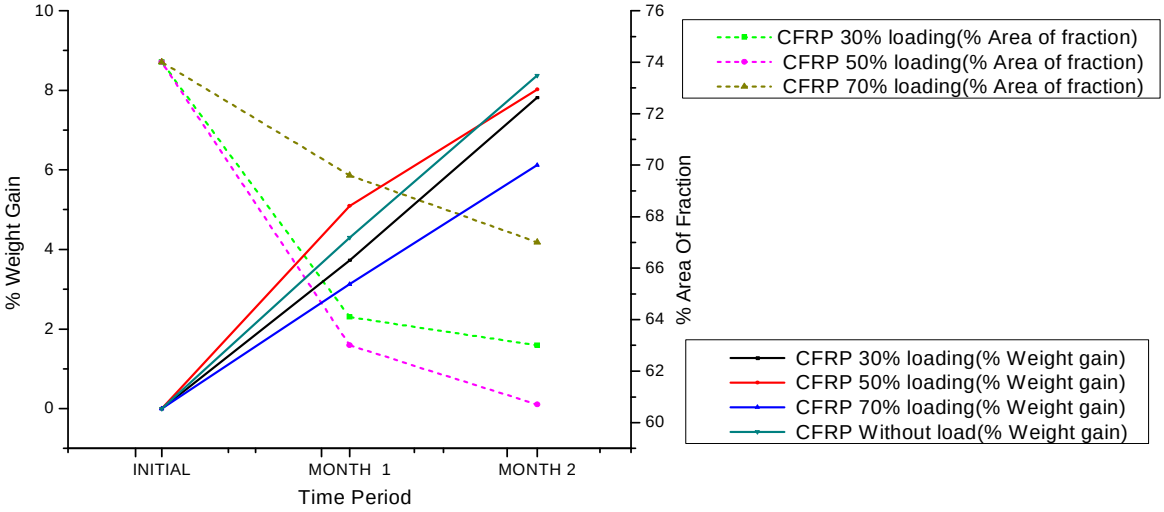


**Fig. 5.92:** Comparison of percentage Weight gain with percentage Area fraction of various CFRP specimen

From the Fig. 5.81 and Fig. 5.92 it is clearly shown that as percentage weight gain increases the percentage area fraction of fibre decreases due degradation of fibre, voids formation in the specimen. In case of 50% UTL GFRP specimen the weight gain had decreased a shown in Fig. 5.91. The CFRP specimen has not yet attained saturation as shown in Fig. 5.92.

### 5.2.6.2.5. Comparison of Capacitance with Micro hardness

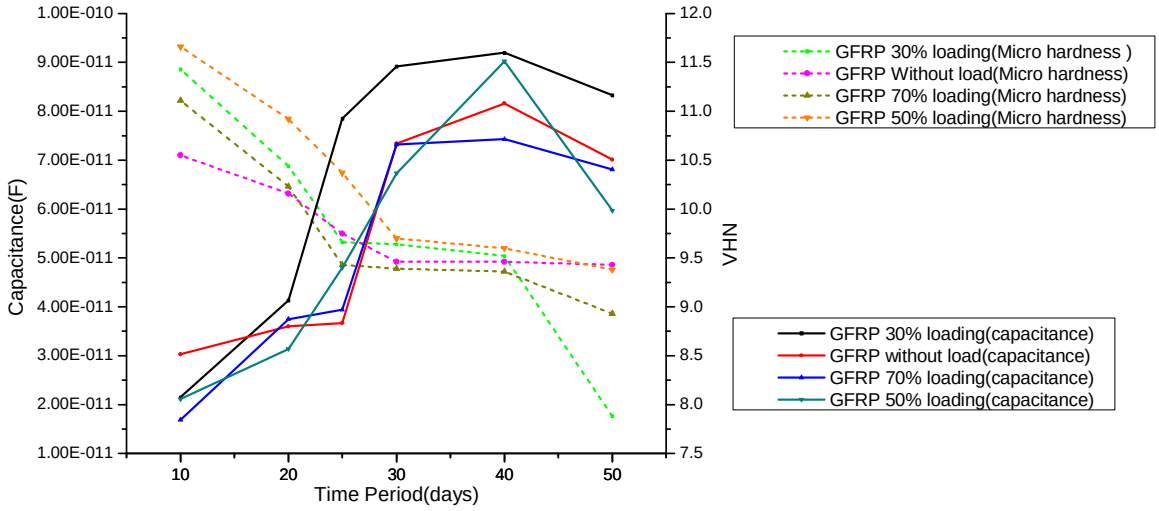


**Fig. 5.93:** Comparison of Micro hardness with Capacitance of various GFRP specimen

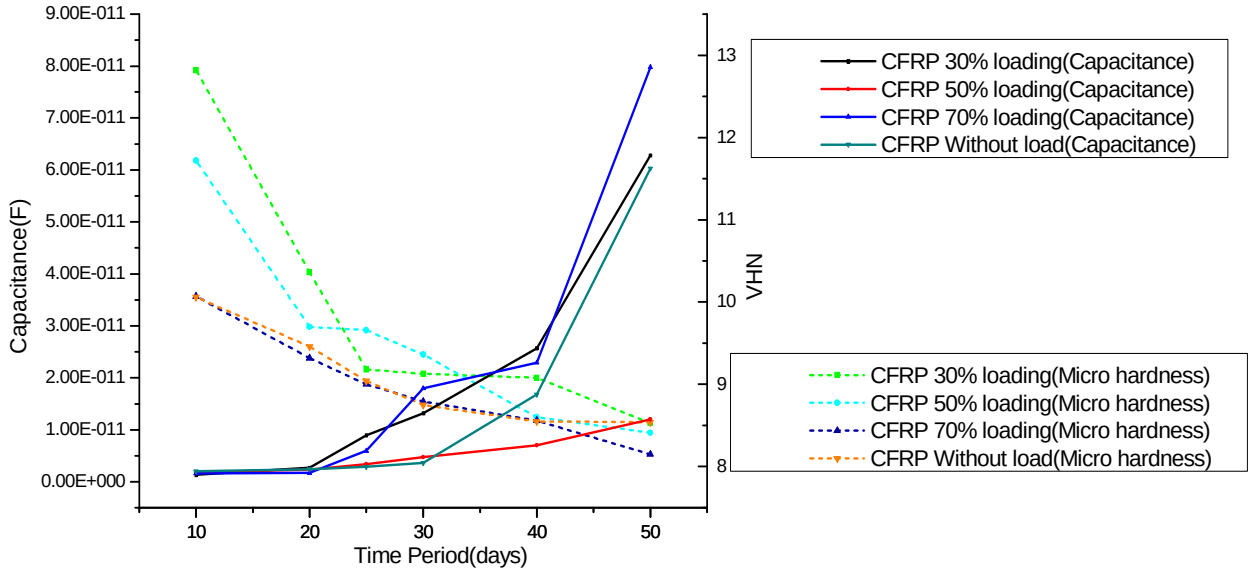


**Fig. 5.94:** Comparison of Micro hardness with Capacitance of various CFRP specimen

From the Fig. 5.93 and Fig. 5.94 it is clearly shown that as Capacitance increases, the Micro hardness of fibre decreases due degradation of fibre, voids formation in the specimen and attains saturation. The capacitance of 50% UTL specimen has drop in capacitance after second month. The capacitance of CFRP specimen was increasing with time and water absorption rate is less comparatively.

### 5.2.6.2.6. Comparison of capacitance with percentage Area fraction

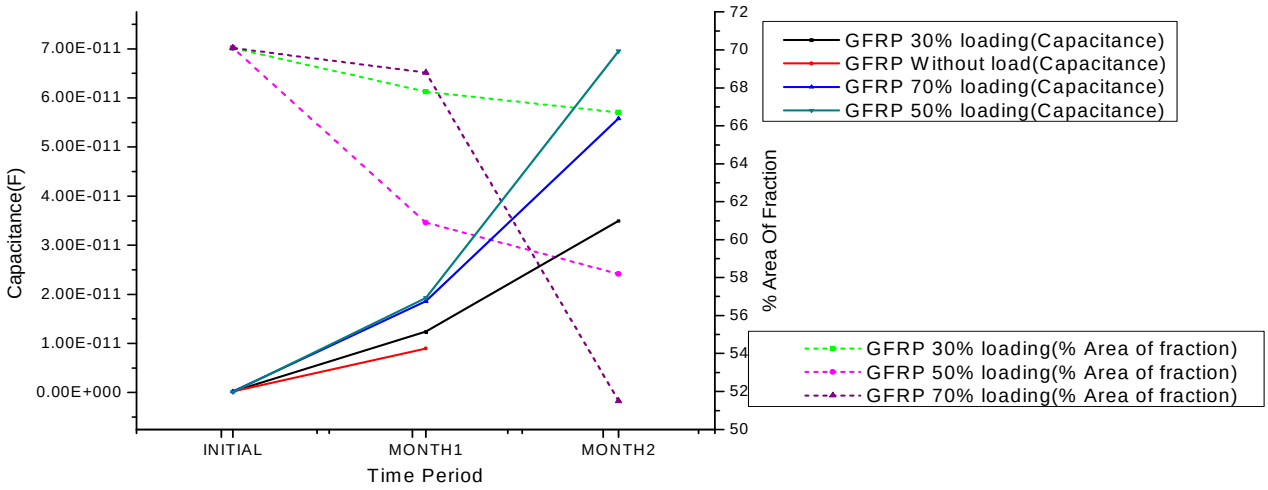


**Fig 5.95:** Comparison of percentage Area fraction with Capacitance of various GFRP specimen

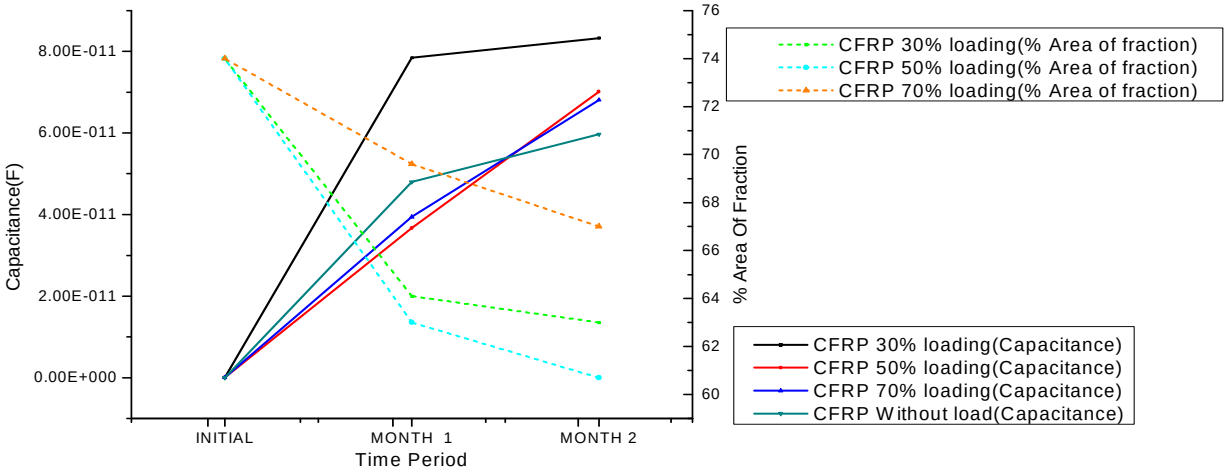


**Fig. 5.96:** Comparison of percentage Area fraction with Capacitance of various CFRP specimen

From the Fig. 5.95 and Fig. 5.96 it is clearly shown that as capacitance increases the percentage area fraction of fibre decreases due to degradation of fibre, voids formation in the specimen. In case of GFRP specimen the capacitance increase is more in 30% UTL GFRP. The 70% UTL GFRP specimen has decreasing value in percentage Area fraction as shown Fig. 5.95.

# CHAPTER-6
# CONCLUSION AND SCOPE OF FUTURE WORK

## 6.1. Conclusion

The flexural strength of GFRP laminates exposed to hygrothermal environment has decreased in range of 25% to 40% after two months. The flexural modulus of GFRP specimen subjected to 50% ultimate flexural load was same up to one month and the sudden decrease in flexural modulus was observed after one month while the GFRP specimen subjected to 30% and 70% ultimate flexural load show continuous decrease in flexural modulus. The flexural strength of CFRP laminates exposed to hygrothermal environment has decreased in range of 10% to 30%. After one month the flexural strength of CFRP specimen subjected to 30% ultimate flexural load is almost same as of initial unexposed specimen while for GFRP specimen subjected to 30% and 70% ultimate flexural load the flexural strength was decreasing continuously. The flexural modulus of CFRP specimen subjected to 50% ultimate flexural load has decreased more compared to other specimen subjected to different pre-load.

The flexural strength of GFRP laminates exposed to room temperature, subjected to 30% ultimate flexural load and without load was almost same after two months while the flexural strength of other specimen decreased with time. The flexural modulus of GFRP specimen exposed to natural conditions subjected to without load decreased up to one month and increased after one month. The flexural strength of CFRP specimen exposed to natural conditions was decreasing with time and the trend was same for all the specimen.

The tensile strength of GFRP specimen subjected to 70% ultimate tensile load decreased and tensile strength of GFRP specimen subjected to 50% ultimate tensile load and 30% ultimate tensile load was almost same up to one month and then decreased after one month. The CFRP specimen have same tensile strength up to one month and then tensile strength decreased after one month where as the tensile strength CFRP specimen without load is almost same up to one month and then decreased.

The CFRP specimen subjected to 70% ultimate flexural load shows sudden increase in percentage weight gain after 6 days where as CFRP specimen subjected to 30% ultimate flexural load shows sudden decrease in percentage weight gain after 40 days. The percentage weight gain of GFRP specimen subjected to 70% ultimate flexural load has increased after 6 days and percentage weight gain GFRP specimen subjected to 30% ultimate flexural load,

50% ultimate flexural load increased after 30 days. The moisture diffusivity of GFRP specimen and CFRP specimen decreased with time.

The percentage weight gain for CFRP specimen subjected to 30% ultimate tensile load was constant after 9 days. The CFRP specimen subjected to 70% ultimate tensile load has decrease in percentage weight gain after 9 days. The CFRP specimen subjected to 30 %ultimate tensile load shows constant percentage weight gain up to 30 days and sudden increase occurred after 30 days. Moisture diffusivity of GFRP specimen is decreasing relatively with time for all specimen whereas for CFRP specimen decrease is almost same up to one month and after one month moisture diffusivity of CFRP specimen has decreased.

The capacitance of GFRP specimen subjected to 30 % ultimate flexural load had attained saturation and for other specimen capacitance was increasing. The CFRP specimen had not attained saturation as water absorption in CFRP specimen is slow and the capacitance was increasing with time.

The capacitance of GFRP specimen subjected to 70 % ultimate tensile load had increased whereas other specimen attained saturation after 30 days. The capacitance of CFRP specimen is almost same up to 20 days compared to initial capacitance and increased after 20 days.

The reduction in strength and damage done in fibre is investigated using SEM images. The area fraction of fibre and circularity of SEM image is obtained using Image-J analysis. The results showed that the area fraction of fibre decreases with time. The fibre circularity decreased more after second month compared to initial circularity.

The area fraction is decreasing with respect to time in GFRP specimen subjected to 50 % ultimate flexural load and 70 % ultimate flexural load. The decrease in percentage area fraction of fibre of GFRP specimen subjected to 70% ultimate tensile load is high compared to other specimen area fraction .The area fraction of CFRP specimen subjected to ultimate flexural load are almost same up to one month.

The micro hardness of GFRP specimen subjected to flexural load were decreasing with time up to 40 days. The micro hardness of GFRP specimen subjected to tensile load was decreasing up to 30 days. The micro hardness of CFRP specimen subjected to flexural load were decreasing with time. The micro hardness of CFRP specimen subjected to tensile load were decreasing with time. The micro hardness of epoxy specimen were decreasing with time.

It was observed that with increase in percentage weight gain, micro hardness of specimen decrease. It was also observed that with time percentage area fraction of fibre decreases due to which flexural strength, tensile strength, young's modulus and flexural modulus of both GFRP and CFRP specimen decrease. As percentage weight gain increases it was observed that there was an increase in percentage area fraction of epoxy with time.

### 6.2. Scope of future work

Pin holed laminated composites under different environmental conditions can be studied as this work is useful to calculate stresses at bearings

Delamination studies on multi directional laminated composites at different environmental conditions can be studied as delamination is main failure occurring in laminates now a day.

Delamination studies by embedding a particle at the interface at different environmental conditions can be studied and analysis of delamination effects can be studied.

The bearing strength of pin holed diameter specimen can be studied at different environmental conditions of different diameters

The delamination of multidirectional laminated composites with an open hole under compressive load can be studied under different environmental conditions

The modeling and analysis of laminated composites can be studied and this can be compared with experimental results of laminated composites exposed at hydrothermal conditions.

# References


[1] www.wikipedia.com/Composite material.html

[2] www.structsource.com/pdf/composite.pdf

[3] www.engr.sjsu.edu/sgleixner/PRIME/FRP.pdf

[4] www.autospeed.com/composites.html

[5] www.bikudo.com/images/glass fibre

[6] www. drdavescience.com/images/carbon fibre

[7] www.rocket materials.org

**[8] Toshio Ogasawara, Yuichi Ishida and Tetsuokasai[2009**],Mechanical properties of carbon fibre/fullerene –dispersed epoxy composites, composites science and technology,vol.69, issues 11-12, pp.2002-2007

**[9] S.K.Panigrahi and B.Pradhan [2009],** through the width delamination damage propagation characteristics in single-lap laminated FRP composite joints, vol.29, issue 2, International journal of adhesion and adhesives.

**[10] Hiroshi Saito and Isao Kimpara [2009],**Damage evolution behavior of CFRP laminates under post impact fatigue with water absorption environment, Composites science and technology, volume69, Issue 6, pp.847-855

**[11] Buket O Kutan,Ramazankarakuzu[2009**], the failure strength for pin-loaded multi-directional fibre-glass reinforced epoxy laminate, journal of composite materials, vol.36, and pp.2695-2712

**[12] S.Yashiro and K.Ogi[2009**], Fracture behavior in CFRP cross ply laminates with initially cut fibres, applied science and manufacturing,

**[13] Xiaodong Shi, Braian R.Hinderliter and Stuart G.Croll [2009**], Environmental and time dependence of moisture transportation in an epoxy coating and its significance for accelerated weathering, presented at the coating tech conference, Indianapolis.

**[14] CHuhne,A-K-Zerbst, G. Kuhlmann, C. Huhne, A-K-Zerbst, G.Kuhlamann**, **C.Steenbock and R.Rolfes[2009],**Progressive damage analysis of composite bolted joints with liquid slim layers using constant and continuous degradation models ,composite structures, vol. 92, issue 2, pp.189-200

**[15] F.Elgabbas, A.A.Ei-Ghandour, A.A.Abdelrahman and A.S.Ei-Dieb [2009**], Different CFRP strengthening techniques for prestressed hollow core concrete slabs: Experimental study and analytical investigation, composite structures, vol.92, issue 2, pp.401-411

**[16] R.M.O Higgins, M.A.Mccarthy and C.T.Mccarthy [2008**], Comparison of open hole tension characteristics of high strength glass and carbon fibre- Reinforced composite materials, composite science and technology, vol.68, issue 13, pp.2770-2778

**[17] Alaattin Aktas and Ibrahim Uzun[2008**], Sea water effect on pinned-joint glass fibre composite materials, volume 85, pp.59-63

**[18] Thomas Schambron, Adrian Lowe and Helen V.Mcgregor [2008**], Effects of environmental ageing on the static and cyclic bending properties of braided carbon fibre/ PEEK bone plates, composites part-B, engineering, vol.39, issue 7-8, pp.1216-1220

**[19] B.Kolesnikov, L.Herbeck and A.Fink [2008**], CFRP/titanium hybrid material for improving composite bolted joints, composite structures, vol.83, issue 4, pp.368-380

**[20] Z. Sereir and E.A.Adda-Bedia[2007**],Use of hybrid composites for the reduction of hygroscopic stresses at the edges of plates exposed to the symmetrical environmental conditions, materials and design, volume 28,Issue 2, pp.448-458

**[21] Sung-Choong Woo and Nak-Sam Choi [2007**], Analysis of fracture process in single-edge-notched laminated composites based on the high amplitude acoustic emission events, composite science and technology, volume 67, Issue 7-8, pp.1451-1458

**[22] Xi Liu and Guoping Wang [2007**], Progressive failure analysis of bonded composite repairs composite structures, vol.81, issue 3, pp.331-340

**[23] K.Nakatani, S Kubo, T Sakagani, D.Shiozawa and M Takagi [2007],** an experimental study on the identification of delamination in a composite material by the passive electric potential CT method, vol.18, pp.49-56, Measurement science and technology.

**[24] Myung-Gonkim, Sang-Gukkang, Chun-Gon Kim and Cheol-Won Kong [2007**], tensile response of graphite/epoxy composites at low temperatures, composite structures, vol.79, issue 1, pp.84-89

**[25] M.De Freitas and R.De Carvalho [2006**], Residual strength of a damaged laminated CFRP under compressive fatigue stresses, Composites science and technology, volume66, Issue 3-4, pp.373-378.

**[26] Z.Sereir, E.A.Adda-Bedia and A.Tounsi[2006**],Effect of temperature on the hygrothermal behavior of unidirectional laminated plates with asymmetrical environmental conditions, Composite Structures, volume 72,Issue 3, pp.383-392.

**[27] B.Pradhan and S.K.Panda[2006],** the influence of ply sequence and thermo elastic stress field on asymmetric delamination crack growth behavior of embedded elliptical delaminations in laminated FRPcomposites, vol. 66, issues 3-4, pp. 417-426, composites science and technology

**[28] Brajabandu Pradhan, Saroja Kanta Panda [2006],** effect of material isotropy and curing stresses on interface lamination propagation characteristics in multiple laminated FRP composites, vol.128, issue3, Journal of engineering materials and technology

**[29] E.C.Botelho, L.C.Pardini and M.C.Rezende [2006**], Hygrothermal effects on the shear properties of carbon fibre/epoxy composites, volume 41, pp.7111-7118

**[30] J.Lee and C.Soutis [2005],** Thickness effect on the compressive strength of T800/924C carbon fibre-epoxy laminates, applied science and manufacturing, vol. 36, issue2, pp. 213-227

**[31] X.W.Wag, I.Pont Lezica, J.M.Harris, F.J.Guild and M.J.Pavier[2005],**Compressive failure of composite laminates containing multiple delaminations, vol.65, issue 2, pp.191-200,composites sciences and technology

**[32] W.J.Hwang, Y.T.Park and W.Hwag [2005**], Strength of fibre reinforced metal laminates with a circular hole, metals and material international journal, vol.11, pp.197-204

**[33] Jorge Borges De Almeida [2005**], Analytical and experimental study on the evolution of residual stresses in composite materials, University of Porto

**[34] Filiz Civgin [2005**], Analysis of composite bars in torsion, Dukuzeylul University

**[35] M. Raghavendra1, C.M. Manjunatha2, M. Jeeva Peter3, C.V. Venugopal3 and H. K. Rangavittal [2004],** Effect of moisture on the mechanical properties of GFRP composite fabric material, International Symposium of Research Students on Material Science and Engineering

[35] **P.K.Ray, A.Bhushan, T.Bera, R.Ranjan, U.Mohanty, S.Vadhera, B.C.Ray[2003],** Mechanical behavior of hygrothermally Conditioned FRP composites after thermal spikes, Emerging trends in structural mechanics and composites

**[36] Z.Zou, S.R.Reid and S.Li[2003],**A continuum damage model for delaminations in laminated composites, Journal of the mechanics and physics of solids, volume 51, Issue 2, pp.333-356.

**[37] B.Pradhan and D.Chakraborthy [2002],** Fracture behavior of FRP composite laminates with embedded two interacting delaminations at the interface, vol.21, pp.681-698, Journal of reinforced plastics and composites

**[38] Buket Okutan [2002**], Effects of geometric parameters on the failure strength for pin-loaded multi-loaded multi-directional fibre-glass reinforced epoxy laminate, composites part-B, engineering, vol.33, issue 8, and pp.567-578

**[39] K.L.Singh, B.Datta Guru, TS Ramamurthy and PD Mangalgiri [2000],** Delamination tolerance studies in laminated composite panels, vol. 25, pp.409-422

**M. A. Aiello and L. Ombre [2000],** Environmental effects on the mechanical Properties of glass-FRP and aramid-FRP rebars, Mechanics of Composite Materials, Vol. 36.

**[40] H.J.Lin, C.C.Tsai and J.S.Shie [1995**], Failure analysis of woven- fabric composites with moulded in holes, composites science and technology, vol.55, issue 3, pp. 231-239

**[41] Sergio Franscino Muller De Almeida and Zabulon Dos Santos Nogueira Neto [1994**], Effect of void content on the strength of composite materials, composite structures, vol.28, issue 2, pp.139-148

**[42] C.Soutis, N.A.Fleck and P.T.Curtis [1991**], Hole interaction in carbon fibre/epoxy laminates under uniaxial compression, composites, vol.14, issue 1, pp. 31-38

**[43] S.Kellas, J.Mortan and P.T.Curtis [1990**], the effect of hygrothermal environments upon the tensile and compressive strengths of notched CFRP laminates part.1: static loading composites, vol.21, issue 2, and pp. 41-51

**[44] C.Soutis and N.A.Fleck [1990**], Static compression failure of carbon fibre T800/924C Composite plate with a single hole, Journal of composite materials, volume 24, Issue 5, pp. 536-558.
[45] Hole in a laminated composite plate, composite structures article in press.
**[46] R.T.Potter [1985**], The interaction of impact damage and tapered thickness sections in CFRP, composites, vol.3, issue 3-4, pp. 319-339
**[47] D.Purslow and R.T. Potter [1984**], The effect of environment on the compression strength of notched CFRP a fractographic investigation, composites, vol.15, issue 2, pp.112-120